“Investigation of microRNA-Protein Complex Recruitment to the Hepatitis C Virus untranslated Regions”

K. Dominik Conrad

Inauguraldissertation “Investigation of microRNA-Protein Complex Recruitment to the Hepatitis C Virus untranslated Regions” zur Erlangung des Dr. rer. nat. im Fachbereich Biologie und Chemie an der Justus-Liebig Universität Gießen.

submitted by K. Dominik Conrad, Dipl.-Biol.

Justus-Liebig-Universität

Gießen, Germany, July 2013

Die vorliegende Arbeit wurde von März 2010 bis Juni 2013 in der Arbeitsgruppe von Prof. Dr. Niepmann im Biochemischen Institut des Fachbereichs Humanmedizin der Justus-Liebig-Universität Gießen angefertigt.

Die Promotion wurde durch die International Research Training Group GRK 1384 “Enzymes and Multienzyme Complexes acting on Nucleic Acids“ und den Sonderforschungsbereich 1021 “RNA viruses: RNA metabolism, host response and pathogenesis“ im Rahmen des Teilprojekts A03 “Hepatitis C Virus RNA plasticity and microRNA action“ gefördert.

Erstgutachter: **Prof. Dr. Albrecht Bindereif**
Institut für Biochemie
Fachbereich für Biologie und Chemie
Justus-Liebig-Universität Gießen

Zweitgutachter: **Prof. Dr. Michael Niepmann**
Biochemisches Institut
Fachbereich Humanmedizin
Justus-Liebig-Universität Gießen

Summary

Hepatitis C virus belongs to the family of *Flaviviridae* and contains a single stranded RNA genome in positive orientation. The genome carries a single polyprotein open reading frame (ORF), which is flanked by two highly structured RNA stretches, the 5'- and 3'-untranslated regions (UTRs). In these UTRs several secondary structures were identified to be necessary for HCV translation and replication.

The internal ribosome entry site (IRES), which is required for translation, comprises three of the four stem loops present in the 5'-UTR. In addition two microRNA-122 (miR-122) binding sites are located upstream of the IRES. The 3'-UTR comprises a variable region (VR), a poly U/C tract and three conserved stem loops. In the VR an additional miR-122 binding site was identified. miR-122 was shown to stimulate HCV translation and replication possibly by protecting the HCV RNA from degradation.

This work focused on the question whether miR-122 recruits a microRNA-protein complex to its binding sites on the HCV RNA and which components this complex contains. Towards this end an anti-Argonaute (Ago) protein-specific – HCV RNA co-immunoprecipitation was developed. Using this method it could be shown that two of the four members of the Ago protein family, Ago1 and Ago2, are recruited to the HCV RNA in a miR-122 dependent manner. For the miR-122 binding site in the VR of the 3'-UTR it has also been shown that Ago2 can be recruited by miR-122. This however is only the case when four nucleotides located in a stem loop in the NS5B coding region are present. These findings give rise to the assumption that for this miR-122 binding site not only the seed sequence but also four additional nucleotides located close to the 3'-end of the miR-122 bind to the HCV RNA.

Finally, employing a time course assay it has been shown that miR-122 prolongs the half-life of a wild type HCV reporter RNA compared to a mutant that is not able to bind miR-122 or compared to the wild type in presence of a control miR-122. This experiment also shows that, besides stabilizing the HCV RNA, miR-122 seems to directly stimulate HCV translation.

Thus, it seems that miR-122 recruits a microRNA-protein complex and positively influences the HCV life cycle via two different mechanisms. Firstly, miR-122 enhances HCV RNA stability, most likely by protecting it from degradation. Secondly, miR-122 improves HCV translation efficiency probably by changing the IRES structure to a conformation favorable for translation.

Zusammenfassung

Das Hepatitis C Virus (HCV) gehört zu der Familie der *Flaviviridae* und besitzt ein einzelsträngiges RNA-Genom in (+)-Strang-Orientierung. Dieses Genom enthält einen einzelnen offen Leserahmen für das Polyprotein. Dieser ist von 5‘- und 3‘-nicht translatierten Regionen (UTRs) flankiert, in welchen sich viele Sekundärstrukturen befinden, die unerlässlich für die Translation und Replikation des Virus sind.
Die sogenannte „*internal ribosome entry site*“ (IRES) in der 5‘-UTR besteht aus drei Haarnadelstrukturen und ist unerlässlich für die Translationsinitiation des HCV ist. Zusätzlich besitzt die 5‘-UTR zwei microRNA-122 (miR-122) Bindestellen stromaufwärts der IRES. Die 3‘-UTR umfasst eine variable Region (VR), einen poly-U/C-Trakt sowie drei konservierte *stem loops*. Auch hier befindet sich, im Bereich der VR, eine miR-122 Bindungsstelle. Des Weiteren wurde für miR-122 nachgewiesen, dass sie stimulierend auf die Translation und Replikation wirkt, möglicherweise indem sie die HCV-RNA vor Abbau schützt.
Das Hauptaugenmerk der vorliegenden Arbeit lag auf der Frage, ob miR-122 einen microRNA-Proteinkomplex (miRNP) an die HCV-RNA rekrutiert und welches die Proteinkomponenten dieses Komplexes sind. Zur Untersuchung dieser Fragestellung wurde eine Argonaute (Ago) Protein spezifische – HCV-RNA Koimmunpräzipitation entwickelt. Mit dieser Methode konnte nachgewiesen werden, dass zwei der vier Mitglieder der Ago-Proteinfamilie, Ago1 und Ago2, durch miR-122 an die HCV-RNA rekrutiert werden. Bezüglich der miR-122 Bindestelle in der VR der 3‘-UTR konnte gezeigt werden, dass abhängig von miR-122 Ago2 auch hier binden kann allerdings nur, wenn neben der bekannten miR-122 Bindesequenz auch vier Nukleotide der NS5B-kodierenden Region vorhanden sind. Folglich ist, nicht nur die *seed*-Sequenz der miR-122 notwendig für die effiziente Bindung an die HCV 3‘-UTR, sondern auch vier Nukleotide am 3‘-Terminus von miR-122.
Zusätzlich wurde ein Zeitverlaufsversuch durchgeführt, um die Stabilität der HCV-RNA zu testen. Dabei wies ein HCV-Reporter-RNA eine höhere Halbwertszeit in Anwesenheit von miR-122 auf als ein vergleichbare Mutante, die miR-122 nicht binden kann, oder der Wildtyp in Anwesenheit einer Kontroll-miR. Zusätzlich scheint miR-122 neben der Stabilisierung der HCV-RNA auch einen direkten positiven Effekt auf die HCV Translation zu haben.
Zusammengefasst rekrutiert miR-122 einen miRNP-Komplex an die HCV-RNA und beeinflusst den Lebenszyklus des HCV positiv durch zwei unterschiedliche Mechanismen. Zum einen erhöht miR-122 die Stabilität der HCV-RNA, möglicherweise durch die Verhinderung des Abbaus der HCV-RNA. Zum anderen verstärkt miR-122 die HCV-Translationseffizienz, möglicherweise dadurch, dass die Bindung von miR-122 die Struktur der IRES beeinflusst und diese in eine Konformation bringt die vorteilhaft für die Translation ist.

Content

1 Introduction

1.1 Hepatitis C Virus Infection

The Hepatitis C virus (HCV) was first cloned by Choo and coworkers in 1989 and was identified as the causative agent of the NonA-NonB hepatitis (Choo et al, 1989). According to the World Health Organization (WHO) about 150 million people worldwide are chronically infected with HCV causing more than 350.000 deaths per year (WHO, 2012).

Two to six weeks after infection only about 20 % of the infected people develop symptoms, which range from fever, fatigue, nausea, abdominal and joint pain to jaundice.

However, in most cases the infection takes a subacute development which increases the risk of chronic infections. It is estimated that about 55 - 85 % of all patients get chronically infected with this liver tropic virus and have a probable chance of 20 % for developing liver cirrhosis which increases the risk for hepatic cancer (Hoofnagle, 2002; Jeong et al, 2012; Seeff, 2002).

Transmission of HCV occurs mainly via blood and blood products as well as with organ transplants. Contaminated medical equipment, like reused syringes and needles, is also a source of infection, which especially poses a threat to drug addicts and patients in countries with poor medical standards.

As a treatment a combination of nucleoside analogues (ribavirin) and polyethylene glycol (PEG)-bound-interferon-α is usually used after diagnosis. In some cases, recently approved inhibitors targeting the NS3-4A protease of HCV are also added to the drug cocktail (Pawlotsky, 2013). Until today no vaccination against HCV is available.

1.2 Classification of HCV

HCV belongs to the family of *Flaviviridae* (Simmonds et al, 1993) which is comprised of the genera Flavivirus, Pestivirus, Pegivirus (Stapleton et al, 2011) and Hepacivirus. The genus Hepacivirus contains only two members, HCV and the recently discovered GBV-B (Muerhoff et al, 1995; Simons, 1995). Well-known members of the Flavivirus family are the yellow fever virus, from which the family name is derived (lat. flavus, yellow), the Dengue fever virus and West Nile virus.

Following the Baltimore classification (Baltimore, 1971) the *Flaviviridae* were categorized in group IV which indicates that the viruses comprising this group contain a single stranded RNA genome in (+)strand orientation. Hepatitis C virus is

subdivided into seven genotypes which are genetically divergent from each other. These genotypes also show a varying distribution across the world, with the subtypes 1a and 1b being the most predominant in Europe (Zein, 2000).

1.3 Hepatitis C Virus

1.3.1 Structure of HCV

Under the electron microscope HCV particles are pleomorphic and have diameters between 30 and 80 nm (Bradley et al, 1985; He et al, 1987; Yuasa et al, 1991). HCV virons contain an approximately 9.6 kilobases (kb) long single-stranded RNA genome with positive polarity. The genome is packed into an icosahedral capsid formed by the viral Core protein. A viral envelope surrounds the capsid and is composed of a lipid bilayer derived from the cellular membrane of the host cell. Two viral glycoproteins E1 and E2 are embedded in the lipid envelope. The viral particle can associate with low-density lipoproteins (Andre et al, 2002; Miyamoto et al, 1992; Nielsen et al, 2006; Thomssen et al, 1992) which are thought to facilitate attachment to the host cell (Bankwitz et al, 2010; Dreux et al, 2006; Prentoe et al, 2011).

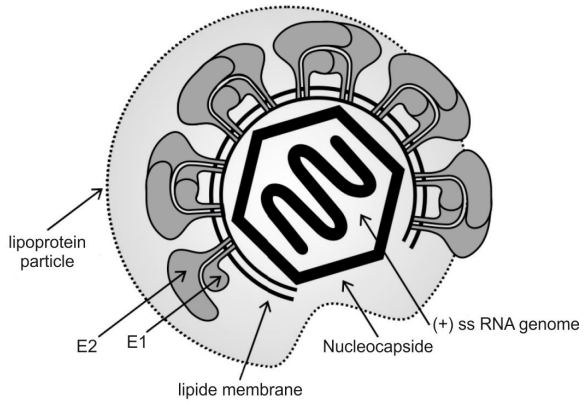

Figure 1: Structure of the HCV particle. The viral particle is made up of the host cell-derived lipid membrane with the embedded viral glycoproteins E1 and E2, and the capsid containing the single stranded RNA genome. The viral particle is associated with a lipoprotein particle. Modified from Bartenschlager et al., 2004 (Bartenschlager et al, 2004).

1.3.2 Genome and polyprotein

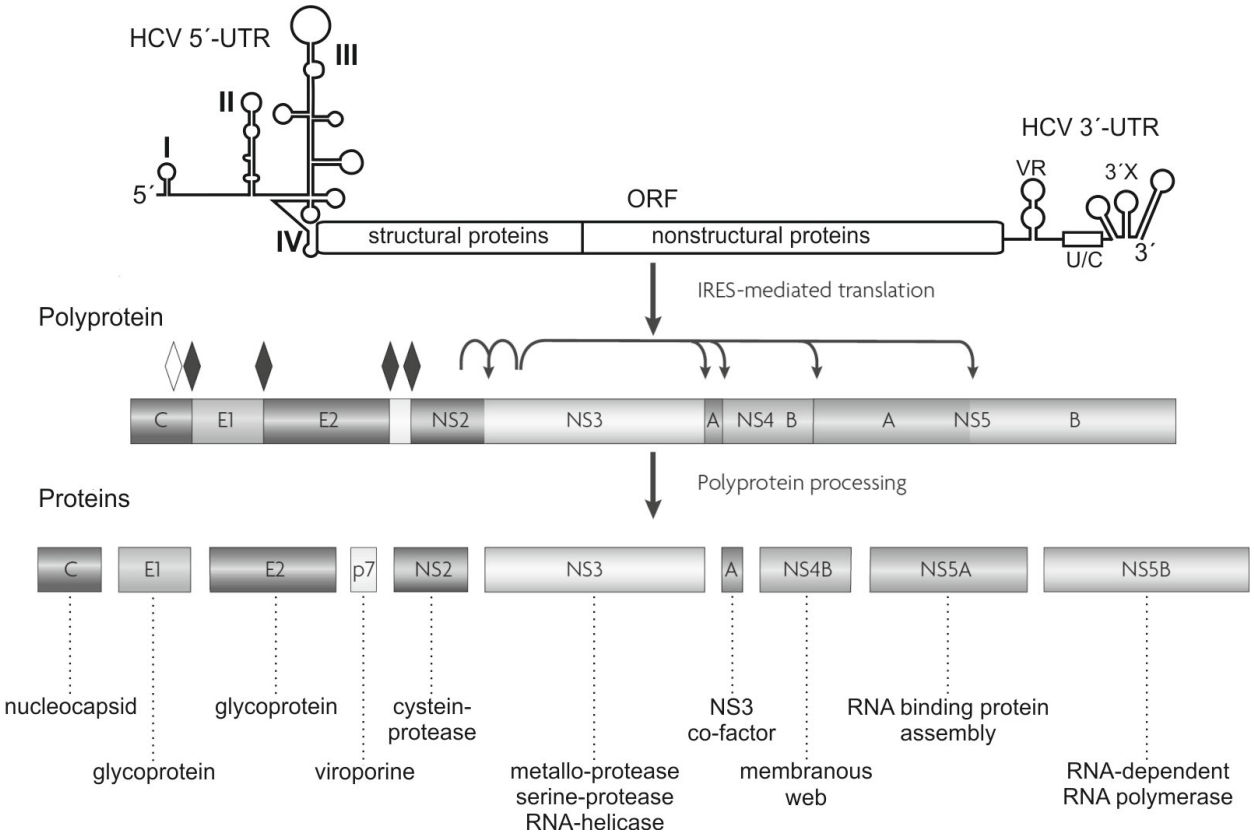

Figure 2: Structure and translation products of the HCV genome. Shown is the approximately 9.6 kb long HCV genome with secondary structures in the 5'- and 3'- UTR. Upon IRES-dependent translation the polyprotein is synthesized and subsequently cleaved into ten sub-proteins. Arrows show autoprotease cleavage by NS2 and NS3, closed diamonds indicate cleavage by the edoplasmatic reticulum signal peptidase while open diamonds indicate cleavage by signal peptide peptidase. The structural proteins shown in the ORF of the genome comprise the core, E1 and E2 protein. Nonstructural proteins are all proteins from p7 to NS5B. Modified from Moradpour et al.,2007 (Moradpour et al, 2007).

The viral genome is approximately 9.6 kb in length and can be roughly divided into three parts; the 5'- untranslated region (5'-UTR), the single open reading frame (ORF) coding for the viral polyprotein and the 3'-UTR.

The 5'-UTR contains four stem loops. Stem loop I and parts of stem loop II were shown to be important for genome replication (Friebe et al, 2001). Stem loop II, III and IV form the viral internal ribosome entry site (IRES) which is used to initiate translation directly at the translation start site (Brown et al, 1992; Tsukiyama-Kohara et al, 1992; Wang et al, 1993). Stem loop IV partly reaches into the core coding region of the polyprotein ORF.

The 3'-UTR contains a variable region (VR), a poly(U/C) tract and the stem loops 1, 2 and 3. It is assumed that the poly(U/C) tract serves as a binding site for the viral

helicase non-structural protein (NS) 3 (Kim et al, 1995; Suzich et al, 1993) and the phosphoprotein NS5A, which was shown to regulate viral replication (Gwack et al, 1996; Huang et al, 2005; Lohmann et al, 1997).

The ORF codes for a single large polyprotein that is post-translationally cleaved, partly autoproteolytically and partly by cellular proteases, to produce ten sub-proteins, the structural proteins Core, E1 and E2 and the non-structural proteins p7, NS2, NS3, NS4A, NS4B, NS5A and NS5B. The RNA secondary structures essential for the viral translation and replication, as well as the cleavage events of the polyprotein and the known functions of the ten sub-proteins (Lohmann, 2013; Moradpour & Penin, 2013; Niepmann, 2013) are illustrated in Figure 2.

In addition the HCV RNA contains several conserved binding sites for the liver specific microRNA-122 (miR-122), two of which are located in the 5'-UTR upstream of the IRES and one is situated in the variable region of the 3'-UTR. It has been shown that miR-122 enhances HCV replication and translation and evidence is emerging that miR-122 protects the HCV RNA from degradation (Henke et al, 2008; Jopling et al, 2005; Shimakami et al, 2012a; Shimakami et al, 2012b; Wilson et al, 2011). In addition there were primate studies suggesting that miR-122 might be a promising target for anti-viral treatment to improve the prospect for chronically infected patients (Lanford et al, 2010).

1.3.3 Replication cycle

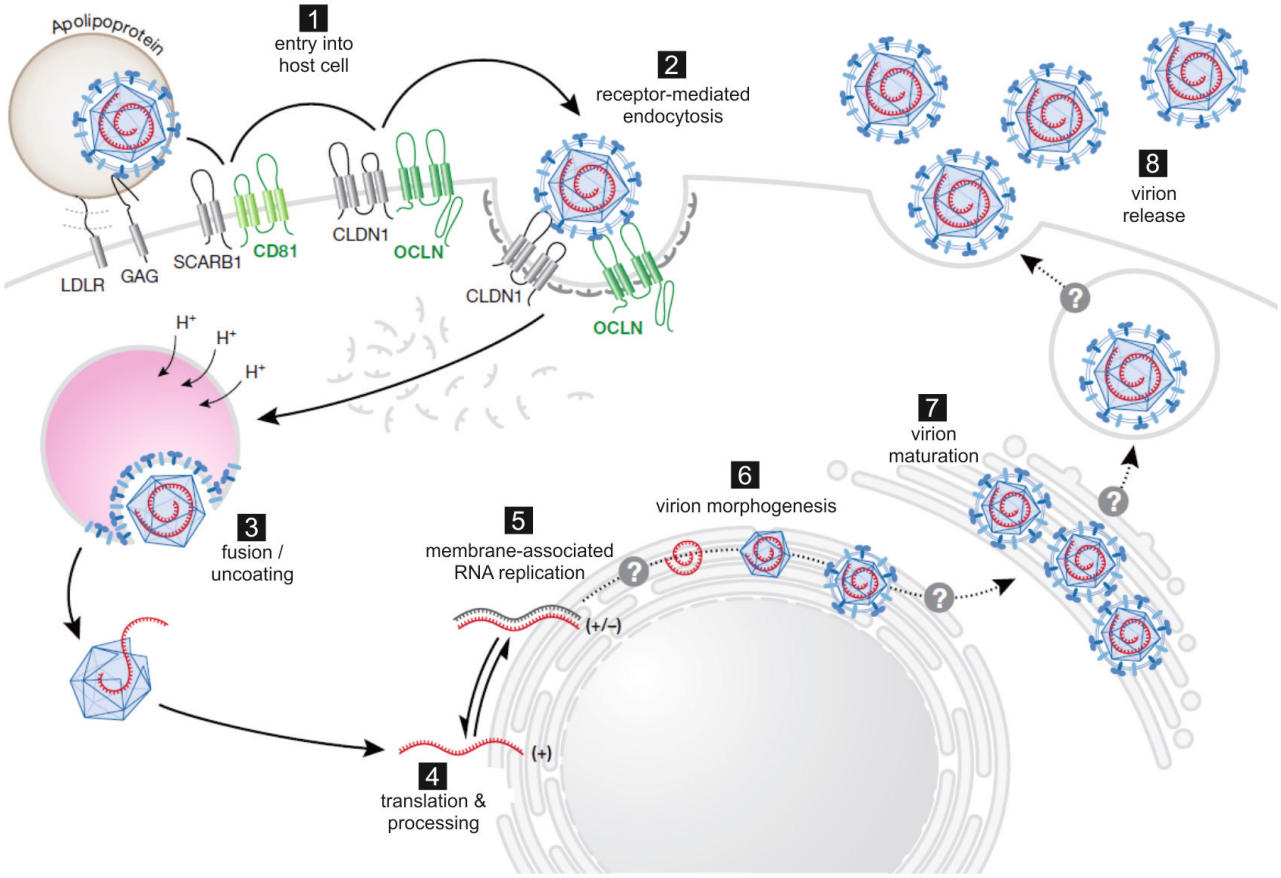

Figure 3: Replication cycle of HCV. HCV recognizes several surface proteins of the host cell using them as receptors to be endocytosed into the cell. Upon acidification of the endosome, the viral RNA is released into the cytoplasm. Subsequently, the IRES-dependent translation and processing of the polyprotein takes place. The genome is then replicated and the newly synthesized genomes are packed into new viral particles and released from the cell. Modified from Ploss and Rice,2009 (Ploss & Rice, 2009).

In the blood stream HCV is associated with lipoprotein particles forming a lipo-viro particle. This association is assumed to facilitate attachment to the host cell via several cellular receptor molecules necessary for cholesterol transport such as SR-BI, LDLR and NOC1L1. A subset of receptors that may be utilized by HCV to enter the host cell has been identified, including OCLN, CLDN1 and CD81 (Ploss et al, 2009; Zeisel et al, 2013). It has been shown that the viral glycoprotein E2 interacts with SR-BI, CD81 and glycosaminoglycans (GAG).

The virus is internalized via clathrine-dependent endocytosis. When the inside of the endophagosome is acidified, it induces fusion of the viral envelope with the endosomal membrane at a pH range of 6.3 - ~4.0 (Pietschmann et al, 2009; Tscherne et al, 2006). It seems that CD81 and CLDN1 together with E1 and E2 play a major role in these events. It is assumed that the acidification of the endosome

triggers a conformational change in the two viral glycoproteins which in-turn initiates fusion, analogous to other viral fusion events (Bressanelli et al, 2004; Modis et al, 2004). After fusion the viral RNA is released into the cytoplasm.

The viral RNA is subsequently translated into protein by IRES mediate translation, which occurs at the endoplasmic reticulum (ER). After cleavage of the polyprotein, all non-structural proteins remain associated with the ER membrane. Next, NS4B induces the formation of invaginations in the ER membrane (Welsch et al, 2009). Together these membrane alterations form the so called membranous web (Egger et al, 2002) and are the sites of viral genome replication (Gosert et al, 2003). Key enzyme in the synthesis of new genomes is the RNA-dependent RNA polymerase NS5B. This enzyme catalyzes the formation of (+)strand genome copies that are used as a template by NS5B for production of a new generation of HCV genomes (Behrens et al, 1996; Lohmann et al, 1997).

Assembly and release of viral particles from the host cell is still not well understood. It has been shown that lipid droplets (Barba et al, 1997; Boulant et al, 2006; McLauchlan et al, 2002; Moradpour et al, 1996) and the endosomal-sorting complex required for transport (ESCRT) pathway (Ariumi et al, 2011b; Corless et al, 2010; Tamai et al, 2012) play a major role in storage and trafficking of viral components and infectious particles but the mechanism stays unclear. Newly formed particles bud into the ER (Gastaminza et al, 2008) and pass through the Golgi before they are released (Vieyres et al, 2010). How and when the viral particle is associated with the lipoprotein particles is unclear, but it has been shown that nascent viral particles are complexed with apolipoprotein ApoE (Coller et al, 2012) indicating that the association occurs during virus assembly.

1.4 Cap-dependent translation versus IRES mediated translation initiation

Like some other positive strand RNA viruses HCV initiates the translation of its genome by employing an internal ribosome entry site (IRES) instead of using a Cap-structure. This IRES is mainly located in the 5'-UTR, spanning from stem loop II to stem loop IV and also comprising a small part of the Core coding region of the polyprotein ORF.

The act of initiating translation at an IRES element differs significantly from the initiation at a Cap structure commonly used in cellular mRNAs and will be discussed in more detail below.

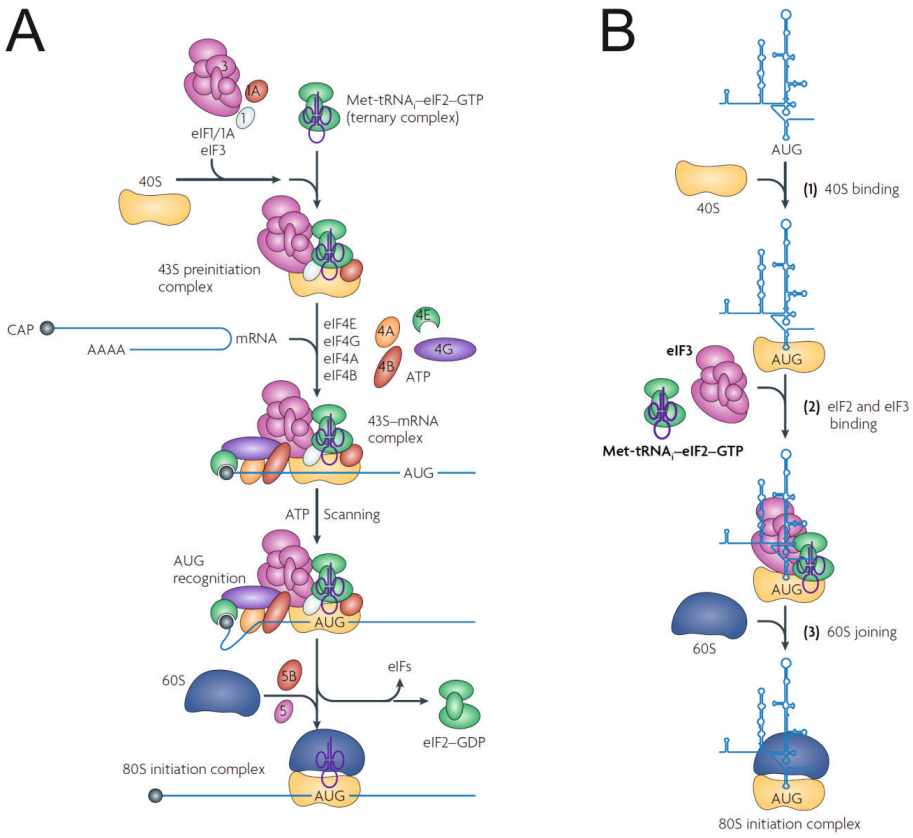

Figure 4: Schematic depiction of the Cap- and HCV IRES-mediated translation initiation. (A) Sequence of the binding events of eukaryotic initiation factors (eIFs) to mRNA in case of Cap-dependent translation initiation. Firstly, the eIF4 subunits bind the Cap structure on the mRNA. Secondly, the preformed 43S pre-initiation complex is recruited. Subsequently, a scanning process for the translation start codon (AUG) occurs. When the AUG is found, the eIFs leave the complex and the 60S large ribosomal subunit is recruited. (B) Sequence of binding events in case of translation initiation at the HCV IRES. The 40S small ribosomal subunit binds directly to the tRNA-like stem loop IV. Afterwards, eIF3 and eIF2 in complex with the methionine carrying starter tRNA are recruited. After eIF5 promoted hydrolysis of the GTP which is part of the eIF2-initiator tRNA complex, the 60S ribosomal subunit is recruited and translation can commence. Modified from Fraser and Doudna, 2007 (Fraser & Doudna, 2007).

1.4.1 Cap-dependent translation initiation

A Cap-structure is comprised of a 7-methyl guanosine bound to the RNA via a 5'-5' tri-phosphate bond. In the event of translation initiation, first the eukaryotic initiation factor (eIF) 4F complex comprised of its subunits A, E, G and the accessory factors B and H is recruited to the Cap, whereas eIF4E is the subunit which is directly interacting with the Cap (Gingras et al, 1999; Jackson et al, 2010). eIF4A possesses a helicase activity which is used to smooth out secondary structures of the mRNA, supported by its co-factors eIF4B and H (Marintchev et al, 2009; Rogers et al, 1999). The 43S pre-initiation complex, containing the small ribosomal subunit and the eIFs 1, 2 and 3, is subsequently recruited by eIF4G (Gingras et al, 1999; LeFebvre et al, 2006). eIF2 is associated with the Methionine carrying initiator tRNA ($tRNA_i^{Met}$). Following the binding, a scanning process occurs in search for the translation start codon AUG (Pestova & Kolupaeva, 2002). When the start codon is found eIF1 leaves the complex and eIF5 induces hydrolysis of the GTP bound by eIF2 in the ternary complex. The eIFs are released and the 60S large ribosomal subunit binds, forming the 80S ribosome (Paulin et al, 2001; Unbehaun et al, 2004). Figure 4 A shows the events taking place at the Cap.

1.4.2 IRES-mediated translation initiation

IRESs are classified by their need of eukaryotic initiation factors for translation initiation. Classically, there are four groups of IRES-structures, class I comprising Entero- and Rhinoviruses, class II of Cardio- and Aphthoviruses, class III containing the Hepatitis A virus, and class IV which HCV was assigned to (Figure 5).
In contrast to the Cap-dependent initiation, the IRES-mediated initiation of HCV translation (Figure 4 B) follows a distinctly different mechanism. Only three of the canonical translation initiation factors, eIF3, eIF2 and eIF5, are used.
Stem loop IV possesses a pseudo knot structure that resembles a tRNA, also including the translation start codon, AUG. The small ribosomal subunit is directly recruited to this structure. After binding of the small ribosomal subunit stem loop IV unfolds, positioning the AUG with adjacent sequences in the mRNA binding cleft (Berry et al, 2011). In the following eIF3 binds to stem loop III contacting the 40S subunit (Jackson et al, 2010). eIF3 is not needed for the recruitment of the 40S subunit to the IRES but it facilitates the binding and stabilizes the formation of the 80S complex (Fraser & Doudna, 2007). Subsequently, the ternary complex comprised of eIF2, the $tRNA_i^{Met}$ initiator tRNA and GTP binds. It has been shown that under certain circumstances like cellular stress eIF2 can be substituted by other factors like eIF5B (Terenin et al, 2008), eIF2D (Dmitriev et al, 2010) or eIF2A (Kim et al, 2011) and thus eIF2 is not absolutely required for translation initiation at the IRES.

eIF5 helps in the recognition of the start codon by the ternary complex and stimulates GTP hydrolysis (Pestova et al, 1998). Finally, the 60S subunit binds releasing the eIFs except for eIF3 which seems to stay associated with the ribosome (Weinlich et al, 2009).

For Cap-dependent translation it is known that the circularization of the mRNA, accomplished by an interaction of eIF4A with the Poly(A) binding protein (PABP), enhances translation efficiency. The proposed mechanism implies that the circularization leads to a more stable binding of the eIF4F complex to the mRNA enhancing the speed of translation (re)-initiation. In case of HCV it has been shown that the 3'-end also enhances the translation efficiency (Bung et al, 2010; Song et al, 2006). It is hypothesized that the circularization of the HCV RNA might also play a role in translation efficiency, but the involved proteins and the mechanism by which it might be accomplished remain unknown. For cellular mRNAs and the HCV RNA both this circularization might be used as a system to ensure the integrity of the RNA, so that only undegraded (i.e. functional) RNAs get efficiently translated.

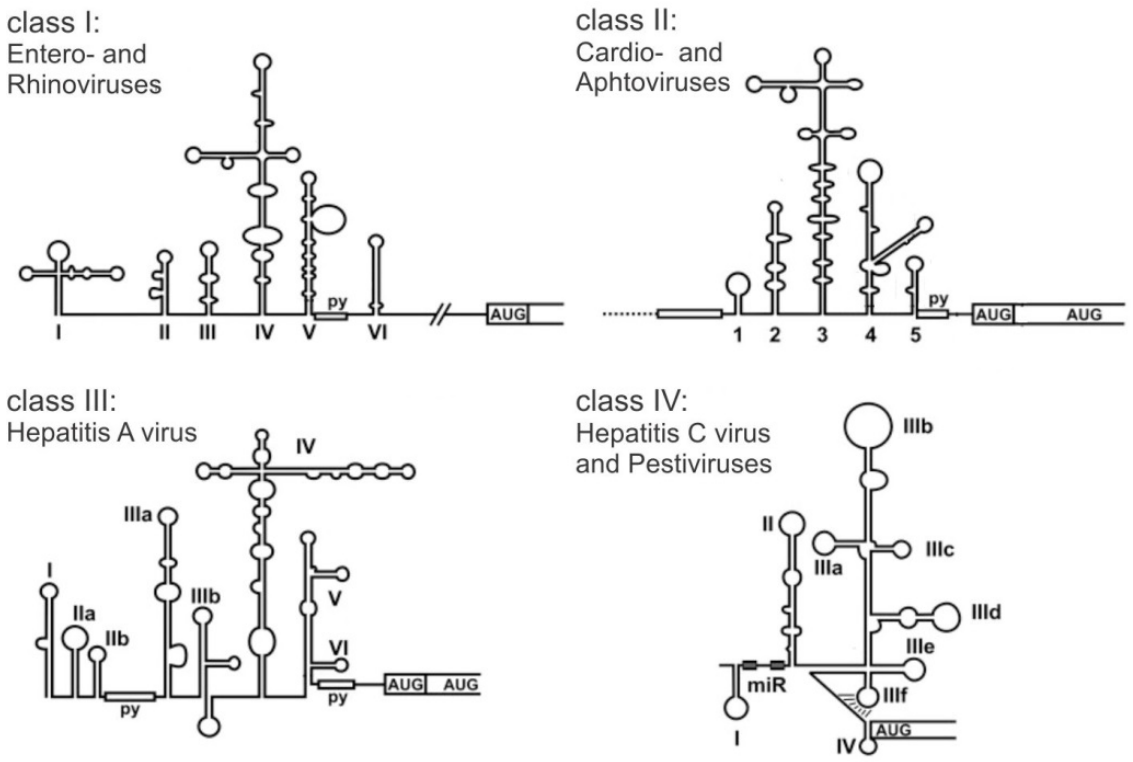

Figure 5: The four groups of classical IRES structures. Shown are the four classical groups of IRES-structures. IRESs are classified according to their needs of canonical initiation factors to initiate translation. Class I shows the IRES of the Entero- and Rhino viruses, class II the IREs of the Cario- and Aphtoviruses, class II the IRES of Hepatitis A virus and class IV shows the IRES of HCV, as a member of the *Flaviviridae* that carries an IRES. The stem loops are shown by either roman (class I, II and IV) or arabic (class II) numbers. py signifies a poly-pyrimidine tract. miR shows the two binding sites of miR-122 in the HCV 5'-UTR. Modified from Niepmann, 2009 (Niepmann, 2009).

1.4.3 IRES trans-acting factors

Besides the canonical eIFs, IRES-dependent translation is known to use IRES transacting factors (ITAFs) to augment translation efficiency. In case of HCV several proteins have been identified that bind to parts of the IRES and influence translation. ITAFs identified for HCV include the La protein, NSAP1, hnRNP L, hnRNP D, IMP-1, Gemin5, LSm1-7 and PCBP2. Figure 6 gives an overview of these proteins showing their structural features and their influence on HCV translation. Most of these proteins contain several RNA interaction domains which enable them to bind to the HCV RNA, like the RNA recognition motif (RRM), the KH domain (Makeyev & Liebhaber, 2002) and the La motif domain (Martino et al). It has been shown that several of these proteins can interact with each other, like La protein with LSm1-7 (Maraia & Lamichhane, 2011) or NSAP1 with IMP-1.
Additionally other factors have been identified that are assumed to stimulate HCV translation but are not counted to the ITAFs such as microRNA-122 and the Argonaute proteins (Henke et al, 2008; Wilson et al, 2011).

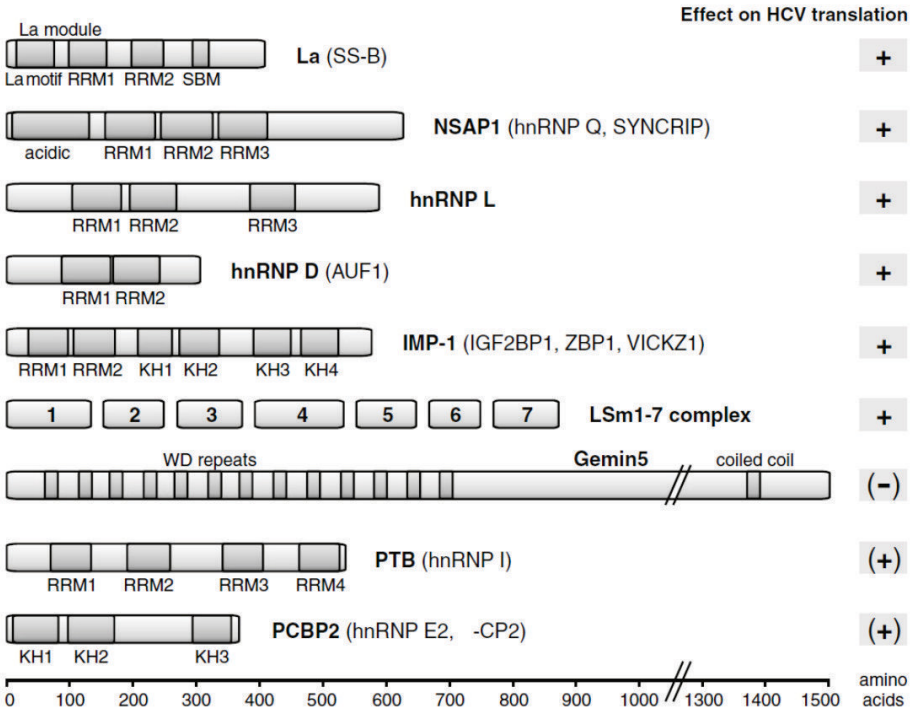

Figure 6: HCV IRES trans-acting factors. Shown are the different IRES transacting factors of the HCV IRES, with domains that are important for RNA interaction (dark grey) like the RNA recognition motif (RRM), the KH domain or the La protein domain. The effect on HCV translation is shown on the right side (+ meaning stimulation; – meaning reduction). Picture taken from Niepmann, 2013 (Niepmann, 2013).

1.5 microRNAs

1.5.1 microRNA biogenesis and function

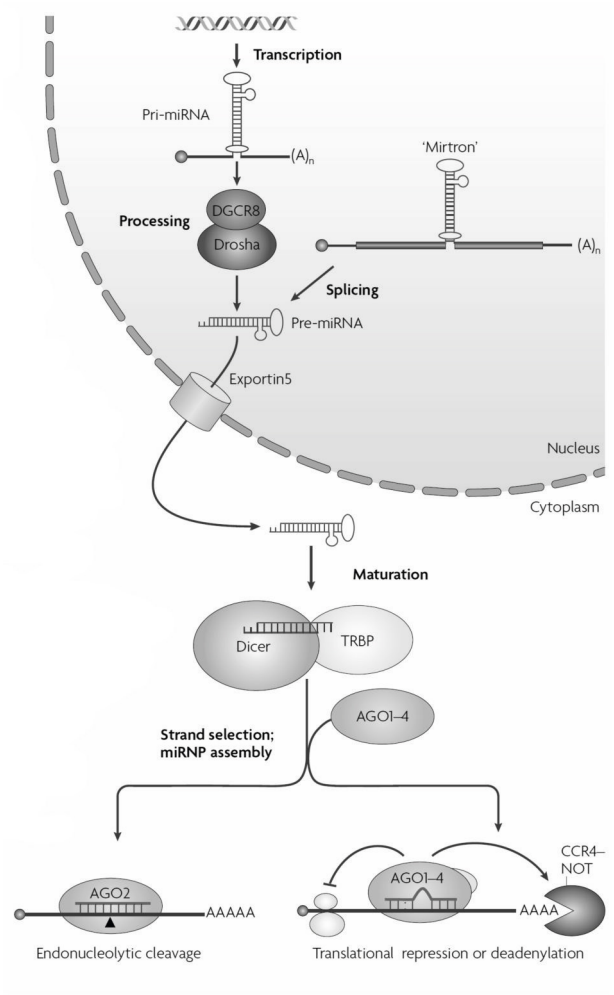

Figure 7: Biogenesis and processing of cellular microRNAs (miRs). miRs are transcribed in the nucleus by RNA polymerase II into primary-microRNA (pri-miR). This pri-miR is then processed down by the endonuclease Drosha/DGRC8, creating a hairpin containing precursor-miR. The pre-miR is subsequently exported into the cytoplasm by Exportin5/Ran-GTP and further cleaved by Dicer. This leads to the creation of a miR duplex, which is unwound by the Argonaute (Ago) proteins. The guide strand is kept in complex with Ago as part of the RNA-induced silencing complex (RISC) and used as a template to identify target mRNAs which, dependent on the matching of the guide strand, are either degraded or translationally repressed. Modified from Filipowitz et al., 2008 (Filipowicz et al, 2008)

microRNAs (miR) are 21-25 nucleotides long RNA molecules, which are transcribed in the nucleus by RNA Polymerase II as capped and polyadenylated primary (pri)-microRNAs. These pri-miRs are encoded either by protein coding intron sequences or by non-coding RNA exons and introns (Rodriguez et al, 2004; Saini et al, 2007). After transcription they are recognized by the microprocessor complex comprised of the RNase III endonuclease Drosha and the double strand RNA binding protein DGRC8, which cleaves them into a 70 nts long precursor miR (pre-miR) containing a hairpin structure, a 5’ phosphate and a 3’ two nucleotides overhang (Gregory et al, 2004). The pre-miR is transported into the cytoplasm by Exportin 5/Ran-GTP where it undergoes an additional cleavage by Dicer, leading to a double stranded about 22 nts long miR duplex containing a guide-strand and a passenger strand as well as two-nucleotides overhangs at the 3’-ends of both strands (Kim et al, 2009; Lund et al,

2004). Dicer can form a complex with TRBP a double-stranded RNA binding protein which also interacts with Ago proteins. Whereas TRBP is not required for pre-miR cleavage by Dicer it was shown to be necessary for the loading of the miR duplex to the Ago-proteins (Castanotto et al, 2007; Chendrimada et al, 2005; Haase et al, 2005). Dicer, TRBP and Ago2 form the minimal requirement for the RISC complex but it has also been shown that the interaction of other proteins like PACT is important for efficient RNA interference (Lee et al, 2006).
During the unwinding of the duplex miR, the guide strand stays in complex with Ago while the passenger strand is degraded. The decision which strand becomes the passenger and which the guide depends on the thermodynamical stability at the ends of the duplex miR. The strand with its 5'-end residing at the less stable end of the duplex becomes the guide (Khvorova et al, 2003; Rand et al, 2005; Schwarz et al, 2003).

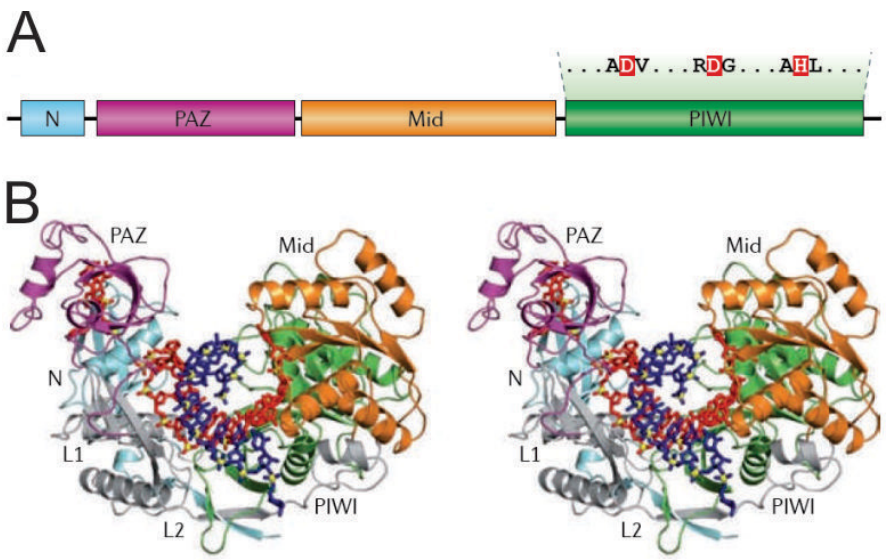

Figure 8: Argonaute protein structure. (A) Schematic depiction of the domains contained in Ago proteins. In red the common Asp-Asp-His motif of Ago proteins with 'slicer' activity is shown. (B) Structure of a Ago protein bound to miR (red) and target mRNA (blue). The PAZ (purple) and Mid (orange) domains interact with the 5'- and 3'-end of the miR, respectively. The PIWI domain interacts with the miR-mRNA duplex. Taken from Czech and Hannon, 2011 (Czech & Hannon).

The Ago protein family contains four members in humans Ago1 to 4, of which only Ago2 has endonuclease (called 'slicer') activity. The miR interacts with three domains in the Ago protein called PAZ, Mid and PIWI. The 3'-end of the miR resides in the Mid domain whereas the 5'-phosphate residue of the miR interacts with the PAZ domain. Figure 8 shows the structure of an Ago protein complexed with miR and target mRNA (Czech & Hannon, 2011)

It is well established that miRs take part in the post-translational repression of gene expression by hybridizing to mRNA and inhibiting their translation. To accomplish this miRs usually bind with their seed sequence to complementary sites in the 3'-UTR of the target mRNA. The seed sequence spans nucleotide 2 to 8 at the 5'-end of the miR, determining the miRs target range. The binding of the seed region does not have to be perfect and bulges in areas where nucleotides are not able to hybridize are common, broadening the possible spectrum of target mRNAs for the miR (Orom & Lund, 2010).
Depending on the matching of the miR seed sequence to the miR binding site and the proteins involved, the translational repression of the mRNA may follow different mechanisms. A perfect matching seed sequence leads to cleavage and subsequent degradation of the mRNA. In humans this process occurs only with the involvement of Ago2 since it is the only human Argonaute protein that carries a 'slicer' activity, enabling it to cleave the target strand. This 'slicer' activity is harbored in the PIWI domain of the Ago protein and often shows an Asp-Asp-His motif (Czech & Hannon, 2011). In contrast, formation of bulges during the binding of the miR leads to sequestration of the mRNA in so called processing-bodies (P-bodies) (Liu et al, 2005). P-bodies are sites in the cytoplasm of cells for storing not needed mRNAs that are either eventually released when the need arises or are degraded. The biogenesis of miRs is summarized in Figure 7.
In addition to translational repression of mRNAs miRs have been shown to stimulate translation of a target RNA (Henke et al, 2008; Orom et al, 2008; Vasudevan et al, 2007) by a yet unknown mechanism.

1.5.2 Function of miR-122

The single locus for miR-122 lies on chromosome 18 and is part of an exon of the non-coding hcr RNA (Chang et al, 2004). miR-122 is highly liver-specific where it represents more than 70 % of the total miR population (Lagos-Quintana et al, 2001) with about 66000 copies per cell in an adult liver (Chang et al, 2004).
It has been shown that miR-122 plays a role in the regulation of cholesterol biosynthesis (Esau et al, 2006; Krutzfeldt et al, 2005) as well as iron homeostasis by influencing the expression of hemochromatosis and hemojuvelin (Castoldi et al, 2011).
Furthermore, data suggests that in hepatocellular carcinoma (HCC) miR-122 levels are typically low (Kutay et al, 2006) which in most cases predicts a bad outcome for the patient (Coulouarn et al, 2009). It has been shown that in cancerous liver cells overexpression of miR-122 may have a tumor-suppressing effect (Bai et al, 2009).

1.5.3 Effect of miR-122 and Ago proteins on HCV

The effect of miR-122 on the HCV lifecycle caused a lot of controversy in the last couple of years. In 2005 Jopling and coworkers reported a direct interaction of miR-122 with the HCV 5'-UTR in the region of two predicted miR-122 binding sites located upstream of the HCV IRES. They observed that sequestration of endogenous miR-122 in cells transfected with a HCV-specific replicon RNA resulted in a reduction of HCV RNA abundance compared to cells where miR-122 was present. During the course of their experiments the authors could neither attribute this effect to HCV translation stimulation nor to the stabilization of the HCV RNA so they assumed that the increase in RNA abundance was due to a stimulation of RNA replication (Jopling et al, 2005).

These findings were questioned when Henke, Goergen et al. published a study in which they showed that HCV translation was positively influenced by miR-122. Their results also gave rise to the assumption that miR-122 might have more than one effect on the HCV RNA since the stimulating effect of miR-122 that they observed was more pronounced when using replication competent HCV RNA rather than the replication deficient RNA (Henke et al, 2008).

In the context of virus production it has been shown that a direct interaction of miR-122 with the HCV genome is necessary to gain infectious virus and that binding site 1, the one closer to stem loop I in the HCV 5'-UTR, seems to be more important in this context than site 2 (Jangra et al, 2010). The authors of this study also claimed that the stimulation of translation is a rather moderate effect of miR-122 and proposed a possible stabilization of the HCV genome or stimulation of RNA synthesis as the main effect of miR-122 binding to the HCV RNA.

The idea of stabilization of the HCV RNA was supported later by Shimakami et al. who have showed that the half-life of replication deficient HCV RNA is strongly increased in the presence of miR-122. They further showed that a non-translationally effective artificial Cap-structure at the HCV 5'-UTR mimics the role of miR-122, and that it protects the HCV RNA from degradation (Shimakami et al, 2012a).

Experiments on the miR-122-HCV RNA complex formation revealed that the binding of miR-122 to the two 5' binding sites is unusual. It seems that not only does the seed sequence of miR-122 bind to its respective counterparts on the HCV RNA, but also several nucleotides 3' of the miR-122 seed sequence hybridize to sequence elements upstream of the binding sites. In this context especially the nucleotides 15 and 16 of miR-122 seem to be crucial for the accumulation and stabilization of HCV RNA (Machlin et al, 2011; Shimakami et al, 2012b).

This mode of binding of miR-122 to the HCV RNA leads to the formation of a bulge and a tail region in the miR (Figure 9). Furthermore, the tail region is thought to play an important role in miR-122-dependent up-regulation of HCV RNA translation and accumulation (Machlin et al, 2011; Roberts et al, 2011).

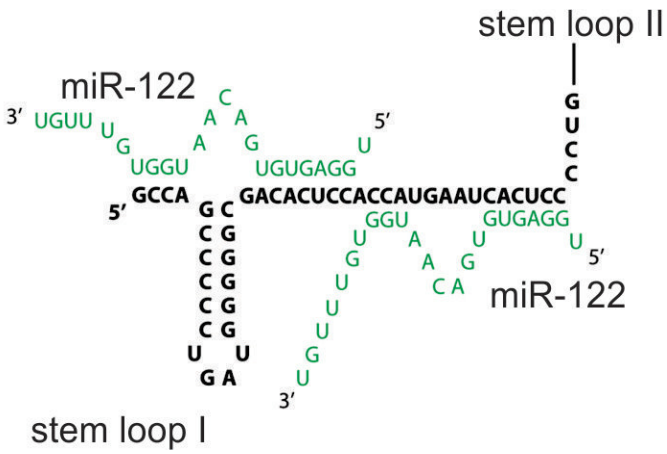

Figure 9: miR-122 forms an unusual RNA complex with the HCV 5'-UTR. Shown is the proposed binding behavior of miR-122 (green) to the HCV 5'-UTR (black). miR-122 binds not only with its seed sequence to the binding sites (ACACUCC / CACUCC) but also forms an interaction with three or four nucleotides 3' of the seed sequence, forming a bulge and tail region. Modified from Machlin et al., 2011 (Machlin et al, 2011).

Recent studies revealed that the Ago proteins also have a stimulatory effect on HCV translation, RNA accumulation and virus production which seem to be linked to the action of miR-122 on the HCV RNA (Machlin et al, 2011; Randall et al, 2007; Roberts et al, 2011; Wilson et al, 2011). It is hypothesized that Ago delivers miR-122 to the HCV RNA as part of a miRNP effector complex. In fact, another recent study published in 2012 by Shimakami and coworkers, showed a direct interaction of Ago2 and to a lesser degree Ago1 with the HCV RNA in a miR-122-dependent manner (Shimakami et al, 2012a). The involvement of other components of RISC in the action of miR-122 and the Ago proteins on HCV remains unclear.

1.6 Aims of the Work

It is well established that Ago proteins have a positive effect on HCV replication (Machlin et al, 2011; Randall et al, 2007; Roberts et al, 2011; Wilson et al, 2011). Thus it was hypothesized that this effect of Ago is linked to the stimulation of HCV RNA accumulation and translation displayed by miR-122. The main goal of this body of work was to investigate whether Ago proteins directly interact with the 5'-UTR of the HCV RNA and if this binding would be miR-122 dependent, by using an Ago protein-specific co-IP assay. Furthermore, this method was used to explore if the highly conserved miR-122 binding site in the variable region of the HCV 3'-UTR is accessible for miR-122-dependent Ago binding.

In addition, the role of spacing between miR-122 binding sites in the 5'-UTR and the IRES as well as the function of the two miR-122 binding sites was addressed. Sequence analysis of several HCV sub-types showed that the distance between the miR-122 binding sites in the 5'-UTR and the IRES is highly conserved. It was assumed that miR-122 recruits a microribonucleoprotein (miRNP) complex the miR-122 binding sites in the HCV 5'-UTR, which is able to interact with the translation initiation machinery bound by the IRES and thus stimulates HCV translation. Thus, mutants were created that carry several nucleotides long insertions in between the IRES and the miR sites and it was tested whether those insertions impair translation stimulation by miR-122.

Next, the individual effect of the two miR-122 sites in the 5'-UTR on the HCV RNA was explored. It has been shown that both replication and translation of the HCV RNA can be stimulated by miR-122 (Henke et al, 2008; Jopling et al, 2005). This gave rise to the question whether both miR sites present in the 5'-UTR contribute equally to these effects or if both sites perform separate tasks. To address this question one mutant in which both miR-122 binding sites can be addressed separately by using two different artificial miRs was created.

Finally, the role of miR-122 in protection of the HCV RNA from degradation was explored. Therefore, a mutant in which the miR-122 sites are masked in a stem loop rendering it unable to interact with miR-122 was produced. This mutant was used in time course assays to see if its reporter activity diminishes more quickly than the activity of the wild type HCV RNA. The reporter activity is a direct measure of RNA abundance and thus was used as an indicator of RNA degradation over time.

2 Results

2.1 Establishing an anti-Ago – HCV RNA co-immunoprecipitation

At the beginning of this work it was known that microRNA-122 (miR-122) enhances the replication of HCV, but the exact mechanism accounting for this effect remained unclear. Jopling and coworkers claimed that miR-122 directly elevates the production of new genomes (Jopling et al, 2005), while results from the Niepmann group showed that miR-122 also stimulates HCV RNA translation (Henke et al, 2008), thereby not excluding additional modes of action. The current general opinion by now is that both of these effects are most likely due to the protection of the HCV RNA from degradation by miR-122 (Jangra et al, 2010; Shimakami et al, 2012a; Shimakami et al, 2012b).
The identification and characterization of cellular proteins involved in the stimulating effect of miR-122 is important to generate a comprehensive model of how miR-122 enhances HCV replication. Since only double stranded miR-122 showed an effect in the cellular context (Goergen & Niepmann, 2012) it was assumed that a protein complex might be involved in the unwinding of the miR-122 duplexes and delivering the guide strand to the site of action. The most likely candidates to accomplish this task are the proteins of the Argonaute (Ago) family. The four members of this protein family, Ago1 to Ago4, recognize and unwind micro-RNA duplex precursors, which are then used to specifically target certain cellular mRNAs.
To identify the Ago proteins associated with the HCV RNA in the presence of miR-122 an anti-Ago protein HCV RNA co-immunoprecipitation (co-IP) was established.

2.1.1 Testing of the co-IP components

Because Ago2 is the most abundant Argonaute in HeLa cell lysate, making 60 % of the total Ago proteins (Petri et al, 2011), it was chosen for the co-IP experiments. Firstly a highly specific anti-Ago2 antibody for the anti-Ago protein - HCV RNA co-IP was needed, preferably one that has been already used for an immunoprecipitation of Ago2. Thus it was decided to try the rat-anti-Ago2 antibody clone 11A9 that was used by Rüdel and coworkers (Rüdel et al, 2008). This antibody was tested in a Western Blot assay, using HeLa cell lysate (Figure 10). In the beginning non-purified antibody from hybridoma supernatant (kindly provided by G. Meister, Figure 10, left lane) was used, later the 11A9 became also available from Sigma Aldrich as a

purified antibody (Figure 10, right lane); the usage of either antibody is indicated. Results obtained from Western Blots using both of the anti-Ago2 11A9 antibodies show only one specific band, representing Ago2, at about 100 kDa with no detectable background in HeLa lysate. Thus there is no cross reaction of these antibodies with unrelated HeLa cell proteins.

The reason to favor HeLa cells above the human hepatoma cell line HuH-7 is that HeLa cells show no detectable levels of endogenous miR-122 (Henke et al, 2008) that might lead to false positive results in the following co-IP assays.

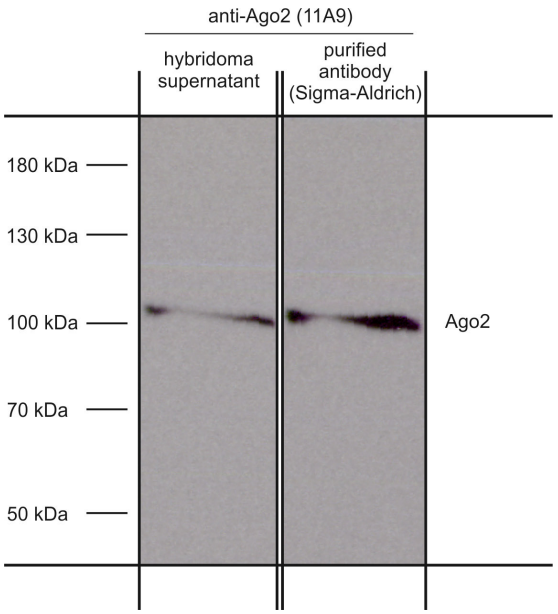

Figure 10: Western Blot using two different anti-Ago2 11A9 antibody preparations. HeLa cell lysate was separated on an SDS - 8 % polyacrylamide gel and blotted on a PVDF membrane. The left blot was stained using a rat-anti-Ago2 antibody clone 11A9 provided as hybridoma supernatant (dilution 1:50). The right blot was stained using the same anti-Ago2 antibody provided as purified solution (dilution 1:1000). As secondary antibody a goat-anti-rat antibody specific for the IgG light chain and coupled to peroxidase was used (dilution 1:20000).

Since the concentration of the 11A9 antibody in the hybridoma supernatant was unknown, a Dot Blot assay was carried out to approximate the binding capacity of the antibody to the magnetic beads that were to be used. It was decided to use protein G magnetic beads, since protein A does not bind rat IgG. Therefore 5 µl of the protein G magnetic beads (as provided by supplier, NEB) were rotated for 1 hour at 4 °C in the presence of varying amounts of hybridoma supernatant. The results indicate that the best ratio to obtain beads saturated with antibody is 5 µl of beads complemented with 15 µl of supernatant. This ratio results in a good binding of antibody to the beads (Figure 11, lower panel) and a low amount of unbound antibody in the supernatant (Figure 11, upper panel).

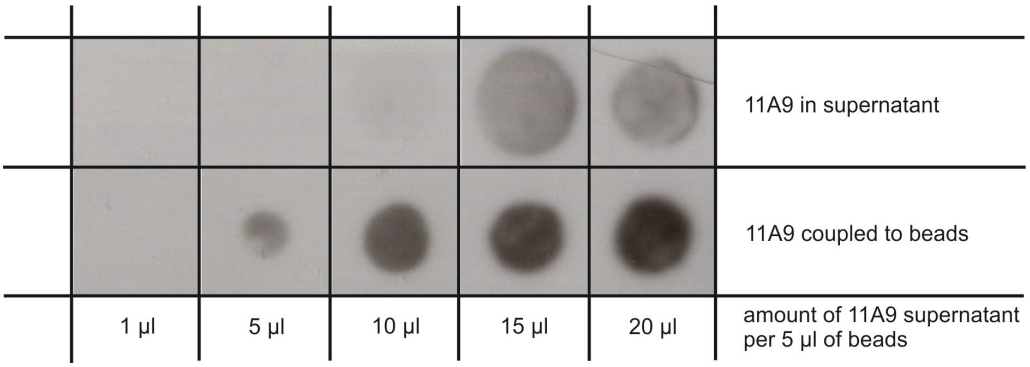

Figure 11: Titration of 11A9 antibody versus magnetic beads. 5 µl of magnetic protein G beads were incubated with varying amounts of rat-anti-Ago2 11A9 hybridoma supernatant. The beads-bound antibody and the residual antibody in the supernatant were blotted on a PVDF membrane and stained with a goat-anti-rat peroxidase (POD) secondary antibody (dilution 1:10000).

The next step was to find out how efficiently the antibody binds Ago2 protein during an immunoprecipitation. Therefore, four 9 cm dishes of approximately 80 % confluent HeLa cells were lysed and pooled to a final volume of 800 µl. The pooled lysate was pre-cleared at 4 °C for 1 h using non-coupled protein G beads (25 µl beads per 200 µl lysate). The pre-cleared lysate was then was divided into four samples at 200 µl, each representing a 9 cm dish into which different amounts of fresh beads and anti-Ago2 11A9 antibody were added (at a constant ratio of 15 µl antibody per 5 µl of beads). The samples were rotated for 2 h at 4 °C. The beads were subsequently washed and cooked for 5 minutes in SDS-sample buffer. Finally a Western Blot assay was performed.

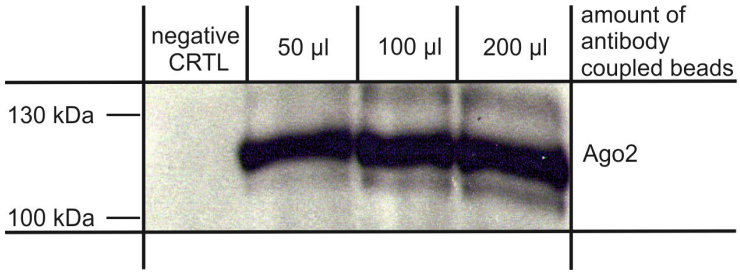

Figure 12: Titration of antibody coupled magnetic beads versus HeLa cell lysate. 200 µl cell lysate obtained from one 9 cm dish of ~80 % confluent HeLa cells was rotated for 2 hours at 4 °C with different amounts of magnetic protein G beads and rat-anti-Ago2 11A9 hybridoma supernatant. As a negative control 200 µl beads without antibody were used. After washing, the beads were cooked with SDS-sample buffer and the supernatant was separated on an 8 % SDS-polyacrylamide gel. Finally, the gel was transferred to a PVDF membrane. The rat-anti-Ago2 antibody clone 11A9 provided as hybridoma supernatant was used as a primary antibody (dilution 1:50). The secondary antibody used for staining was a goat-anti-rat POD (dilution 1: 20000).

The results indicate that optimal pull-down of Ago2 is achieved by using 100 µl of antibody-coupled beads, using 200 µl of beads and antibody results only in a marginal increase in protein pull-down efficiency (Figure 12).

Summarizing the previous results, it seems that for one 9 cm tissue culture dish with ~80 % confluent HeLa cells one should use 100 µl of the magnetic protein G beads complemented with 300 µl of the rat-anti-Ago2 11A9 antibody to obtain optimal results.

2.1.2 Anti-Ago2 - HCV RNA co-IP with following reverse transcriptase - PCR

Having done the preliminary experiments, the next question was whether the HCV RNA could be pulled down along with Ago2 in a miR-122 dependent manner. Therefore, a co-immunoprecipitation protocol was employed using reverse transcriptase - RCR (RT-PCR) to detect the co-precipitated RNA.
The two miR-122 binding sites in question are located in the 5'-UTR of the HCV RNA genome, upstream of the IRES element. To cover this region two primers were designed for RT-PCR that produce a fragment 245 nucleotides (nts) in length. The forward primer covers the loop of stem loop I and reaches across the first miR-122 binding site, while the reverse primer is located slightly upstream of the 3'-end of stem loop III (Figure 13).

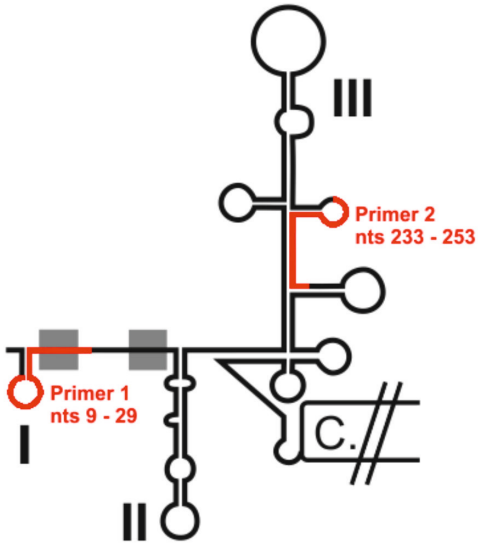

Figure 13: Localization of RT-PCR primers in the HCV 5'-UTR. Shown is a schematic depiction of the HCV 5'-UTR and parts of the core protein coding region. Indicated are the relative positions of the two RT-PCR primers (red). Forward primer 1 (RT-HCV pos. 9 - 29) spans from nucleotides 9 - 29, covering part of stem loop I and reaching into the first miR-122 binding site. Reverse primer 2 (RT-HCV pos. 233 – 253) spans nucleotides 233 through 253 and thus covers parts of stem loop III. The expected fragment produced by these primers is 245 nts in length.

For the co-IP HCV-SIN RNA was *in vitro* transcribed using a double stranded DNA template generated by PCR from the pHCV-SIN plasmid. The HCV-SIN RNA comprised a small in-frame linker sequence of 96 nts consisting of the part of the

Core coding sequence necessary for IRES formation and the 5'-part of the firefly luciferase open reading frame, flanked by the HCV 5'- and 3'-UTR.

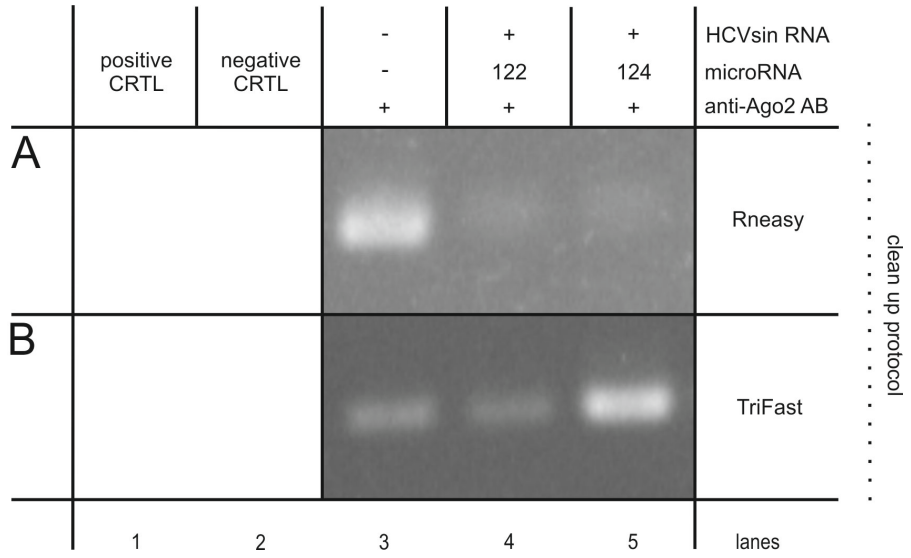

Figure 14: Results of two different co-IP experiments with subsequent RT-PCR. HeLa cells were transfected with HCV-SIN RNA together with either miR-122 or miR-124. After 4 h the cells were lysed and used in an anti-Ago2 immunoprecipitation for 2 h, using anti-Ago2 11A9 antibodies from supernatant coupled to magnetic protein G beads. The beads were washed and the co-precipitated RNA was released from the proteins and used in an RT-PCR. Given are two different experiments using two different RNA release and cleanup protocols.

The *in vitro* transcription was carried out at 37 °C in the presence of T7 RNA polymerase. HeLa cells, seeded on 9 cm-dishes, were subsequently transfected with HCV-SIN RNA and lysed after 4 h. Following the immunoprecipitation protocol described before the lysates were pre-cleared with native beads. After pre-clearing beads and anti-Ago2 11A9 hybridoma supernatant were added and the samples were rotated at 4 °C for 2 h. The Ago2-bound RNA was then extracted from the beads and purified following the specifications of the Qiagen RNeasy RNA clean-up Kit using a buffer containing guanidine thiocyanate and β-mercaptoethanol. The cleaned RNAs were then used in a RT-PCR assay and the products were then separated on an agarose gel and stained with ethidium bromide.

Unfortunately, the results obtained with this method were not convincing (Figure 14 A). The sample in which no microRNA was present shows a strong band, both samples with miR-122 or miR-124, respectively, show very faint bands. If Ago2 would bind miR-122 independently all samples should show the same outcome. Thus it was assumed that the bands were unspecific background. To make sure that those artifacts were not due to varying RNA recovery from the column-based RNA clean-up it was decided to use the phenolic peqGOLD TriFast™ solution from peqlab to detach the RNAs from Ago2. In the following, the RNA was precipitated with

Isopropanol. However, this approach was also found to be insufficient to avoid unspecific background (Figure 14 B).

2.1.3 Attempts to improve RT-PCR detection of HCV RNA

Since the previous experiments showed high amounts of unspecific products it was decided to check if this background might stem from DNA contamination in the samples that might have been introduced during the experimental procedure. To ensure the exact length of the 3'-end of the transfected RNA a DNA template was created by PCR from the plasmid pHCV-SIN and used for *in vitro* transcription. Both the template and the plasmid are possible sources of contamination during RT-PCR. The exact way of how this DNA might be carried into the samples is not clear, either it was residual DNA from the *in vitro* transcription that was still mixed with the RNA or it could also be possible that the used co-IP buffers contained traces of the pHCV-SIN plasmid. To detect and remove both possible contaminations a DNase I digest as well as a DNA test PCR were introduced into the work flow. The primers for the test PCR were the same as the ones used for template production and thus should be able to detect both, the DNA template and the plasmid (Figure 15).

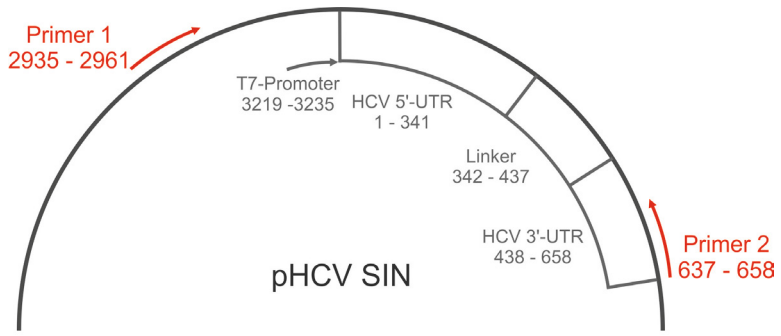

Figure 15: Primer positions for the DNA contamination control PCR in pHCV-SIN. Shown are the relative positions of the two primers (red arrows) in the pHCV- SIN plasmid. Primer 1 (HCMV-4986 for) reaches from nucleotide 2935 – 2961, primer 2 (3X rev) covers the nucleotides 637 – 658. The arrows indicate the direction of the primers. Together both primers produce a fragment of 959 nts which is equivalent to the DNA template for the in vitro RNA synthesis.

Applying these changes, samples were treated with DNase I for 1 h after release and isopropanol precipitation of the RNA. Subsequent purification was carried out following the TriFast protocol. These steps were repeated at least twice before the samples were tested for DNA contamination. If this test for the presence of DNA was positive, the procedure of DNase digest and clean-up was repeated until PCR showed no DNA background, and only then the samples were used in RT-PCR. The last row of Figure 16 gives an example of a test PCR without DNA background. The

implementation of these changes in the protocol at first had promising results (Figure 16 C), showing a single band only in the sample containing miR-122. Unfortunately, these results were not reproducible (Figure 16 D).

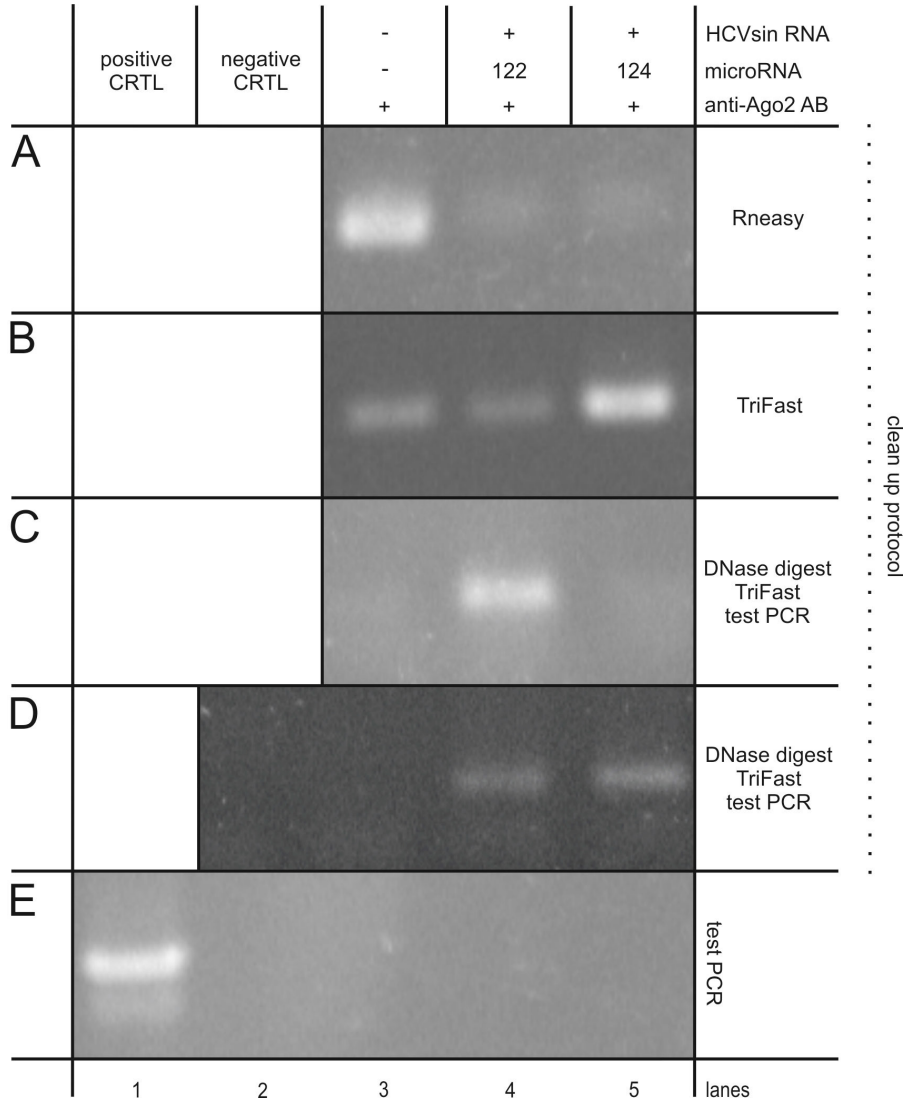

Figure 16: Results of different co-IP experiments with subsequent DNA test PCR and RT-PCR. HeLa cells were transfected with HCV-SIN RNA together with either miR-122 or miR-124. After 4 h the cells were lysed and used in an anti-Ago2 immunoprecipitation for 2 h, using anti-Ago2 11A9 antibodies from supernatant coupled to magnetic protein G beads. The beads were washed and the co-precipitated RNA was released from the proteins and used in an RT-PCR. Given are four different experiments using three different RNA release and cleanup methods. The lowest panel gives an example of the test PCR used to detect DNA contaminations arising from either the pHCV-SIN plasmid or the DNA template used to synthesize the transfected RNA. As a positive control (CRTL) 10 ng of pHCV-SIN plasmid was used, the negative CRTL consisted of double distilled and autoclaved water.

In total the co-IP experiments using RT-PCR as a readout system did not work out in these experiments. All experiments showed either high unspecific background or low reproducibility. Since DNA contamination does not seem to be the issue it was

assumed that the amount of RNA recovered after multiple DNase I digest and clean-up rounds was too low and variable to give reliable results. To avoid the necessity for multiple clean-up rounds of the RNA and for PCR amplification, it was decided to change the readout from RT-PCR products to radioactively labeled RNA which could be directly analyzed on a gel after detachment from Ago2 protein.

2.1.4 Anti-Ago2 - HCV RNA co-IP using radioactively labeled HCV RNA

Since the previous co-IP experiments with subsequent RT-PCR did not provide convincingly reproducible results, most likely due to too low RNA recovery from the clean-up steps, it was decided to circumvent the necessity for extensive RNA clean-up and amplification procedures by using radioactively labeled HCV RNA for a direct readout.

As before a double stranded DNA template was amplified from the pHCV-SIN plasmid and used in an *in vitro* transcription to produce HCV-SIN RNA. During the transcription process the RNA was labeled using ^{32}P-UTP.

HCV-SIN RNA was then transfected along with either miR-122 or miR-124 into 80 % – 90 % confluent HeLa cells grown on a 6-well plate. 6 h post-transfection the cells were harvested and lysed. For the co-IP the lysate was pre-cleared and the HCV RNA was subsequently co-precipitated with Ago2 using 100 µl of protein G magnetic beads coupled with anti-Ago2 antibody from hybridoma supernatant. After washing, the RNA was extracted from the beads following the RNeasy clean-up protocol.

The samples were then separated on a 10 % polyacrylamide gel in the presence of 7 M urea and the radioactive RNA was detected by autoradiography.

Figure 17 gives the results of two independent co-IP experiments. These experiments showed that sometimes there was a very small increase in band intensity favoring RNA recovery in the sample with miR-122 (Figure 17 A), but those results were also not consistently reproducible (Figure 17 B). Furthermore, for some of the experiments carried out following this protocol it was problematic to recover any RNA from the samples at all (data not shown).

In summary, the co-IP experiments using radioactively labeled HCV RNA as readout did not work out as expected and failed to provide constantly reliable results. The detected bands were most likely the result of unspecific background binding of radioactive RNA to the magnetic beads. This could also possibly explain the massive problems encountered during the co-IP assays with consecutive RT-PCRs for detection. These results led to the assumption that the readout was not the most pressing issue in the experiments, but rather the co-IP procedure itself was flawed.

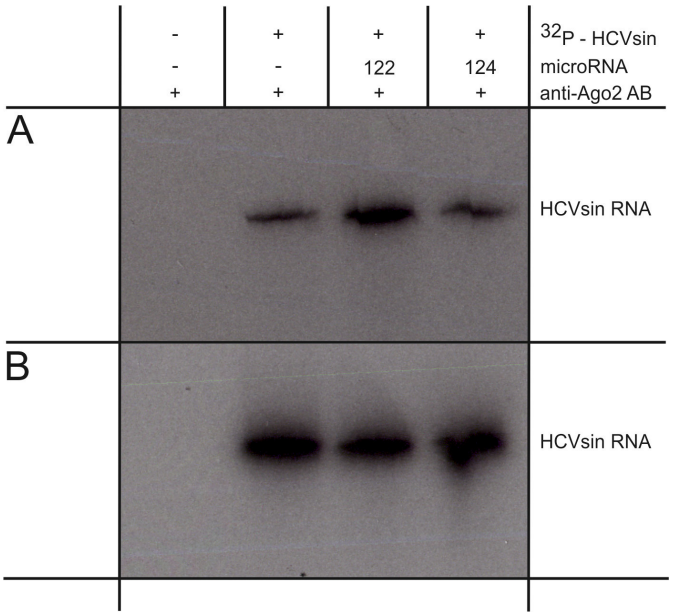

Figure 17: Results of two co-IP experiments using radioactively labeled HCV RNA. HeLa cells grown to ~80 % to 90 % confluency in a 6-well plate were transfected with radioactively labeled HCV-SIN RNA along with either miR-122 or miR-124 or no microRNA. The cells were lysed and the lysate was used in an anti-Ago2 immunoprecipitation. After pull-down the co-precipitated RNA was released from the proteins, cleaned and separated on a 10 % polyacrylamide gel with 7 M urea. Shown are the results of two experiments, following the same protocol.

Concerning the experiments so far it was assumed that the amount of RNA recovered from the samples was much too low for reliable results. Possible factors influencing the recovery of RNA were either the transfection efficiency or the co-IP itself. Factors influencing transfection efficiency would be the amount of cells and RNA, as well as the transfection time. In the previous assays 6-well plates with approximately 80 % confluent HeLa cells were used and transfected for 4 h with 1 µg of radioactively labeled RNA.

Regarding the co-IP some possible points that may need troubleshooting are the compositions of the lysis and washing buffers as well as the amount of washing steps. Furthermore, the transfection of RNA into the cells and the detachment of RNA from Ago2 protein might also be steps that need optimization.

Very helpful discussions with other scientist showed that some of these points are really critical. A breakthrough was finally accomplished when numerous changes from the Ago2-co-IP protocol published by Dr. Beitzinger from Prof. Meister's laboratory in Regensburg, Germany (Beitzinger & Meister, 2011), were implemented. Those changes concerned mostly the co-IP procedure itself by altering the lysis buffer, the amount of washing steps and the RNA detachment and clean-up protocol. All changes to the co-IP protocol are shown in detail below in Table 1.

Finally, the RNA used was changed from HCV-SIN RNA to a much smaller fragment comprising only the first 386 nucleotiodes (nts) of the HCV-SIN RNA covering the complete HCV 5'-UTR and parts of the luciferase open reading frame (ORF). That way it was expected to get a more favorable RNA fragment to transfection reagent ratio as well as less RNA degradation during the co-IP. Later this fragment was further shortened by 23 nts (see Figure 19).

	Previous co-IP protocol	New co-IP protocol
Cell amount	6-well plate with ~80 % HeLa cells	9 cm dish with ~80 % HeLa cells
RNA amount	1 µg radioactively labeled HCV-SIN RNA	3 µg radioactively labeled HCV 5'-UTR
RNA size	full HCV-SIN RNA	HCV-SIN RNA fragment comprising the first 386 nts (later the first 363 nts)
Transfection time	4 h	6 h
Lysis buffer	20 mM Tris-HCl, pH 7.5; 150 mM NaCl; 0.5 % Nonidet P-40; 2 mM EDTA; 0.5 mM DTT, 1 mM NaF; 1 mM Pefablock (Roche)	25 mM Tris-HCl, pH 7.5; 150 mM KCl; 0.5 % Nonidet P-40; 2 mM EDTA; 0.5 mM DTT
Preclearing of lysate	Yes	No
Antibody	Anti-Ago2 11A9 hybridoma supernatant provided by Prof. G. Meister	Anti-Ago2 11A9 purified antibody provided by Sigma Aldrich
coupling of Antibody to magnetic beads	during co-IP; rotated for 2 h at 4 °C	before co-IP; rotated overnight at 4 °C
co-IP time	2 h	3 h
Washing buffer	50 mM Tris-HCl, pH 7.5; 300 mM NaCl; 5 mM $MgCl_2$; 0.05 % Nonidet P-40	50 mM Tris-HCl, pH 7.5; 300 mM NaCl; 5 mM $MgCl_2$; 0.05 % Nonidet P-40
Washing steps	three repetitions at room temperature	at least four repetitions with washing buffer and one time with PBS at room temperature
RNA detachment from Ago2 and clean-up	RNeasy RNA clean-up protocol	Proteinase K digest for 15 minutes at 65 °C and phenol-chloroform extraction and ethanol precipitation

Table 1: Changes in the co-IP protocol after unsuccessful experiments with subsequent RT-PCR or autoradiography.

2.2 Anti-Ago2-HCV RNA co-IP using a HCV 5'-UTR RNA fragment

Applying the previously discussed changes (Table 1) to the co-IP protocol it was finally possible to achieve constantly reliable results.
In short, on the first day purified anti-Ago2 11A9 from Sigma Aldrich was pre-coupled to magnetic beads. On the second day 3 µg of the radioactively labeled short HCV 5'-UTR RNA fragments along with the same amount of either miR-122 or miR-124 were transfected for 6 h into HeLa cells, grown to approximately 80 % confluency on a 9 cm tissue culture dish. The cells were lysed and the lysate was mixed with the pre-coupled beads. 10 % of the lysate was saved as an input control. The co-IP was carried out for 3 h at 4 °C under constant rotation. Subsequently, the beads were washed and 10 % of the washed beads were stored for a Western Blot assay to detect the bound Ago2 protein. The rest of the sample and the input control were treated with Proteinase K, the RNA was purified by phenol-chloroform extraction and precipitated overnight with ethanol and sodium acetate. On the third day the precipitated RNA was separated on a polyacrylamide gel and exposed to an X-ray film.

2.2.1 Anti-Ago2-RNA co-IP using HCV 5'-UTR-386 RNA

Following the new co-IP protocol, small RNA fragments comprising the first 386 nts of the HCV-SIN RNA (HCV 5'-UTR-386) along with miR-122 or miR-124 were transfected into HeLa cells. In total four samples were produced (Figure 18 B), three including miR-122 and one including miR-124. After cell lysis the supernatant was used for co-IPs utilizing three different antibodies for the three miR-122 positive samples. The first sample was precipitated with an anti-eIF3a antibody. eIF3a is known to bind the HCV IRES microRNA independently and thus served as a positive control for the co-IP reaction. The second antibody targeted the FLAG epitope which does not naturally occur in cells. This sample served as a negative control to detect unspecific background. The last antibody was the anti-Ago2 11A9 antibody provided by Sigma Aldrich and was used for the last miR-122 sample as well as for the miR-124 sample.
As described before, for each sample RNA input and anti-Ago2 Western Blot controls were carried out to ensure an equal RNA transfection and Ago2 precipitation efficiency (Figure 18 A and C).

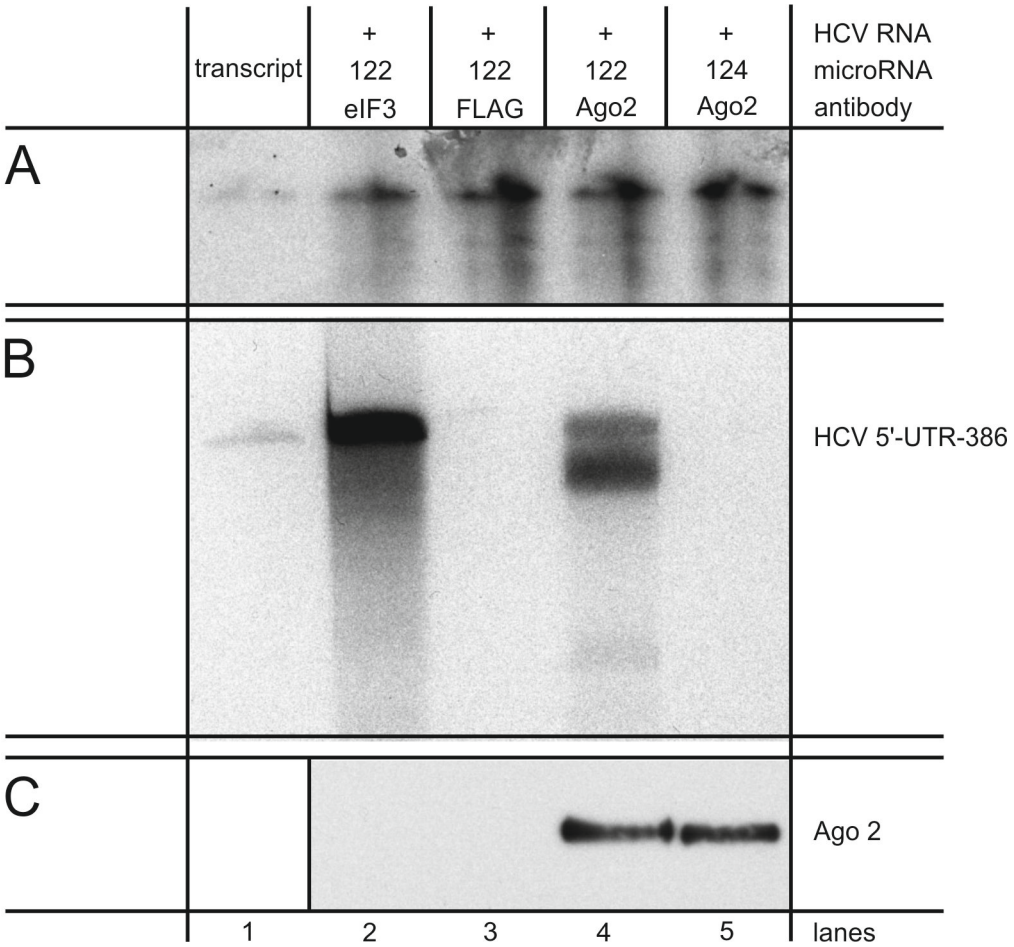

Figure 18: Anti-Ago2-RNA co-IP using HCV 5'-UTR-386 RNA. HeLa cells were transfected with radioactively labeled HCV RNA (HCV 5'-UTR-386) along with either miR-122 or miR-124 as a negative control. 6 h post-transfection, the cells were lysed, and 10 % of the lysate was saved as an input control (A). The rest of the lysate was used in anti-Ago2 immunoprecipitation. anti-eIF3a and anti-FLAG antibodies were used as positive and negative control. After washing 10 % of the magnetic beads used for the precipitation were stored for Western Blot analysis (C). The co-precipitated RNA was released from the proteins by Proteinase K digest, purified by chloroform - phenol extraction and precipitated with ethanol. The input controls were treated likewise. All RNAs were then separated on a 6 % Polyacrylamide gel with 7 M urea (B). Purified transcript was used as a marker for RNA integrity. The gel was subsequently dried and exposed to film.

The experiment shows a miR-122 dependent recovery of the HCV RNA (lane 4) with no binding detectable in the sample with miR-124. The input and Western Blot control show no significant differences in transfection and pull down efficiency among the samples. The input control was problematic, obviously the resuspension of the RNA pellet after ethanol precipitation was not satisfactory, but it was possible to solve this issue in later experiments by heating the RNA to 65 °C during the resuspension process (see Figure 20 A).

Based on these results it was concluded, that Ago2 binds to the HCV 5'-UTR in a miR-122 dependent manner. Surprisingly, during the experiments two very prominent bands appeared in the miR-122 sample precipitated with the anti-ago2 antibody of

the co-IP. One band representing the HCV RNA fragment at the same height as the transcript used for transfection (lane 1) and another slightly smaller. The occurrence of the lower band was reproducible during all the experiments even though it was highly variable in its intensity (data not shown). For the eIF3a sample that band was not detected so prominently but in this case also HCV 5'-UTRs were precipitated that have not yet been bound by miR-122 and Ago2. This gave rise to the question whether Ago2 induces cutting of the test RNA and if the cutting occurs at the 5'- or 3'-end of the RNA.

2.2.2 Anti-Ago2-RNA co-IP using HCV 5'-UTR-363 RNA

As described in the previous chapter the experiments showed two RNA bands after co-IP representing the HCV 5'-UTR-386 RNA, which suggests that the RNA was probably cut after transfection. The question was whether this cut occurred on the 5' or 3'-end of the RNA and if it was induced by the binding of Ago2 or an artifact coming from the method.
Since the HCV RNA fragment used so far also included part of firefly luciferase open reading frame the question arose, if this was the part that was degraded during the co-IP procedure. It was likely that this part of the RNA was not tightly packed with cellular proteins like the rest of the HCV 5'-UTR and thus was more accessible for RNases.

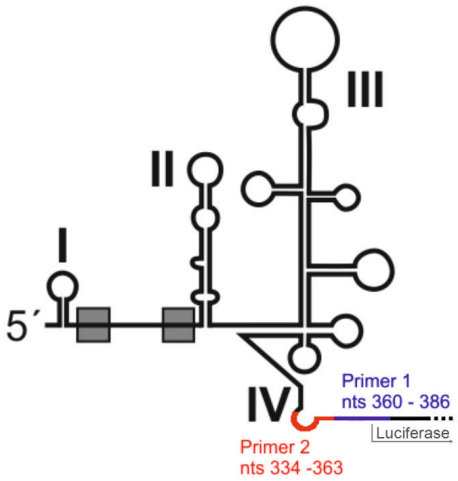

Figure 19: Positions of reverse primers for HCV 5'-UTR template production. Given are the positions of the two reverse primers (primer 1: pHCV-FL pos 360-386 (blue), primer 2: pHCV-FL pos 334 – 363 (red)) used to produce the DNA templates for the in vitro transcription of the HCV 5'-UTR-386 and HCV 5'-UTR-363 RNAs. The forward primer for these DNA templates was HCMV-4986 for.

To check this hypothesis a new RNA fragment, 23 nucleotides shorter than the HCV5'-UTR-368 RNA, was created reaching into stem loop IV of the IRES (Figure 19). This short RNA fragment, called HCV 5'-UTR-363, was transfected into HeLa cells and a co-IP assay was performed as described before (Figure 20).

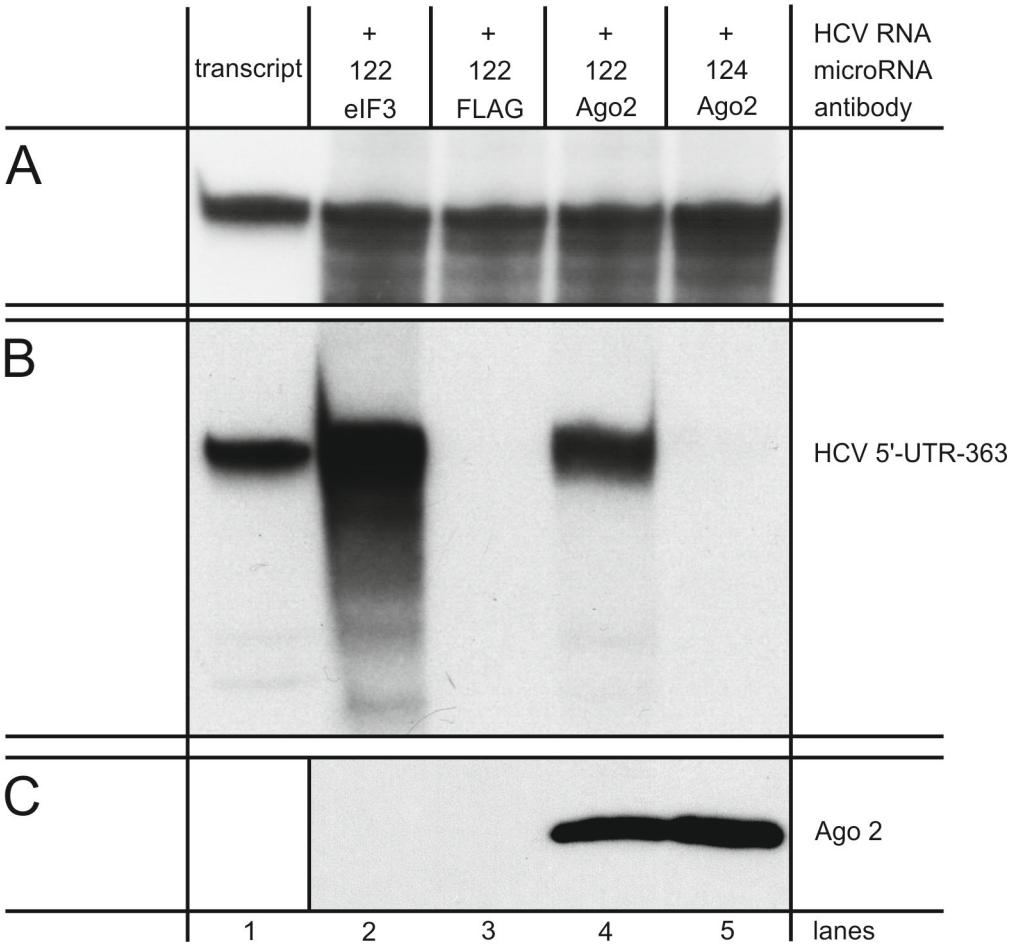

Figure 20: Anti-Ago2-RNA co-IP using HCV 5'-UTR-363 RNA. HeLa cells were transfected with radioactively labeled HCV RNA (HCV 5'-UTR-363) along with either miR-122 or miR-124, as a negative control. 6 h post-transfection, the cells were lysed and 10 % of the lysate was saved as an input control (A). The rest of the lysate was used in anti-Ago2 immunoprecipitation. anti-eIF3a and anti-FLAG antibodies were used as positive and negative control. After washing 10 % of the magnetic beads used for the precipitation were stored for Western Blot analysis (C). The co-precipitated RNA was released from the proteins by Proteinase K digest, cleaned by chloroform - phenol extraction and precipitated with ethanol. The input controls were treated likewise. All RNAs were then separated on a 6 % Polyacrylamide gel with 7 M urea (B). Purified transcript was used as a marker for RNA integrity. The gel was subsequently dried and exposed to X-ray film.

Using this shorter RNA fragment only one distinct band in the miR-122 sample (Figure 20 lane 5) was present. This led to the conclusion that the degradation of the HCV 5'-UTR-386 RNA occurred at the 3'-end of the fragment. Furthermore, it was concluded that the observed cutting of the RNA was not due to Ago2 binding, but rather it was an artifact that stems from a sequence stretch in the luciferase open reading frame, that is not tightly associated with protein during the co-IP.

2.2.3 co-IP assay of the HCV 5'-UTR using an anti-Ago1 antibody

Since miR-122 dependent binding of Ago2 to the HCV 5'-UTR was detected it was decided to test whether other members of the Argonaute protein family were able to bind to it as well. Ago1 was chosen as a new target since it is the second most abundant Ago protein in HeLa cell lysate, making up 22 % of the whole Ago protein population (Petri et al, 2011).

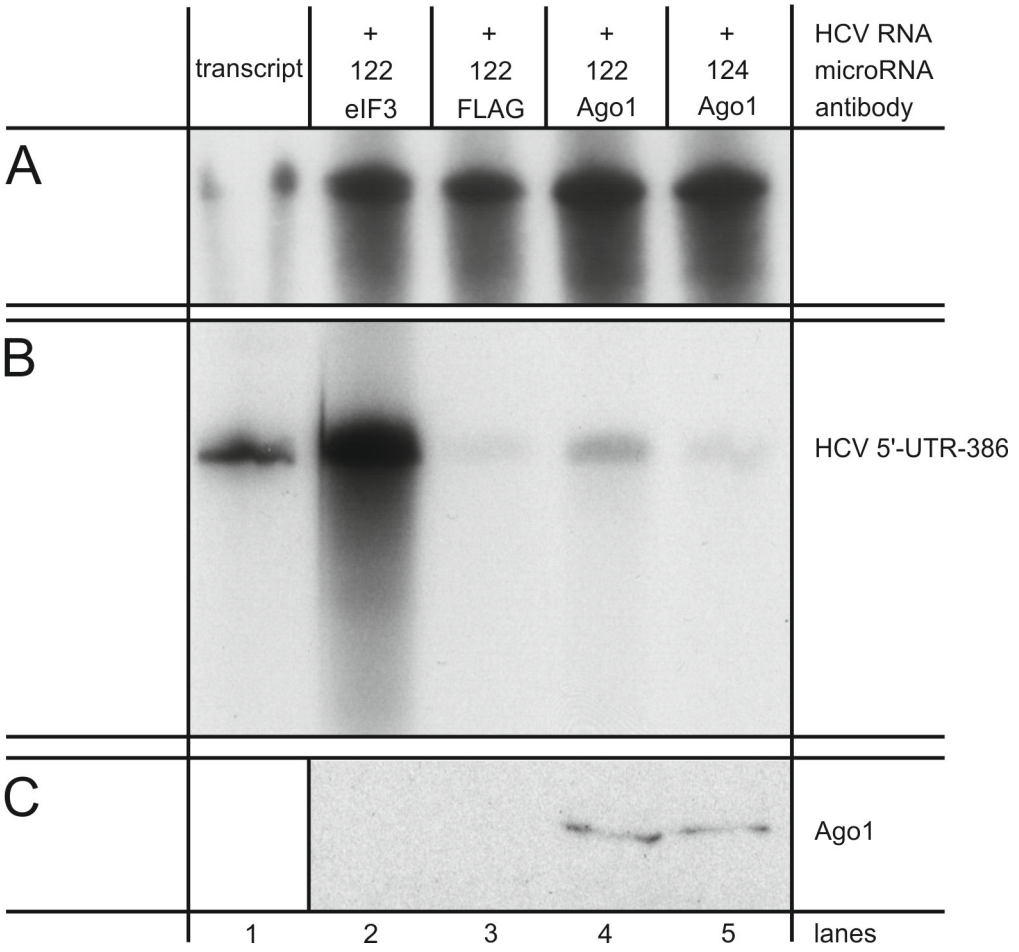

Figure 21: Anti-Ago1-RNA co-IP using HCV 5'-UTR-386 RNA. HeLa cells were transfected with radioactively labeled HCV RNA (HCV 5'-UTR-383) along with either miR-122 or miR-124, as a negative control. 6 h post-transfection, the cells were lysed and 10 % of the lysate was saved as an input control (A). The rest of the lysate was used in anti-Ago2 immunoprecipitation. anti-eIF3a and anti-FLAG antibodies were used as positive and negative control. After washing 10 % of the magnetic beads used for the precipitation were stored for Western Blot analysis (C). The co-precipitated RNA was released from the proteins by Proteinase K digest, cleaned by chloroform - phenol extraction and precipitated with ethanol. The input controls were treated likewise. All RNAs were then separated on a 6 % Polyacrylamide gel with 7 M urea (B). Purified transcript was used as a marker for RNA integrity. The gel was subsequently dried and exposed to X-ray film.

The co-IP was performed following the same protocol as before except that now the rat-anti Ago1 clone 4B8 antibody was used which is commercially available from Sigma Aldrich (Figure 21).
In those assays a miR-122 dependent association of Ago1 with the HCV 5'-UTR (lane 5) could be detected, even though the detected band appears to be much weaker than the one seen with Ago2. The explanation for this result might be the differences in Ago protein abundance as well as the quality of the two used antibodies. Looking at the Western Blot assay for the experiments with Ago2 and Ago1 it can be seen that the amount of precipitated Ago1 is much lower than the amount of precipitated Ago2, hinting to a significant difference in their protein binding affinity.
Thus it seems that both Ago1 and Ago2 are able to bind to the HCV 5'-UTR in a miR-122 dependent manner, but it is not possible to draw any conclusions concerning the stability or efficiency of that binding.

2.3 Creating a HCV 5'-UTR with separately addressable microRNA binding sites

The HCV 5'-UTR carries two binding sites for miR-122, one close to stem loop I, the other directly in front of stem loop II. Machlin and coworkers (Machlin et al, 2011) found evidence that not only the seed sequence of miR-122 binds to the HCV RNA but also three to four nucleotides further to the 3'-end of the microRNA might bind to the HCV RNA as well, thus upon binding the microRNA would form bulge and tail region. It was furthermore shown that this unconventional miR binding was necessary to stabilize the HCV RNA by possibly protecting it from degradation.
Those findings raised the question whether miR-122 could perform two different tasks in the HCV 5'-UTR, firstly maintaining HCV RNA integrity by protecting it from RNases and secondly recruiting cellular factors that influence HCV translation. Furthermore, it would be interesting to elucidate if both sites are necessary for both effects or if one site conveys only one effect.
Therefore, it was decided to mutate both miR-122 binding sites and additional binding areas in the HCV RNA, so that it would be possible to address them separately with two artificial microRNA. The sequences of the new mutated sites are given in Figure 22.

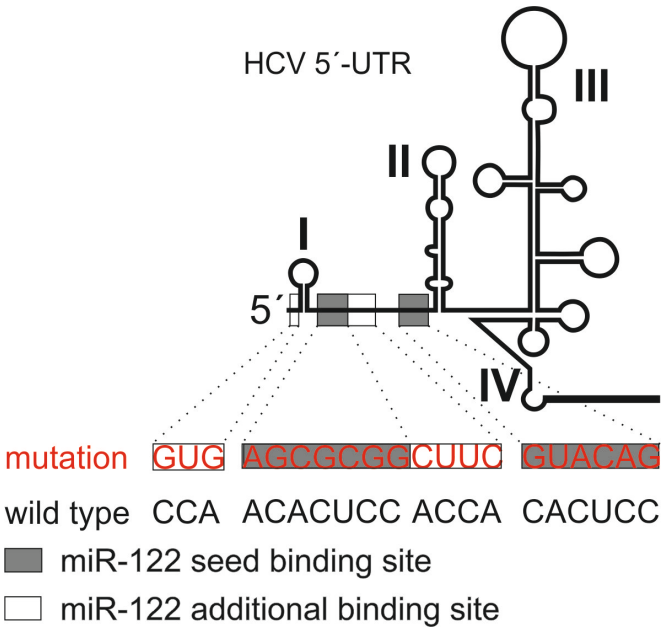

Figure 22: Schematic depiction of the HCV m1/m2 5'-UTR. Given are the sequences of the wild type and mutated m1/m2 HCV 5'-UTR and their relative position. Shown in grey are the mutations in the miR binding sites that match the miR-122 seed sequence. Mutations in the regions, which presumably bind to nucleotides in the 3'-region of miR-122 (Machlin et al, 2011) are highlighted in white.

The new sequences were introduced by a two-step mutagenesis PCR, which is described in detail in the method section. In short, at first two PRCs were performed, creating two DNA fragments carrying the desired mutations in the miR-site 1 and miR-site 2 (Figure 23 A). Both fragments overlap partially so they can serve as a template for the third PCR using the two outermost primers to fill in gaps and amplify the mutated insert which then can be cloned into the vector backbone (Figure 23 B).

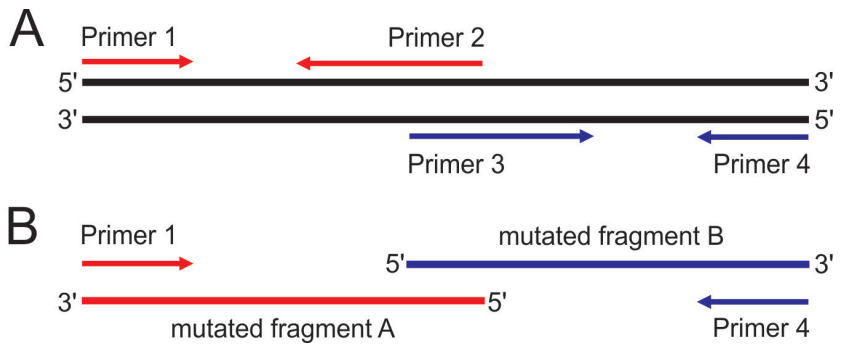

Figure 23: Model of the two-step mutagenesis PCR to create HCV m1/m2. In the first step the mutations were introduced by two separate PCRs using mutagenesis primers 1 and 2 for the first PCR and primers 3 and 4 for the second (A). The resulting DNAs from both PCRs partially overlap and can be used as a template for the third PCR (B) in which primers 1 and 4 are used to fill up the gaps and amplify the mutated final fragment.

The mutated HCVm1/m2 5'-UTR was cloned into the HCV-FL construct to replace the wild type HCV 5'-UTR and sequencing showed that the mutations were correctly introduced into the HCV sequence.

Before starting the final experiments, the secondary structure of HCVm1/m2 from the first nucleotide to the 3'-end of stem loop II was predicted. The result of this prediction is shown in Figure 24. Unfortunately, this test revealed a high probability that the mutations interfere with the natural folding of the HCV 5'-UTR, destroying stem loop I and II and masking the mutated miR-binding sites in newly formed stems. These results forced the cancellation of all experiments concerning this part of the project until a new clone is created and tested *in silico*.

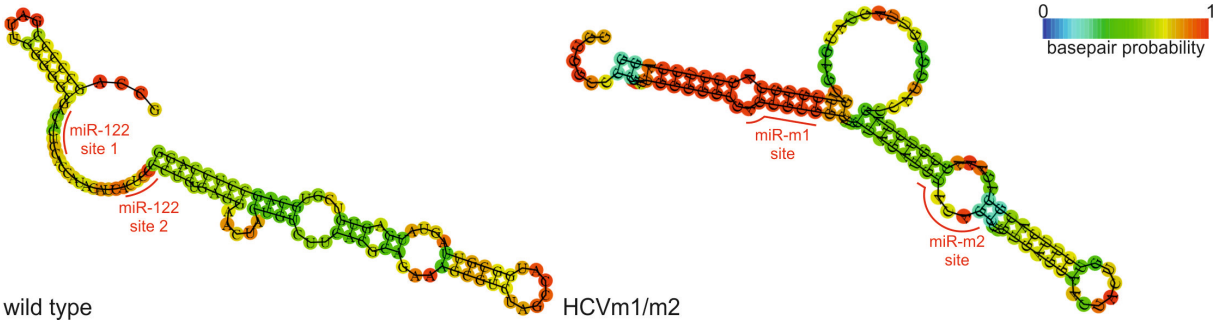

Figure 24: Secondary structure prediction of the wild type HCV 5'-UTR compared to the HCm1/m2 5-UTR. *In silico* model of the HCV wild type and HCV m1/m2 5'-UTRs including the sequence to the 3'-base of stem loop II. Given in red are the positions of the two miR-122 binding sites. Colors indicate base pair probabilities. The program used was provided online (http://rna.tbi.univie.ac.at/cgi-bin/RNAfold.cgi). The parameters applied were "minimum free energy and partition function", "no dangling ends energy", "Andronescu model, 2007" and "avoid isolated base pairs" at 37 °C.

2.4 Anti-Ago2-HCV RNA co-IP using HCV 3'-UTR RNA fragments

In addition to the two miR-122 binding sites in the 5'-UTR of the genome, HCV also carries one conserved potential binding site for miR-122 in the variable region of the 3'-UTR. So far it could not be shown that this site has any significant effect on HCV translation stimulation by miR-122 (Henke et al, 2008), neither have there been any reports of effects on replication for this site. It was decided to test whether this highly conserved site is used as a target for miR-122 and Ago2 binding.

2.4.1 Anti-Ago2 co-IP using a RNA fragment carrying only the HCV 3'-UTR

To test if Ago2 is also recruited to the HCV 3'-UTR it was decided to perform anti-Ago2-RNA co-IP assays using a RNA fragment derived from the pHCV 3'-UTR only plasmid, containing a small part of the luciferase ORF and the full HCV 3'-UTR. The protocol for those experiments was the same as for the 5'-UTR co-IP assays.
In three out for four experiments no binding of Ago2 to the HCV 3'-UTR, neither in the presence (Figure 25 B, lane 4) nor in the absence of miR-122 (lane 5), was detected.

In one case a very weak band in the miR-122 positive sample appeared with no background in the miR-124 sample. As a positive control (lane 2) an anti-PTBP1 antibody was used, since PTB was shown to strongly bind to the HCV 3'-UTR.
In summary, these data suggests that Ago2 does not significantly bind to the HCV 3'-UTR. This result was surprising due to the high degree of conservation and the positioning of the site. Since miR-122 forms an unusual complex at the HCV 5'-UTR, involving also sequence elements 5' of the miR-122 binding sites (Machlin et al, 2011) the question arose whether this might also be the case with the 3'-UTR.

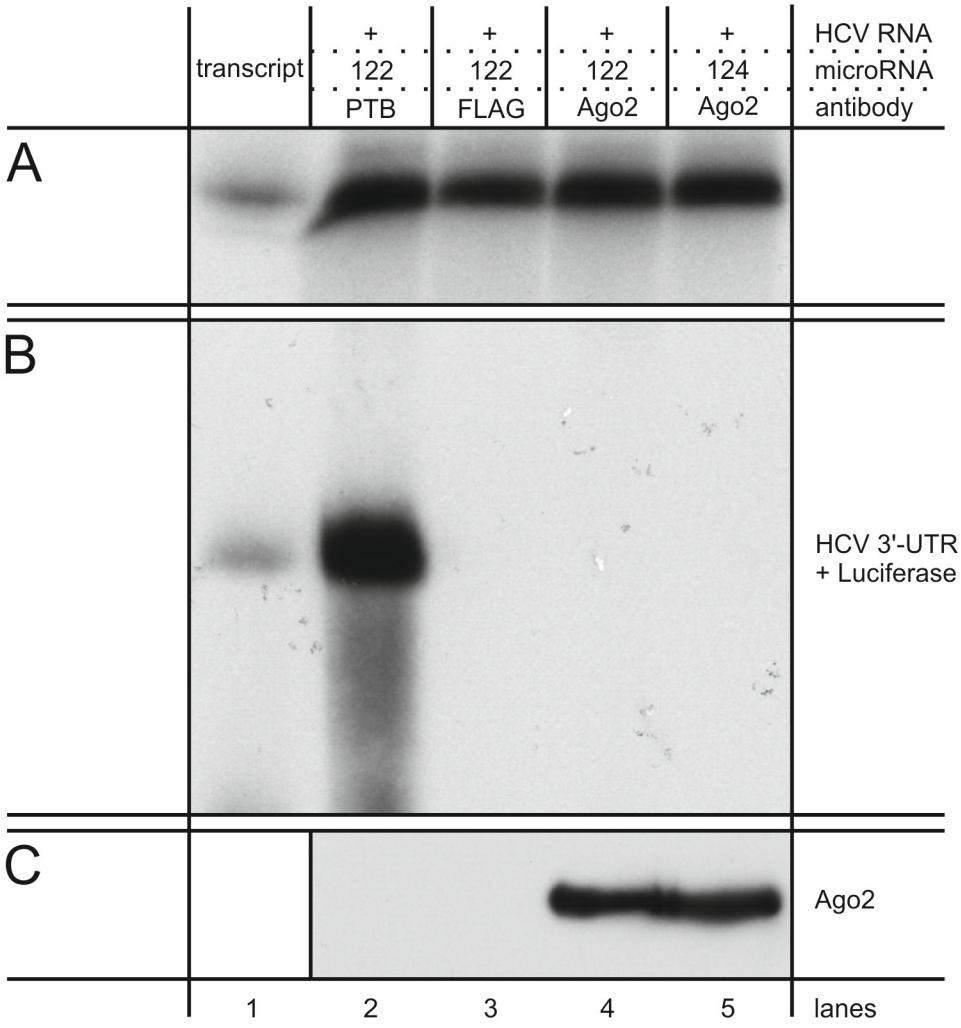

Figure 25: Anti-Ago2-RNA co-IP using HCV 3'-UTR with luciferase RNA. HeLa cells were transfected with radioactively labeled HCV 3'-UTRs including last 41 nts from the firefly luciferase open reading frame along with either miR-122 or miR-124, as a control. 6 h post-transfection, the cells were lysed and 10 % of the lysate was saved as an input control (A). The rest of the lysate was used in anti-Ago2 immunoprecipitation. anti-PTBP1 and anti-FLAG antibodies were used as positive and negative control. After washing 10 % of the magnetic beads used for the precipitation were stored for Western Blot analysis (C). The co-precipitated RNA was released from the proteins by Proteinase K digest, cleaned by chloroform - phenol extraction and precipitated with ethanol. The input controls were treated likewise. All RNAs were then separated on a 6 % Polyacrylamide gel with 7 M urea (B). Purified transcript was used as a marker for RNA integrity. The gel was subsequently dried and exposed to X-ray film.

2.4.2 Anti-Ago2 co-IP using a RNA fragment carrying parts of the NS5B ORF and the 3'-UTR

Machlin and coworkers (Machlin et al, 2011) showed that in order to have an effect miR-122 not only needs to bind to the target region of its seed sequence but also needs to bind certain nucleotides further upstream of the binding site, forming a bulge at not paired areas.

To see if there might be an additional binding area for miR-122 close to the 3'-UTR, for nucleotides of miR-122 not part of the seed sequence, a sequence comparison focusing on the 3'-end of the NS5B coding region was performed (Figure 26).

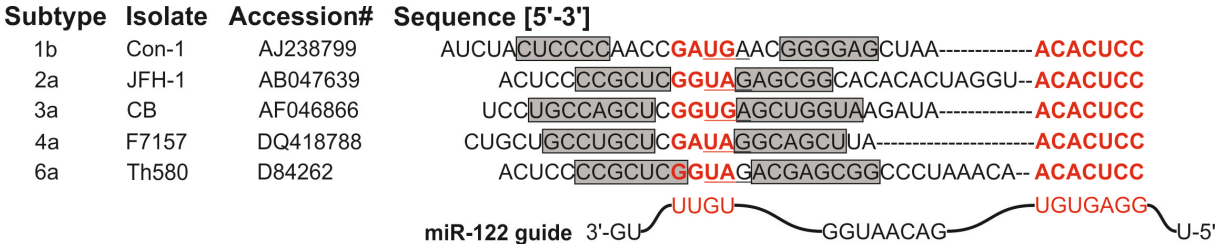

Figure 26: Sequence comparison of the 3'-End of NS5B and parts of the variable region of five different HCV subtypes. Shown are the sequences of five different HCV subtypes, including the last stem loop of NS5B and the predicted miR-122 binding site in the variable region. The areas that form a stem are marked in grey. Highlighted in red are the regions that might serve as a binding site and extended binding area for miR-122. The stop codon of the HCV ORF is underlined. Also shown are the nucleotides of the miR-122 guide strand that would be used for the interaction.

Interestingly four nucleotides were found (including two nucleotides of the stop codon) positioned in the non-paired region of a stem loop formed between the NS5B coding region and the variable region. These nucleotides might be able to pair with four nucleotides very close to the 3'-terminus of the miR-122 guide strand (Figure 26). The identified sequence stretch belongs to two different codons in the HCV genome, coding for arginine and the translation stop.

Subtype	Isolate	Accession#	Codons	
1b	Con-1	AJ238799	CGA	UGA
2a	JFH-1	AB047639	CGG	UAG
3a	CB	AF046866	CGG	UGA
4a	F7157	DQ418788	CGA	UAG
6a	Th580	D84262	CGG	UAG
		Aminoacid	ARG	**Stop**

ARG codons	Codon usage
CGA	10.9 %
CGG	20.1 %
CGC	18.3 %
CGU	7.9 %
AGA	21.2 %
AGC	21.5 %

Figure 27: Comparison of the last two codons of the NS5B coding region of five different HCV subtypes. Given are the last two codons of the NS5B coding region of five different HCV subtypes. Highlighted in red are the nucleotides that possibly pair with parts of the miR-122 3'-end. The right box shows all possible codons for arginine and the codon usage in human cells (recalculated from Spencer, 2012).

Arginine is coded by six different codons, these six codons vary quite significantly in their usage in human cells (Figure 27, right side). Strikingly, only two of the six possible codons are used for the arginine in the predicted stem loop. More interestingly these are not the codons that display the highest codon usage rate (Figure 27). This led to the assumption that not only the arginine is critical at this position of NS5B, but also the sequence by which it is coded.

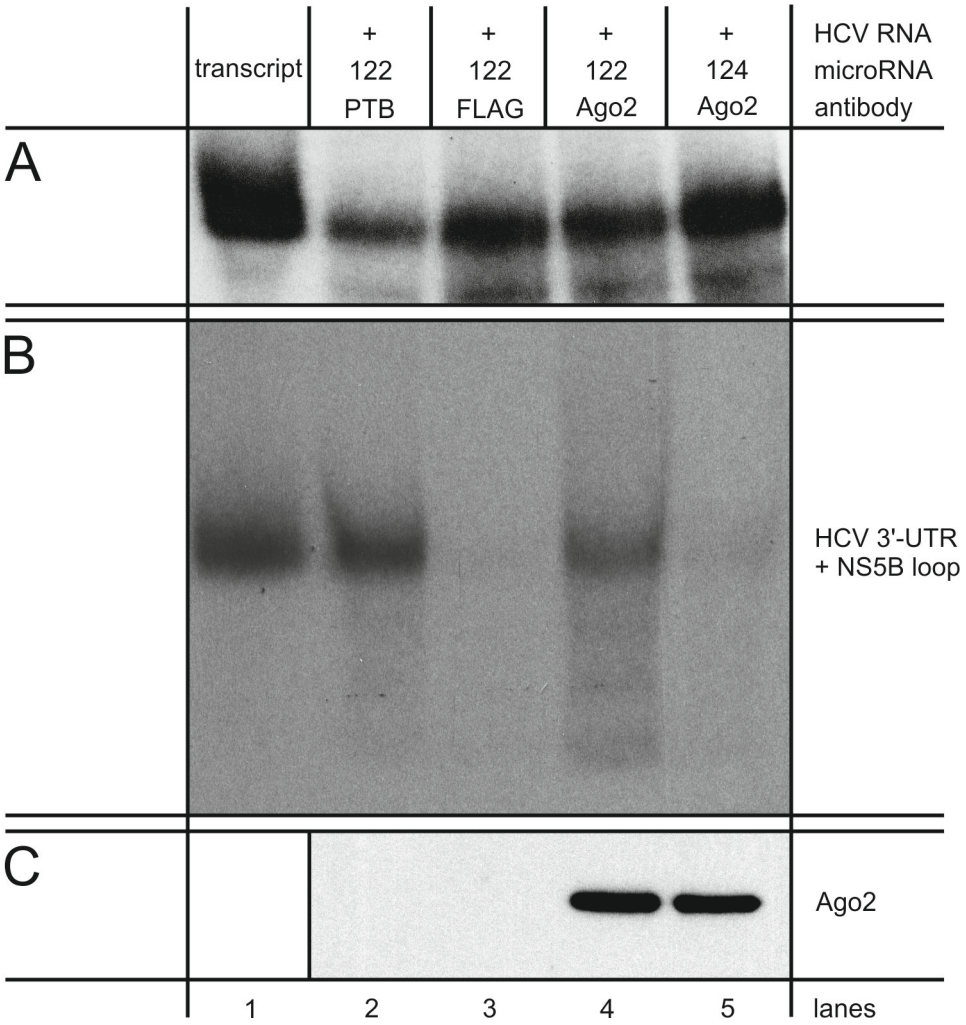

Figure 28: Anti-Ago2-RNA co-IP using HCV 3'-UTR + NS5B loop RNA. HeLa cells were transfected with radioactively labeled HCV 3'-UTRs including the last 18 nts of the HCV NS5B open reading frame along with either miR-122 or miR-124, as a control. 6 h post-transfection, the cells were lysed and 10 % of the lysate was saved as an input control (A). The rest of the lysate was used in anti-Ago2 immunoprecipitation. anti-PTBP1 and anti-FLAG antibodies were used as positive and negative control. After washing 10 % of the magnetic beads used for the precipitation were stored for Western Blot analysis (C). The co-precipitated RNA was released from the proteins by Proteinase K digest, cleaned by chloroform - phenol extraction and precipitated with ethanol. The input controls were treated likewise. All RNAs were then separated on a 6 % Polyacrylamide gel with 7 M urea (B). Purified transcript was used as a marker for RNA integrity. The gel was subsequently dried and exposed to X-ray film.

To test this hypothesis it was decided to repeat the previous experiment now using RNA comprising the HCV 3'-UTR and the last stem loop of the NS5B coding region. This RNA was transcribed from a DNA template generated from the pHCV-FL plasmid by using a primer which paired at the start of the HCV 3'-UTR and also carried a long non-pairing region including the T7-RNA polymerase promoter and the last 18 nucleotides of NS5B sequence.

The results of the experiments using this RNA construct are given in Figure 28. The experiment clearly shows a miR-122-dependent recruitment of Ago2 to the HCV 3'-UTR (Figure 28, lane 4).This led to the conclusion, that the predicted additional miR-122 binding region is really needed for efficient microRNA binding.

2.5 Creation and characterization of mutants carrying insertions between the miR-122 binding sites of the HCV 5'-UTR and the IRES

The HCV subtypes display a low variance concerning the spacing of structural elements that are important for translation. It seems that the miR-122 binding sites are positioned in a fixed distance relative to the IRES and it was wondered whether insertions between the IRES and the miR-122 binding sites might disrupt the stimulation effect of miR-122 on HCV translation. The hypothesis was that the fixed distance is necessary for proteins recruited by miR-122 to properly interact with the IRES elements or with the ribosomal subunits binding the IRES.

2.5.1 Insertion of nucleotides between the miR-122 binding sites and the IRES

Therefore mutants were created that carried insertions of either five, ten or twenty nucleotides (nts) in between the second miR-122 binding region and stem loop II which is the first stem loop belonging to the IRES.
The insertions were introduced via the Quick Chnage *in vitro* mutagenesis protocol. Two complementary mutagenesis primers that carried the desired insertion were used in the mutagenesis PCR, to amplify and mutagenize the pHCV-FL plasmid. The pHCV-FL construct that was used as a template was grown in Escherichia coli and thus was methylated by the Dam methylase. Using this fact it was possible to digest the initial template pHCV-FL in the PCR samples with the DpnI nuclease that only digests hemi-methylated DNA. The residual mutated DNA was subsequently transformed and amplified in bacteria. After small scale plasmid preparation (mini prep) the sequence of the three new plasmids, pHCV-FL 5nts, pHCV-FL 10nts and pHCV-FL stem, was confirmed by sequencing.

In silico analysis of the structure of the three mutants (Figure 29) revealed that the folding of the 5 nts insertion mutant was the same as the one of the wild type. For the 10 and 20 nts mutants it could be seen that the miR-122 binding sites were partially (in case of the 10 nts mutant) or even completely (in case of the 20 nts mutant) integrated in a newly formed stem loop covering most of the miR-122 binding sites. Therefore, the pHCV-FL 20nts mutant was renamed pHCV-FL stem.

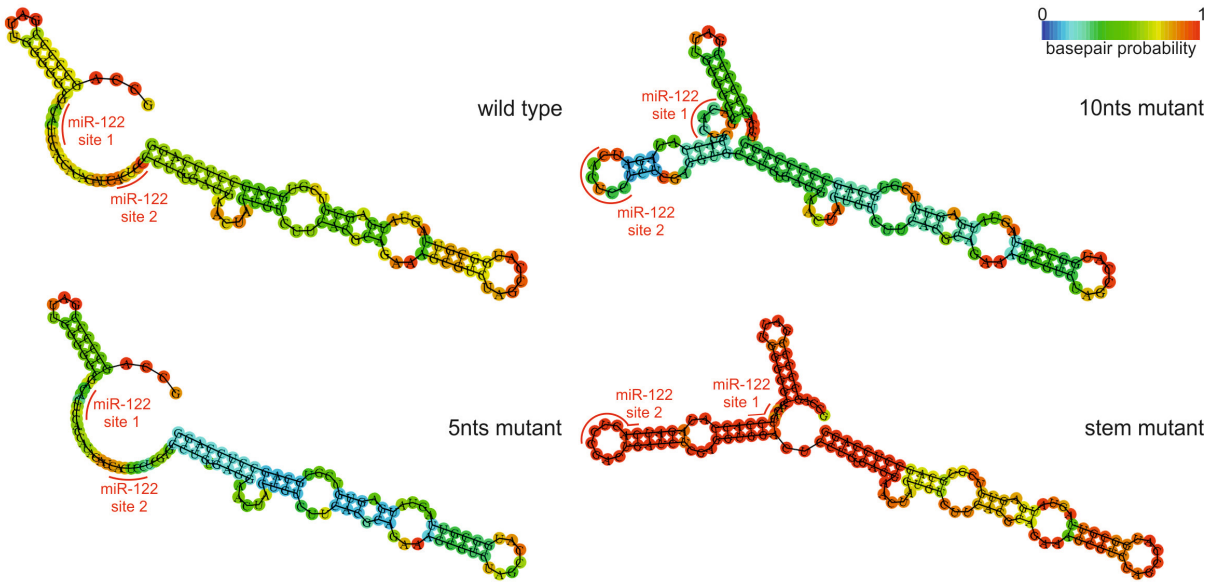

Figure 29: Predicted folding of the HCV insertion mutants. *In silico* model of 5'-UTR of the 5 nts, 10 nts and the stem mutant compared to the wild type. The prediction comprises all nucleotides from the start to the 3'-base of stem loop II. Given in red are the positions of the two miR-122 binding sites. Colors indicate base pair probabilities. Program used was provided online (http://rna.tbi.univie.ac.at/cgi-bin/RNAfold.cgi). The parameter given were "minimum free energy and partition function", "no dangling ends engery", "Andronescu model, 2007" and "avoid isolated base pairs" at 37 °C.

2.5.2 Testing of the insertion mutants in a luciferase reporter assay

Despite the partial masking of the miR-122 sites in a stem loop for some of the mutants, it was decided to test them in a luciferase reporter assay to see if their translation was stimulated by miR-122. Those reporter assays were carried out by Florian Giering (Giering, 2013). After *in vitro* transcription, HuH-7 cells grown in a 24-well tissue culture plate were transfected with 400 ng of the respective mutant RNA along with either 400 ng of miR-122 or miR-124. For normalization a capped and polyadenylated Renilla-luciferase expressing RNA was co-transfected. Cells were harvested and lysed 4 h post-transfection and the lysate was used in a luciferase assay.

As shown in Figure 30 B both the 5 and 10 nts insertion mutants are stimulated by miR-122 to a level similar compared to the wild type (Figure 30, B). This indicates that neither the insertion nor the partial masking of the miR-122 binding sites in case of the 10 nts mutant impaired miR-122 binding and a possible interaction of recruited proteins with the IRES. The stem mutant however proved to not be affected by miR-122. Thus leading to the assumption that miR-122 is not able to disrupt the stem loop and bind to its binding sites on the HCV mutant RNA. To explore this possibility it was decided to perform an anti-Ago2 a co-IP assay with this mutant and compare it to the wild type HCV RNA. If miR-122 is really not capable to bind to the stem mutant anymore the HCV stem RNA should not be coprecipitated along with Ago2.

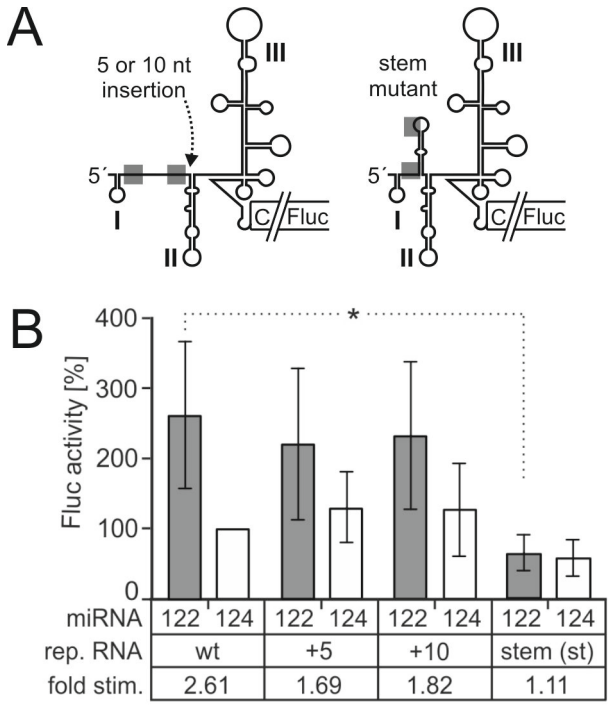

Figure 30: Luciferase assay using HCV mutants carrying insertions between the second miR-122 binding site and the IRES. (A) Schematic drawing of the 5 and 10 nts mutants and the stem mutant. The 5 and 10 nts mutants both carry an insertion of either 5 or 10 nucleotides, between the second miR-122 binding site and the IRES. The stem mutant carries an artificial stem loop which comprises both miR-122 binding sites and thus renders them unable to hybridize with miR-122. miR-122 binding sites are highlighted in grey. (B) HuH-7 cells were transfected with a RNA reporter construct comprised of the open reading frame of the Firefly-luciferase (Fluc) and either the wild type (wt) HCV 5'-UTR or one of the mutations shown in (A). Furthermore, ectopic miR-122 (or miR-124 as a control) and a capped and polyadenylated Renilla-luciferase (RLuc) RNA were added to the samples. The RLuc values were used to normalize the measurements from the FLuc RNAs. The readouts from samples including the wild type 5'-UTR and miR-124 were set to 100 % and all other values were calculated relative to this sample. P-values were calculated using a student's t-test (* = p< 0.05). Experiments were carried out by Florian Giering. Modified from (Conrad et al, 2013).

2.5.3 Anti-Ago2 co-IP assay using the 5'-UTR of the HCV stem mutant

Finding out that the translation of the HCV stem mutant RNA is not stimulated by miR-122 it was decided to check whether miR-122 is even able to bind to this mutant. Therefore, an anti-Ago2 co-IP assay was performed to see if Ago2 is also recruited to the HCV stem 5'-UTR in the presence of miR-122. It was reasonable to assume that if miR-122 was not able to bind to the mutant, Ago2 binding would be impaired as well.

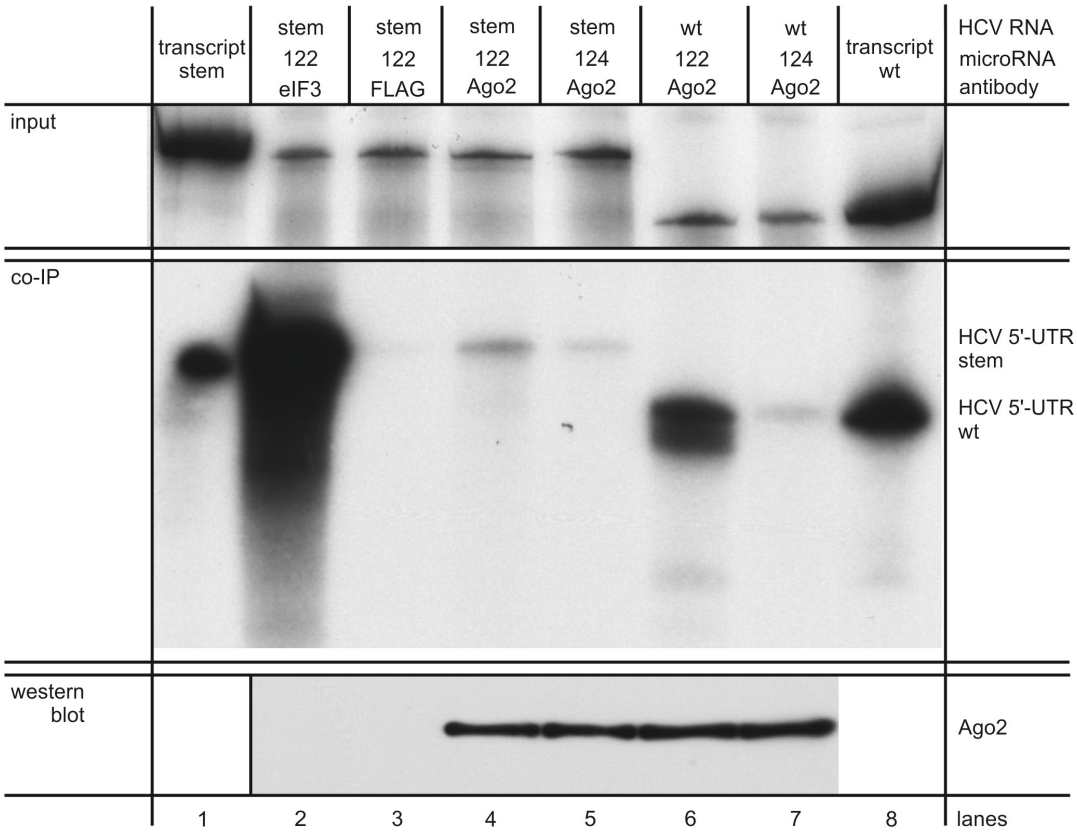

Figure 31: Anti-Ago2-RNA co-IP using HCV 5'-UTR stem mutant RNA. HeLa cells were transfected with radioactively labeled HCV 5'-UTRs carrying the stem mutation along with either miR-122 or miR-124, as a control. Furthermore, a set of cells was transfected with wild type HCV 5'-UTRs and either miR-122 or miR-124, to directly compare the binding efficiencies of the wild type RNA versus the stem mutant RNA. HCV 5'-UTR-386 RNA was used as wild type control. 6 h post-transfection, the cells were lysed and 10 % of the lysate was saved as an input control (A). The rest of the lysate was used in anti-Ago2 immunoprecipitation. anti-eIF3a and anti-FLAG antibodies were used as positive and negative control. After washing 10 % of the magnetic beads used for the precipitation were stored for Western Blot analysis (C). The co-precipitated RNA was released from the proteins by Proteinase K digest, cleaned by chloroform - phenol extraction and precipitated with ethanol. The input controls were treated likewise. All RNAs were then separated on a 6 % Polyacrylamide gel with 7 M urea (B). Purified transcript was used as a marker for RNA integrity. The gel was subsequently dried and exposed to X-ray film.

Following the previously described protocol for a Ago2 specific co-IP RNA fragments were used that comprised the 5'-UTR of the stem mutant and compared to the wild type HCV 5'-UTR in the presence or absence of miR-122 (Figure 31).
The results clearly show that for the stem mutant RNA the binding of Ago2 is massively impaired (Figure 31, B, lane 4) compared to the wild type (Figure 31, B, lane 6). The band derived from the sample containing miR-122 and the mutant RNA is just insignificantly stronger than the background in the samples containing the control miR-124 (Figure 31, B, lanes 5 and 7).
Therefore, it was concluded that masking the miR-122 binding sites in the stem loop interferes with Ago2 binding to the HCV 5'-UTR most likely by preventing miR-122 to interact with its complementary sequences.
Now that a translationally competent mutant RNA that does not efficiently bind miR-122 was available, it was wondered whether this mutant would also show a lower stability in cells compared to the wild type HCV RNA in presence of miR-122.

2.5.4 Comparison of the stability of the wild type HCV RNA and the HCV stem mutant

Shimakami and coworkers proposed that the stimulation of HCV translation and replication by miR-122 could be a secondary effect. They assumed that the main impact of miR-122 is to protect the HCV RNA from degradation (Shimakami et al, 2012a). To check this hypothesis HuH-7 cells were transfected with reporter constructs coding for the firefly luciferase (Fluc) that carried either the wild type HCV 5'-UTR or the stem mutant 5'-UTR. Additionally ectopic miR-122 or miR-124 was added. The cells were harvested after 3, 6 or 9 h after transfection and a luciferase assay was performed.
The Fluc measurements from this experiment should directly represent the amount of RNA present in the cells. On the one hand, if miR-122 protects the HCV RNA from degradation a slower decrease in luciferase activity in the wild type 5'-UTR with miR-122 (wt/miR-122) sample should be detected compared to the samples containing the stem mutant or miR-124. On the other hand, a higher luciferase activity in the wt/miR-122 sample compared to the wild type with miR-124 with nearly the same relative drop in luciferase activity over time would argue for a stimulating effect of miR-122 on HCV translation.
Figure 32 shows the results of this assay. All values were calculated relative to their respective 3 h measurement which was set to 100 % for each kind of sample. In the presence of either microRNA, the stem mutant showed an average decrease of about 53 % in the two 3 h intervals between the first and the last time point. The sample containing wild type and miR-124 (wt/miR-124) lost in average 36 %

luciferase activity in a 3 h period, showing a shallow decline of about 27 % in the first 3 h and a steeper one of about 45 % in the second 3 h. The difference in the decline between the stem mutant and the wt/miR-124 sample is supposedly due to the fact that HuH-7 cells have a natural background of miR-122 which can bind to the wild type HCV RNA in the wt/-miR-124 sample. The wt/miR-122 sample however shows no loss in reporter activity between the first two time points, but later a decrease of about 35 % could be detected. These results show that the interaction of miR-122 and its binding sites really seems to contribute to HCV RNA stability over time.

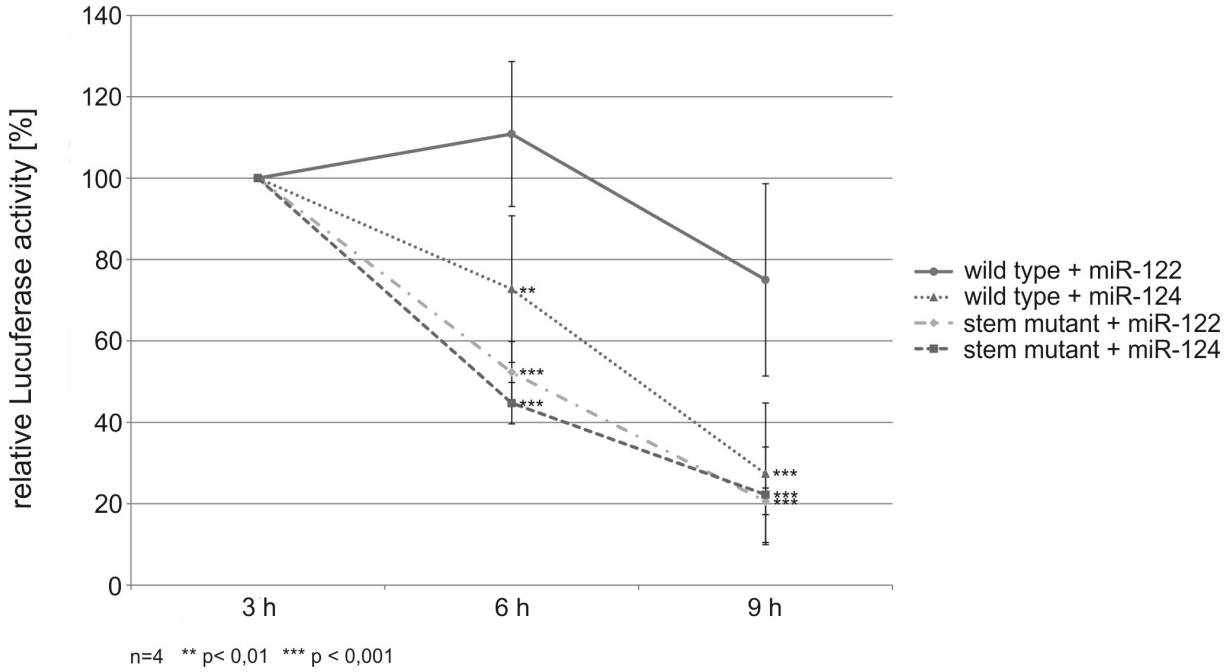

Figure 32: Stabilization effect of miR-122 on HCV RNA. Huh- 7 cells were transfected with either wild type HCV FL or the stem mutant RNA along with miR-122 or miR-124, respectively. After 3, 6 and 9 hours the cells were harvested and lysed. The lysate was then used to perform a luciferase assay. The 3 hour values for all RNA combinations were set to 100 %. For statistical purpose a two-way ANOVA with a 95% confidence interval was carried out using PRISM 5.0.

Nevertheless, this effect does not seem to be the only effect of miR-122. After normalization of all measurements relative to the 3 h time point of wt/miR-122 (Figure 33) there is a significant gap between the luciferase activities of wt/miR-122 and the wt/miR-124 at the 3 h time point. According to Shimakami et al. the half-life of HCV RNA in presence of miR-124 is 3.6 h (Shimakami et al, 2012a). Since equal amounts of RNA were transfected into the cells, this difference of translation efficiency of about 70 % between the wt/miR-122 and the wt/miR-124 sample at the 3 h time point can't be explained by RNA decay alone. Such a large difference in luciferase activity short after transfection is most likely explained by differences in translation efficiency

of the respective RNA invoked by miR-122. Thus it seems that besides stabilizing the HCV RNA, miR-122 also stimulates translation efficiency.

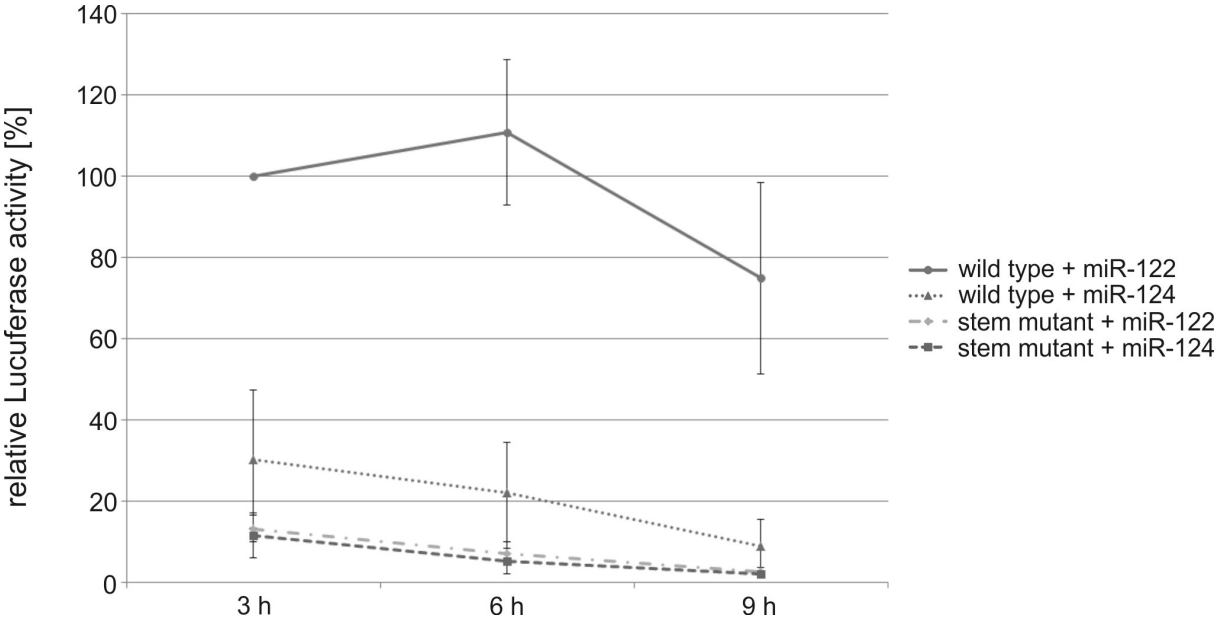

Figure 33: Translational effect of miR-122 on HCV RNA. Huh- 7 cells were transfected with either wild type HCV FL or the stem mutant RNA along with miR-122 or miR-124. After 3, 6 and 9 hours the cells were harvested and lysed. The lysate was then used to perform a luciferase assay. All values were normalized relative to the measurement of wild type with miR-122 sample at the 3 h time point.

3 Discussion

The data presented in this work show that microRNA-122 (miR-122) recruits proteins of the Argonaut (Ago) family, Ago1 and Ago2, to the HCV 5'-UTR. For Ago2 it could also be shown that this protein interacts with a binding site in the variable region (VR) of the HCV 3'-UTR in a miR-122-dependent manner. This binding however, seems to be dependent not only on the binding of the seed sequence of miR-122 but also on the hybridization of nucleotides close to the 3'-end of the miR to the HCV RNA. Four nucleotides were identified in the HCV NS5B coding region that seem to be necessary for efficient miR-122 binding to the HCV 3'-UTR. Furthermore, the experiments presented in the previous chapters give hint that miR-122 binding to the HCV RNA has two effects. Firstly, the binding of miR-122 seems to prolong the half-life of HCV RNA most likely by protecting it from degradation. Secondly, the data shows that upon binding miR-122 enhances HCV translation efficiency. Thus, it seems that there are at least two different mechanisms in place through which miR-122 is able to positively influence the life cycle of HCV.

3.1 Recruitment of Ago proteins to HCV RNA

The purpose of this work was to investigate whether Ago proteins directly bind to HCV RNA in a microRNA-122 dependent manner. For Ago1 and Ago2 a miR-122-dependent recruitment to the HCV 5'-UTR could be established, for Ago2 also a miR-122-dependent binding to the HCV 3'-UTR was found. These data correlate with the findings of Shimakami and coworkers (Shimakami et al, 2012a), who also found an association of these two Ago proteins with the HCV RNA in the presence of miR-122. Furthermore, it was shown that Ago1 seems to associate less efficiently with HCV RNA than Ago2, which is supported by Shimakami et al. (Shimakami et al, 2012a). However, neither my experiments nor their data give any explanation whether the difference in Ago protein binding to HCV RNA is due to a lower abundance of Ago1 compared to Ago2 in the cells or if this is a specific effect. Roberts and coworkers showed that knock out (KO) of Ago1 or Ago2 had a strong negative effect on HCV translation stimulation by miR-122, with only a slightly stronger influence seen with the Ago2 KO (Roberts et al, 2011). It is possible that Ago1 plays a more important role in the action of miR-122 on HCV translation than the binding experiments suggest.

In addition, Roberts et al. showed that KO of all four Ago proteins resulted in only a small additional decrease of HCV translation stimulation by miR-122 compared to

Ago2 KO alone (Roberts et al, 2011). In comparison, Randall et al found that KO of Ago4, which is the least abundant Ago protein in humans, had the biggest negative impact of all the Ago proteins on HCV RNA abundance and production of infectious virus (Randall et al, 2007). Based on the latter findings, it could be speculated that different Ago proteins influence the HCV lifecycle at several stages. Whether the influence of Ago proteins on HCV replication is directly or indirectly mediated by other miRs is not yet clear.

3.2 Effect of miR-122 binding to HCV RNA

The data presented in this work suggests that HCV RNA is stabilized by the binding of miR-122. It was found that the wild type HCV RNA reporter construct, in the presence of a control miR or a mutant deficient for miR-122 binding, display a much more pronounced drop in luciferase activity over time than the wild type HCV reporter RNA in the presence of miR-122. Using the luciferase activity as a direct measure of RNA abundance in transfected cells, it could be shown in a time course assay that the average decrease in luciferase activity for the mutant HCV RNA construct in the presence of miR-122 or miR-124 and for the wild type HCV reporter RNA in the presence of miR-124 ranges around 35 - 53 % in a 3 h period. For the wild type HCV RNA in the presence of miR-122 no reduction in luciferase activity was found during the first 3 h and only a 35 % decrease in reporter activity in the second 3 h interval. These data correlate well to the calculated half-life ($t_{1/2}$) of HCV RNA of approximately 3.6 h in the presence of miR-124 published by Shimakami et al. (Machlin et al, 2011; Shimakami et al, 2012a). However, Shimakami and coworkers calculated the half-life of HCV RNA in presence of miR-122 to be 5.3 h. This result differs a bit from the data shown in this work where a decrease of luciferase activity of about 35 % in 9 h was measured. This discrepancy might be due to the differences in the testing system. Shimakami et al. checked directly for HCV RNA abundance, whereas measuring luciferase activity as an indicator for RNA stability could proof to be less accurate in the long run due to possible differences in $t_{1/2}$ of the HCV RNA and the luciferase.

Due to the stabilization of HCV RNA by miR-122, it was assumed that miR-122 might act as a homologue of a Cap-structure on HCV RNA protecting it from degradation (Roberts et al, 2011; Shimakami et al, 2012a). Adding a translationally inactive non-methylated guanosine Cap analog to the 5'-end of the HCV RNA Shimakami et al. did not see any difference in stability in the presence or absence of miR-122. Furthermore, they were not able to detect stimulation of translation by miR-122 for this RNA.

Contrary to the findings by Shimakami and coworkers (Shimakami et al, 2012a), the data presented here in this work suggests that there might also be a moderate effect of miR-122 on HCV translation. A difference of approximately 70 % in translation efficiency in the sample with wild type HCV RNA and miR-122 and the sample with miR-124 was found. Since this difference occurs only 3 h after transfection, RNA degradation cannot be the exclusive explanation for it. It can rather be assumed that this difference occurs due to variations in the inherent translation efficiency of the HCV reporter RNA in the presence of miR-122 compared to miR-124. This indicates that miR-122 has a moderate, but direct influence on HCV translation, which is not due to stabilization of HCV RNA by miR-122. This idea is supported by the finding from the group of Catherine Jopling who found that the binding of miR-122 to its target sequences in the HCV 5'-UTR has a positive effect on translation only when the complete HCV IRES is present. For these experiments Roberts et al. exchanged the HCV IRES by the IRES elements of either the structurally similar IRES of the classic swine fever virus (CSFV) or the IRES of foot and mouth disease virus (FMDV). The results showed no positive effect of miR-122 on translation in both cases. Not even a chimeric IRES derived from HCV and CSFV could rescue miR-122-dependent translation stimulation (Roberts et al, 2011). Recently two other papers from different groups gave rise to the assumption that binding of miR-122 to the HCV 5'-UTR might induce structural changes in the IRES. Performing *in vitro* structural analysis with the HCV IRES in presence and absence of miR-122 both groups found that binding of miR-122 changes the accessibility of several nucleotides in the in structures known to be necessary for HCV translation. For example a the area around the translation start codon as well as nucleotides in the loop region of stem loop (SL) II showed decreased reactivity whereas parts of the stem regions of SLII and IV became more accessible (Mortimer & Doudna, 2013; Pang et al). Strikingly, SLII and IV are both necessary for efficient initiation of translation and the areas of both loops that showed a lower reactivity upon miR-122 binding were described to interact with each other (Filbin & Kieft, 2011). Thus it seems that miR-122 binding might induce and alteration in the structure of the HCV IRES leading to an increase in translation.

3.3 Impact of RNA stabilization on control samples during Ago-specific co-IP assays

Despite the fact that the data from the time course experiments suggest a 36 - 53 % decrease in HCV RNA abundance during 3 h it is surprising to see no differences between the anti-Ago2 co-IPs input control samples with HCV RNA and miR-122 present compared to the ones with HCV RNA and miR-124. Based on the data

gathered from the time course experiments, that suggest an increase in the half-life for HCV RNA in the presence of miR-122 during the first 6 h, it would be expected to see the difference in HCV RNA abundance between the miR-122 and miR-124 co-IP input sample on the gels. However, no difference in the ability to stabilize HCV RNA between miR-122 and miR-124 was observed.

There have been reports that liposome-mediated transfection of eukaryotic cells, which was used for the experiments, might pose problems. It has been described that fractions of the transfected RNAs do not get properly transported into the cells but rather accumulate in punctuate structures inside and outside the cell where the RNA stays biologically inactive (Barreau et al, 2006). During cell harvest those inactive RNAs mix with the portion of RNAs that got properly transported into the cytoplasm and might falsify results on stability. However, Roberts et al. reported no significant difference in RNA abundance between liposome-mediated transfection and electroporation when using HCV RNA reporter constructs containing the firefly luciferase ORF flanked by the HCV 5'- and 3'-UTR (Roberts et al, 2011). Since the RNA fragments used for co-IP were derived from a very similar construct, it could be possible that the reason why no difference between the miR-122 and miR-124 co-IP input sample could be observed is not due to a bias stemming from the method of transfection.

A possible explanation for the same abundance of HCV RNA in the presence of miR-122 and miR-124 comes from the fact that for the experiments only small fragments of HCV RNA (comprising only the 5'- or 3'-UTR) have been used. These RNA fragments are highly structured and contain several stem loops. Furthermore, it is known that these structures are tightly packed with proteins, possibly making them less accessible to RNases compared to longer RNAs and protecting them from efficient degradation. Such an explanation is supported by the results gathered during the co-IP experiments in which two versions of the HCV 5'-UTR were used. One 5'-UTR comprised 386 nucleotides and also included parts of the firefly luciferase ORF. The other HCV 5'-UTR fragment was shortened by 23 nts and thus contained only HCV specific sequences. Using the HCV 5'-UTR construct, that contained parts of the firefly luciferase ORF, two bands of different sizes were detected in the miR-122 co-IP sample. When a shortened HCV RNA fragment which excluded the firefly luciferase part was used, only one band occurred in the co-IP sample. This observation gave rise to the assumption that the luciferase part of the fragment was degraded, whereas the HCV specific part was protected from RNases. These findings suggest that the HCV RNA fragments used for co-IP assays are more stable than the HCV RNA reporter constructs used during the time course experiments, and thus show no difference in HCV RNA abundance 6 h post-transfection.

3.4 Binding of Ago2 to the HCV 3'-UTR

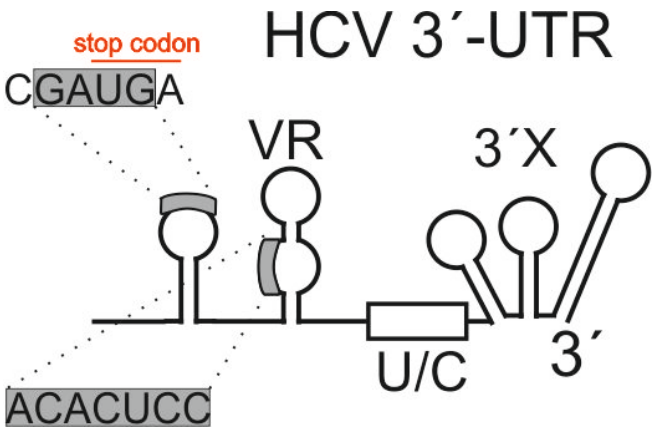

Figure 34: Schematic depiction of the binding sequences for miR-122 present in the HCV 3'-UTR and NS5B coding region. Shown is the positioning of the two regions (grey) necessary for miR-122 binding in the 3'-UTR and NS5B coding region of HCV. The sequence of those binding sites is derived from the HCV 1b Con1 isolate. In red the position of the translation stop of the polyprotein ORF is given.

The binding of miR-122 to the HCV 5'-UTR is peculiar. It has been shown that in addition to the seed sequence other nucleotides of miR-122 are also involved in the binding to the target sequences on HCV RNA. In the case of the first miR-122 binding site on the HCV RNA (the one closer to the 5'-end), the nucleotides 14-17 of miR-122 are hybridizing to the first 4 nucleotides of the HCV RNA. In case of the second miR-122 binding site in the HCV 5'-UTR the nucleotides 14-16 of the miR interact with three nucleotides directly behind the first miR-122 binding site. This unusual binding of miR-122 leads to the formation of a bulge and a tail region on the miR (Machlin et al, 2011). *In vitro* data suggests an even more pronounced binding of miR-122 to the second binding site, involving even more nucleotides outside of the seed sequence than described by Machlin et al. Mortimer and coworkers proposed that additionally to the seed sequence and nucleotides 14-16 also the nucleotides 10 and 12 could hybridize to the HCV RNA. Thus, the G residue at position 10 of miR-122 would bind to position 37 of the HCV 5'-UTR and the C at position 12 of the miR could pair to a G at position 34 of the HCV RNA (Mortimer & Doudna, 2013). It is unclear however whether this binding also occurs under in vivo conditions, when in addition to miR-122 also proteins are recruited to the HCV 5'-UTR.

The data gathered from anti-Ago2 - HCV RNA co-IP experiments suggest that an unusual complex between miR-122 and the HCV RNA is not only formed at the HCV 5'-UTR but also during binding of miR-122 to a highly conserved miR-122 binding site in the variable region of the HCV 3'-UTR. My data indicates that for efficient binding of miR-122 to this site in the variable region additional nucleotides, present in a stem loop in the coding region of NS5B, are necessary (Figure 34).

These four nucleotides, comprising parts of the stop codon of the polyprotein open reading frame, hybridize to the nucleotides 17-20 of miR-122. This binding would lead to the formation of a large bulge of eight nucleotides and a very small tail region

of two nucleotides on miR-122. Until now this binding site present in the variable region of the 3'-UTR was not shown to be functionally relevant for the HCV life cycle (Henke et al, 2008; Nasheri et al, 2011), but a majority of studies focused exclusively on the two miR-122 binding sites present in the 5'-UTR. However, Nasheri et al. analyzed the accessibility and affinity of the miR-122 binding sites on HCV RNA for miR-122 in vitro and found that the site in the variable region of the 3'-UTR showed a higher affinity for miR-122 binding compared to the second site in the 5'-UTR. Furthermore, they identified a fourth miR-122 binding site located in the coding region of NS5B (Figure 35) and postulated that this binding site might be a repressor for HCV translation and replication with a high affinity for miR-122 (Nasheri et al, 2011). It would be worthwhile to investigate whether the binding of miR-122 to this fourth miR-site also leads to the same unusual complex formation as the one seen with miR-122 binding to the 5'-UTR and supposedly to the 3'-UTR.

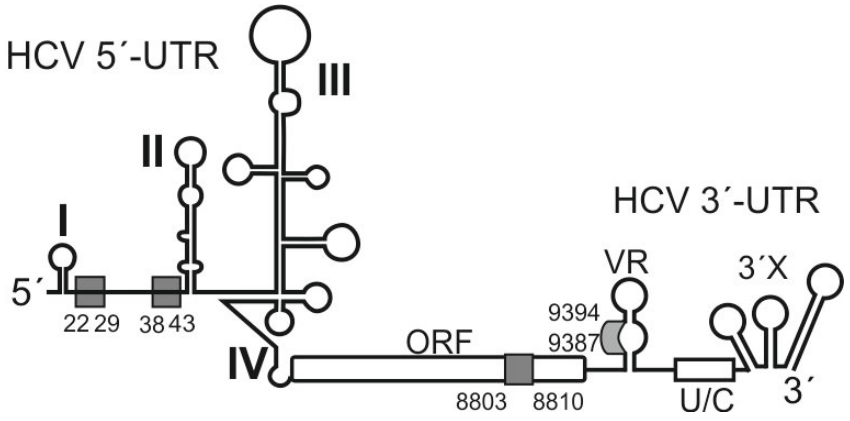

Figure 35: Localization of miR-122 binding sites in the HCV genome. This graphic shows the localization of the four identified miR-122 binding sites (grey) on the HCV genome. Two are situated in the 5'-UTR upstream of the IRES. A third binding site was predicted in the variable region (VR) of the 3'-UTR and a newly found fourth miR-122 binding site (Nasheri et al, 2011) is located in the NS5B coding region of the polyprotein ORF. The numbers signify the first and the last nucleotide that is part of the binding site in the HCV 1b Con1 isolate.

3.5 Relocation of cellular proteins during HCV infection

It is known that during infection HCV remodels the host cell to fit its purpose. For example HCV interferes with P-body and stress granule formation by recruiting several proteins localized in these compartments to lipid droplets (LDs) (Ariumi et al, 2011a). Amongst those are DDX3 and 6, ATX2, PABP1 and G3BP1. Furthermore, components involved in miR maturation, like Ago2 and Dicer, have also been shown to be redirected to LDs during infection (Berezhna et al, 2011). LDs are believed to take part in viral RNA synthesis and virion assembly due to their association with virus components like the Core protein and NS5B (Lindenbach, 2013; Lohmann, 2013).

Knock out (KO) studies revealed that some of the P-body and stress granule proteins redirected to LDs have impact on the HCV life cycle. KO of PABP1, ATX2, DDX3 and DDX6 lead to a dramatic drop in HCV RNA abundance and protein synthesis, especially in case of DDX6 (Ariumi et al, 2011a). The DEAD-box helicase and supposedly RISC component DDX6 (Chu & Rana, 2006) was recently in the focus of investigation since it was reported that DDX6 influences HCV translation and replication (Scheller et al, 2009). The fact that DDX6 is able to interact with Ago2 gave rise to the question whether DDX6 takes part in the translation stimulation of HCV by miR-122. Recent studies however, formed the general opinion that DDX6 influences HCV translation and replication in a miR-122-independent manner (Huys et al, 2013; Jangra et al, 2010). Even though DDX6 does not seem to be part of the miRNP complex necessary for HCV translational stimulation, the need for DDX6 for efficient gene silencing by miR-122 (Huys et al, 2013) supports the idea that the miRNP complex recruited for increasing HCV translation differs from the one recruited for RNA silencing.

3.6 Influence of other microRNAs on the HCV lifecycle

In addition to remodeling the cell for its advantage, several publications indicate that HCV infection can alter the miR expression profile of the host cell (Bhanja Chowdhury et al, 2012; Bruni et al, 2011; Ishida et al, 2011; Liu et al, 2010; Shwetha et al, 2013; Zhang et al 2013). Some of these miRs have been assumed to have influence on HCV replication as well as to modulate the response of the immune system of the host. For instance it has been demonstrated that HCV influences the host cell immune response, apoptosis and proliferation pathways by stimulating the expression of miR-491, miR-320c and miR-473-5p. Notably miR-491 and miR-320c have been predicted to act on the PI3/Akt signaling pathway and thus are assumed to modulate the host cell response to HCV infection (Ishida et al, 2011; Shwetha et al, 2013). Shwetha and coworkers furthermore reported that miR-320c and miR-483-5p seem to have putative targets in the Map-kinase and NFκB signaling pathways and thus seem to take part in the regulation of apoptosis, immune response and cell proliferation (Shwetha et al, 2013).

The effect of another microRNA, miR-130a, on HCV remains controversial. Liu et al. as well as Zhang and coworkers reported that miR-130a is down regulated in HCV infected cells (Liu et al, 2010; Zhang et al, 2013), whereas Bhanja Chowdhury and coworkers showed an up-regulation of miR-130a by HCV. In addition, Bhanja Chowdhury et al. demonstrated that sequestration of miR-130a resulted in a lower replication efficiency of HCV, which is most likely due to repression of the interferon-

induced transmembrane protein, IFITM1, a protein known for its antiviral function (Bhanja Chowdhury et al, 2012).
In contrast to the miRs described above, several other miRs have been reported to have negative effects on HCV replication. For example, Murakami et al. predicted a binding site for miR-199a* in stem loop II of the HCV 5'-UTR which is part of the HCV IRES. It was shown that the inhibition of HCV replication by miR-199a* seems to be accomplished by recruitment of the RISC (Murakami et al, 2009). Pedersen et al. identified two IFN-inducible miRs, miR-196 and miR-448, which have binding sites in the HCV genome and which down regulate HCV replication (Bruni et al, 2011; Pedersen et al, 2007). For miR-196 Bruni et al. reported that HCV negatively effects the expression of this miR (Bruni et al, 2011).
In addition, the miR-30(a-d) cluster as well as miR-130a, miR-192, miR-301 and miR-324-p5 have been shown to be down-regulated by HCV infection and up-regulated in response to IFN-α (Liu et al, 2010; Zhang et al, 2013). It has been shown that down-regulation of miR-30c enhances HCV genome replication. Furthermore, some of these miRs are assumed to have impact on endocytosis as well as TGF-β signaling, a pathway involved in cell growth and apoptosis (Zhang et al, 2013) .
Overall, the observed alterations in miR expression in the host cell induced by HCV infection seem to facilitate HCV reproduction as well as to maintain its persistence. Understanding how HCV influences miR expression in the host cell might be advantageous for developing new antiviral drugs, by either sequestering miRs that are hijacked by the virus or by supplementing miRs that are down-regulated during HCV infection. The sequestration approach was recently tested for miR-122 in a phase 2a trial with promising results concerning viral clearance and emergence of viral resistance (Janssen et al, 2013).

3.7 Current model of miR-122 action on HCV RNA

The current model, based on the data presented in this work, is shown in Figure 36. It implies that miR-122 recruits a miRNP complex, including the Ago proteins, to the HCV 5'-UTR by interacting with the two miR-122 binding sites. This binding does not only involve the seed sequence of the miR but also several nucleotides downstream of the seed region, thus protecting the HCV RNA from degradation by cellular RNases. Furthermore, binding of miR-122 to HCV RNA enhances translation efficiency. It is assumed that this stimulation occurs at the step of translation initiation, possibly by interaction of proteins that are part of the miRNP complex with the translation initiation machinery. Several groups reported that for the stabilization of HCV RNA and translational enhancement the tail region of miR-122 bound to the 5'-UTR seems to play a major role (Machlin et al, 2011; Roberts et al, 2011;

Shimakami et al, 2012a). The nucleotides 20-23 of miR-122 have been shown to be important for HCV translation stimulation and RNA abundance, but were dispensable for translational repression by the RISC complex (Machlin et al, 2011; Roberts et al, 2011). In this context it would be interesting to identify the components of the microRNA-protein (miRNP) complex which is supposedly recruited by miR-122. It is reasonable to assume that the composition of the stimulating miRNP complex differs from the repressive one.

Another explanation for HCV translation stimulation by miR-122 could be that binding of the miRNP complex alters the structure of the IRES changing its binding affinity for other cellular factors that influence translation. Such a model would accommodate data from the Niepmann group which suggest that miR-122 binding to HCV RNA competes with the binding of the heat shock cognate protein 70 (HSC 70) (Henke, 2010). HSC 70 has been shown to associate with HCV particles and seems to be involved in the assembly and budding of HCV (Parent et al, 2009). Thus it could be possible that HSC 70 only binds HCV genomes that show a conformation not favorable for translation but rather genomes that are ready to be incorporated into viral particles.

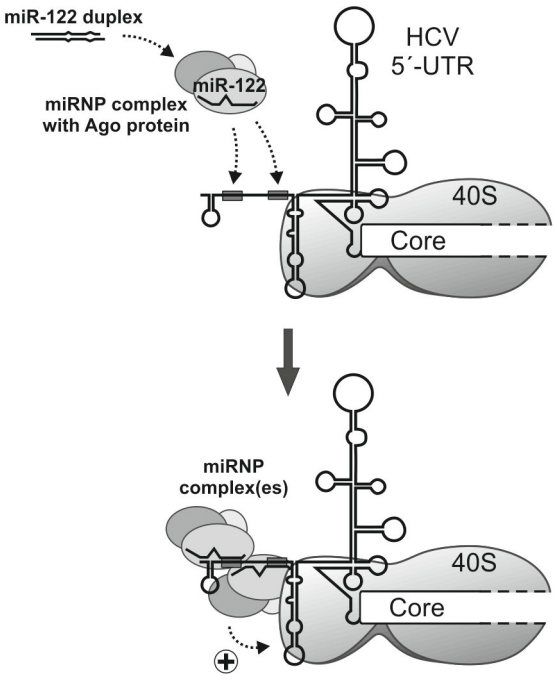

Figure 36: Model: The effect of miR-122 on HCV translation and replication through binding to the HCV 5'-UTR. miR-122 is loaded into a miRNP complex and recruits this complex to the HCV 5'-UTR. When bound to the HCV RNA, the miRNP complex protects HCV RNA from degradation but also interacts with the HCV IRES or factors bound to it and thus stimulates HCV translation.

For the binding of miR-122 to the HCV 3'-UTR no biological function has been described so far. In one of the few approaches to elucidate the function of this miR-122 binding site Henke, Goergen et al. found that mutating the binding site for miR-122 in the 3'-UTR had no effect on HCV translation stimulation by miR-122 but showed changes in overall translation efficiency possibly caused by altering the

structure of the VR (Henke et al, 2008). For these experiments the authors used a reporter constructs containing the firefly luciferase ORF flanked by the HCV 5'- and 3'-UTR. This construct however lacked the nucleotides in the HCV NS5B coding region that have been identified to be necessary for efficient miR-122 and Ago2 binding. Since the results presented in this thesis suggest that the miR-122 binding site in the HCV 3'-UTR also includes parts of the NS5B coding region of HCV, it might be worthwhile to revisit the question whether this miR-122 binding site influences HCV translation stimulation by miR-122. For this purpose a reporter construct should be created that comprises an ORF coding for a reporter protein prolonged by the last nucleotides of the NS5B coding region, thus including the last two codons of NS5B and the stem loop in which they are located.

In summary, the data presented in this work supports the idea that miR-122 positively influences HCV taking part in at least two different mechanisms. By recruiting a miRNP complex in which the ago proteins are involved in miR-122 prolongs the half- of HCV RNA as well as stimulates translation. It can only be speculated on how much each of the miR-122 binding site in the 5'-UTR adds to each of these mechanism. It could be possible that due to their position and binding behavior the first site protects the HCV 5'-end from degradation and the second site is involved in translation stimulation. The questions however, whether both of these miR-122 binding sites are bound by a miRNP complex at the same time and what biological function the binding of miR-122 to the third binding site in the VR of the 3'-UTR has, stay to be answered.

4 Methods and Materials

4.1 Methods

4.1.1 Tissue Culture Techniques

All steps involving eukaryotic cells were carried out in using a biosafety cabinet (BSC), sterile pipettes and pipette tips, as well as sterile buffers and media. All pipettes and pipette tips contained filters to eliminate any carryover of aerosols. All buffers and media were warmed to 37 °C before use. Everything that was carried into the BSC was decontaminated by wiping it down with 70 % denatured ethanol.
To properly identify the cells all cultures were marked with name of the cell line, date and passage number. The Lot number from the ECACC was also included if available.

4.1.1.1 Thawing of eukaryotic cells that were stored in a liquid nitrogen tank

To thaw cells stored in liquid nitrogen it is necessary to work carefully. The use of protective eyewear as well as gloves is recommended since nitrogen may reside in the vial.
The cryotubes were partially opened in a BSC to release any residual nitrogen. Following this the cryovials were placed in a 37 °C water bath to accelerate the thawing process. The cells were then transferred to a 25 cm^2 tissue culture flask containing 5 ml of pre-warmed Dulbecco's Modified Eagles Medium supplemented with 10 % fetal bovine serum (FBS) and 1 % Penecillin/Streptomycine (Pen/Strep) (DMEM 10 %) and incubated at 37 °C for several hours until they adhered to the bottom of the flask. When the cells have attached the medium was changed to fresh DMEM 10 %. This change of medium is necessary to remove cells that died during the freezing and thawing procedure, as well as to remove residual DMSO that was part of the freezing medium.

4.1.1.2 Passaging eukaryotic cells

To ensure a constant growth of an adherent cell line it is necessary to split the cells on a regular basis to keep them from getting too confluent. Cell cultures that are grown too thickly have the tendency to detach from the growing surface and to die.
Usually cells were passaged when they reached 80 % - 95 % confluency to ensure that they are in the log phase of growth.
The old culture medium was discarded and the cells were washed twice with PBS. Afterwards, the cells were treated at 37 °C with an appropriate amount of 0.5 % Trypsin-EDTA until they detached (for 75 cm^2 flasks 3 ml Trypsin were used, for 175 cm^2 flasks 5 ml Trypsin were used). Trypsin was inactivated by adding at least the same amount of fresh DMEM 10 %.
The cells were resuspended in the DMEM 10 % by pipetting up and down. Subsequently, an appropriate amount of cell suspension was given into a new flask along with fresh DMEM 10 % and cultured for several days. A normal amount of HeLa cells that was given into the new flask was 1/20 – 1/30 of the cell suspension for 4 days of cultivation.

4.1.1.3 Counting eukaryotic cells

To determine the total amount of cells in a cell suspension the cells were counted using a Neubauer improved hemocytometer. The counting chamber has a depth of 0.1 mm and is divided into several squares of different sizes. For determining the cell number the squares of 1 mm^2 (Figure 37, highlighted in blue) were counted. Cells that touched the upper or right edge of the square were not included in the calculations. Cells touching the left or lower edge of the square were included into the count. The total cell number of all four 1 mm^2 squares was averaged and this mean value was multiplied by 10000, resulting in the number of cells per ml.

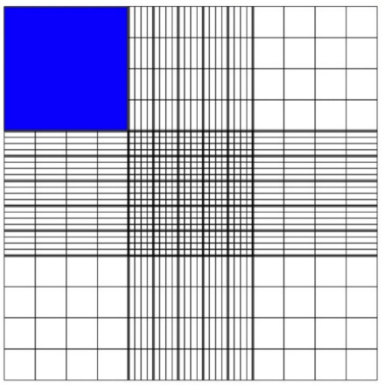

Figure 37: Partition of a Neubauer improved hemocytometer. The hemocytometer has a depth of 0.1 mm and is divided in several squares ranging from 0.0025 mm2 to 1 mm2. The square used to determine the amount of cells in a suspension is highlighted in blue and has an area of 1 mm2. The count of four of these 1 mm2 squares was averaged and multiplied by 10000 to approximate the total number of cells per ml. Cell touching the right and upper rim of the square were not counted. The picture was taken from http://www.microbehunter.com and modified.

4.1.1.4 Seeding eukaryotic cells

For all experiments HeLa or HuH-7 cells were seeded in either 24-well plates or 6-well plates or 9 cm dishes. The cells were washed twice with PBS and detached with 0.5 % Trypsin EDTA. Afterwards the cells were resuspended in an appropriate amount of DMEM 10 %, usually leading to a final volume of 10 - 15 ml. Subsequently, the cells were counted using a Neubauer improved hemocytometer. After counting, a certain amount of cell suspension was diluted in DMEM 10 % and seeded in the desired tissue culture plate size. The appropriate amounts of cells have been determined for every cell line by previous empiric testing. Since the growth rate varies during the life of a cell line it may be necessary to reconsider the appropriate amount of cells once in a while, depending on the number of passages and general treatment of the cell line. The final volumes of cell suspension with DMEM 10 % in the wells of the tissue culture plates were 1 ml for 24-well plates, 3 ml for 6-well plates and 10 ml for 9 cm dishes.

4.1.1.5 Transfection of eukaryotic cells using Lipofectamine 2000

Eukaryotic cells were transfected by using Lipofectamine 2000 (Invitrogen) transfection reagent. This reagent contains liposomal particles that can bind nucleic acids and shuttles them into the cells via endocytosis.
A ratio of 1:3 between transfection reagent and nucleic acids (µg RNA/DNA : µl Lipofectamine 2000) was established as used for optimal transfection efficiency of both HeLa and HuH-7 cells.
Two samples were prepared: one containing RNA/DNA diluted in DMEM, and one containing Lipofectamine 2000 also diluted in DMEM. The appropriate amount of DMEM in those samples varied depending on the size of the tissue culture plate on which the cells were grown; for 6-well plates 250 µl DMEM was used for each sample and for 9 cm dishes 500 µl DMEM were used.
The two samples containing RNA/DNA and Lipofectamine 2000, respectively, were incubated for 5 minutes at room temperature and then merged together by pipetting. The resulting mixture was incubated for additional 20 minutes at room temperature without agitation. Meanwhile the cells were washed twice with PBS and fresh DMEM without any supplements was added. Again, the amount of DMEM varied depending on the size of the tissue culture plate, for 6-well plates 500 µl and for 9 cm dishes 4 ml DMEM were used.
After incubation the transfection mixture containing both RNA/DNA and Lipofectamine 2000 was added drop wise to the cells. Afterwards the cells were incubated at 37 °C with 5 % CO_2 for 3 - 6 hours.

When the incubation time for the transfection before harvesting the cells is 9 hours or less all these steps can be carried out without a BSC.

4.1.1.6 Freezing eukaryotic cells

Eukaryotic cells change their behavior with the number of passages and the time they are cultured. Sometimes transfection efficiencies and growth rate can drop dramatically. At this time point it is necessary to thaw new cells that were stored in the vapour phase of a liquid nitrogen tank. To ensure that low passage cells are always available it is obligatory to propagate and freeze some of the freshly thawed cells from time to time.

Generally the protocol to freeze cells given by the ECACC was used. The cryomedium was made by mixing 20 % FBS with 10 % DMSO as a cryoprotectant. The cells were grown in DMEM 10 % until they reached log phase growth at approximately 80 - 90 % confluency. The old culture medium was discarded, the cells were washed twice with PBS and treated with 0.5 % Trypsin-EDTA until they detached. The trypsination was stopped by adding one volume cryomedium. Subsequently, the cells were centrifuged for 10 minutes at a speed of 150 rcf and 4 °C. The cells were resuspended in cryomedium at a concentration of about 2 - 4 x 10^6 cells per ml and dispersed in to cryovials, 1 ml per vial.

The cryovials were placed in an alcohol bath (Nalgene cell freezing container containing 100 % Isopropanol) that was pre-cooled to 4 °C. The cells were then placed in a -80 °C freezer. After one to two days the cryovials were transferred into the gas phase of a liquid nitrogen tank.

A week after the freezing one sample of the cells was thawed and tested if the cells were still viable.

4.1.2 Microbiological Methods

All steps involving bacteria were carried out in close proximity to a Bunsen burner to ensure sterility of the bacterial culture. Metal and glass ware such as glass pipettes or beakers were either disinfected by dry heat sterilization or were singed. The surface of the working space was disinfected by wiping it down with 70 % ethanol.

4.1.2.1 Cultivation of bacteria

Bacteria were grown either on agar plates forming colonies or in LB medium as a solution.
The powdered LB medium was solved in deionized water according to the manufacturer's specifications and autoclaved. For agar plates, 3.75 g of bactoagar were added per 250 ml of LB medium before autoclaving.
For seeding bacteria on a petri dish, the agar was heated and cooled down to approximately 60 °C, and only then was the antibiotic added (7.5 µg/ml). Following the addition of the antibiotic about 20 ml of the agar were poured into a petridish. After turning solid the bacteria were dropped on the agar and spread with a bacterial spreader until the liquid seeped into the plate.
For liquid cultures it was usually necessary to prepare a pre-culture containing 3 - 5 ml of LB medium (7.5 µg ampicillin /ml). This pre-culture was inoculated with one bacterial colony picked from an agar plate and grown for several hours until the medium turned turbid (approximately OD 0.6), then 1/10 of this culture was used to inoculate a bigger flask of LB medium, ranging in size from 10 ml - 500 ml.

4.1.2.2 Transformation of bacteria by electroporation

For transformation either the *E. coli* strains XL1-Blue or HB101 were used. The bacteria were prepared for electroporation by growing a 10 ml culture over night at 37 °C under constant agitation (180 - 250 rpm). To remove any residual salts that might interfere with the electroporation the bacteria were centrifuged at 5000 rcf for 15 minutes at 4 °C and the pellet was resuspended in ice-cold double distilled autoclaved water (ddH_2O). This step was repeated 3 times. After the third centrifugation the pellet was resuspended in 2 ml ice-cold ddH_2O and the bacteria were divided in 100 µl aliquots. These aliquots could be stored at -80 °C for several weeks.
For electroporation one aliquot was thawed on ice and mixed with approximately 100 ng of plasmid DNA or half the volume of a ligation sample (usually 7.5 µl). Afterwards the mixture was pipetted into an electroporation cuvette, into which an additional 500

µl dd H2O were added to ensure that enough volume resided in the cuvette. Cells were electroporated at 25 µF, 200-400 Ohm and 2.5 kV. Immediately after electroporation 1 ml of LB medium was added to the cells and the bacteria were incubated for 1 hour at 37 °C under constant agitation (180 - 250 rpm). Subsequently, transformed bacteria were spread on an agarplate containing an appropriate antibiotic, usually ampicillin.

4.1.2.3 Alkaline lysis of bacteria and plasmid preparation

The alkaline lysis of bacteria and plasmid preparation is a standard procedure in molecular biology laboratories to amplify plasmid DNA (Sambrook et al, 1989). Bacteria were transformed with the plasmid of choice and grown (usually overnight) at 37 °C under constant shaking at 180 – 250 rpm until they reached log phase growth (approximately OD 0.6).
Afterwards the cells were pelleted by centrifugation (5000 rcf, 4 °C, 10 – 15 minutes) and lysed under alkaline conditions in the presence of SDS, thus denaturing all bacterial DNA and proteins. Neutralization was accomplished by adding a potassium acetate containing buffer. This neutralization leads only the relatively small plasmid DNA to properly renature, all other cell components form a white fall out that can be easily removed from the sample either by centrifugation or filtration. Following the removal of the cell debris, the plasmid DNA was bound to a silica matrix at high salt and low pH conditions. After washing with an ethanol containing buffer, the DNA was eluted with an elution buffer into a fresh collection tube and precipitated by adding isopropanol. Small scale preparation protocols usually directly elute the DNA with ddH_2O, the precipitation step was then omitted.
This method was employed for two different scales of bacterial cultures, leading to different amounts of plasmid gained from the procedure. The first scale, maxi preparation, used 100 - 250 ml of bacterial culture and was performed with the NucleoBond AX 100 Kit from Machery-Nagel. The second scale, mini preparation, used 2 ml of a 3 - 5 ml culture and was carried out with the Wizard Plus SV Minipreps DNA purification System from Promega. Both kits provided all buffers, components and instructions necessary for the protocol.

4.1.3 Methods concerning the Manipulation and Characterization of Nucleic Acids

4.1.3.1 Working with RNA

RNases are ubiquitous proteins that are not completely inactivated by normal means of heat sterilization methods like autoclaving. Therefore, it is necessary to take certain precautions when working with RNA. At least the use and the regular changing of latex or nitrile gloves is recommended.
All glass and metal ware was baked at either 500 °C for 4 hours or overnight at 280 °C. Reusable plastic ware was soaked for 1 hour in 0.1 M NaOH and 1 mM EDTA solution and subsequently rinsed with ddH_2O. Additionally, everything was wrapped or covered with aluminum foil to prevent RNase contamination and autoclaved.
Chemicals used to prepare buffers were specially dedicated to RNA work and only touched with RNase free material, like baked spatula. For weighing these chemicals the RNase-free aluminum wrapping of the used spatula was employed as a scale pan.
All self-made buffers (except gel running buffers like TBE or TAE) were prepared in and after preparation filled into RNase-free glass ware and subsequently autoclaved.
Furthermore, only nuclease-free certified filter tips and sterile serological pipettes were used to handle the buffers and RNA solutions.

4.1.3.1 DNA-template preparation for *in vitro* transcription

Since none of the plasmids coding for the used RNA reporter constructs contained a T7 or Sp6 RNA polymerase terminator sequence at which the elongation of the nascent RNA molecule could stop (e.g. the authentic end of the HCV 3'-UTR could not be guaranteed), it was necessary to prepare a DNA template for *in vitro* transcription (4.1.3.2). To ensure that the T7 or Sp6 RNA polymerase did not add nucleotides to the HCV 3'-UTR a primer was used for amplification that comprised the last 29 nucleotides of the 3'-UTR.
The tables show the standard program employed on the Biometra TProfessional cycler as well as the composition of the sample. Cycle steps 2 - 4 were repeated 30 times. The choice of primers used for each PCR depended on the plasmid used as a PCR template.
During the work for this thesis the vendor of the Taq DNA polymerase changed (from Promega to NEB), which lead to some changes in the PCR protocol. The elongation and final elongation temperature was decreased to 68 °C (initially 72 °C). The addition of $MgCl_2$ to the sample was omitted and the concentrations of the dNTPs, the primers and the Taq DNA polymerase were decreased.

After PCR the resulting DNA fragments were purified either by phonol-chloroform extraction (4.1.3.7) with subsequent ethanol precipitation (4.1.3.8) or following the protocol of Illustra GFX PCR DNA and Gel Band Purification Kit from GE Healthcare and eluted in ddH_2O.

1	95 °C	2 min	initial denaturing
2	95 °C	0.5 min	denaturing
3	70 °C	1 min	annealing
4	72 °C	1 min	elongation
5	72 °C	3 min	final elongation
6	8 °C	pause	storage

component	**concentration (Promega)**	**concentration (NEB)**
DNA	100 ng	100 ng
Taq specific buffer	1x	1x
$MgCl_2$	2.5 mM	
Primer 1	1 µM	0.5 µM
Primer 2	1 µM	0.5 µM
dNTPs	250 µM	200 µM
Taq DNA polymerase	10 U	1,25 U
H_2O	@ 100 µl	@ 100 µl

Table 2: Program and sample composition for DNA-template preparation

4.1.3.2 *In vitro* transcription of radioactive and non-radioactive RNA

To provide RNA constructs for transfection of eukaryotic cells (4.1.1.5) an *in vitro* transcription was performed using a PCR derived DNA template (4.1.3.1). The *in vitro* transcription was carried out at 37 °C for 1.5 hours using T7 or Sp6 RNA polymerase. Transcription buffer was provided by Fermentas and contained 200 mM Tris-HCl (pH 7.9), 30 mM $MgCl_2$, 50 mM DTT, 50 mM NaCl and 10 mM spermidine. Since DTT is not stable for a long time, 10 mM DTT were added in case the transcription buffer was older than one month. All components were pipetted at room temperature for the reason that spermidine may precipitate the DNA template at low temperatures. The concentrations of all components used for transcription are given below. For labeling the RNA product with radioactive Uridine residues, the concentration of rUTPs was reduced to 100 µM and 0.625 µM of α-^{32}P rUTPs were added. Non-radioactive RNA was purified by either phenol-chloroform extraction (4.1.3.7) or using the Qiagen RNeasy RNA clean-up protocol following the manufacturer's specifications. After purification the concentration of RNA was measured by photometric measurement using the Tecan Infinite multimode reader.

The amount of radioactively labeled RNA was determined by separating it on a denaturing polyacrylamide gel (4.1.3.10) and estimating the percentage of incorporated radioactive nucleotides. The ratio of incorporated and free radioactive nucleotides was used to calculate the concentration of the labeled RNA.

total amount of RNA [pMol] = (c (rUTP) [µM] x reaction volume [µl] x incorporated radioactive rNTPs [%]) / (incorporated radioactive rUTPs [%] + nonincoporated radioactive rUTPs [%]) x number rUTPs in RNA

component	amount
DNA template	100 – 200 ng
Transcription Buffer	1x
DTT*	10 mM
rNTPs (AGCU) / rNTPs (AGC)**	0.5 mM (each)
rUTPs**	100 µM
α-^{32}P rUTPs**	0.625 µM
T7 / Sp6 RNA polymerase	0.1 U/µl

* added when the transcription buffer was older than one month

** used only for radioactive labeling of the RNA product

Table 3: Sample composition for radioactive and non-radioactive *in vitro* transcriptions

4.1.3.3 *In vitro* mutagenesis

The *in vitro* mutagenesis is a technique used to easily introduce point mutations or to create small insertions or deletions into plasmid DNA, by amplifying the plasmid. This mutagenesis strategy is based on the commercially available QuickChange mutagenesis protocol by Stratagene.

The mutagenesis is accomplished by performing a PCR using two complementary primers which both carry the desired mutation. The primers should have 25 - 45 nts length and a T_m of 78 °C or above. The mutation should be in the middle of the primers flanked by 10 to 15 nts of correct sequence to each side.

In the first round of amplification the primers anneal leaving an unpaired bulge at the site where the mutation will be introduced, the polymerase will then create newly synthesized mutated DNA strands. During the second and all following rounds of the PCR these new strands will be exponentially amplified. Since the not mutated template DNA was isolated from *E. coli* it was methylated by the Dam methylase. These methylations are recognized by the endonuclease DpnI. The not methylated PCR products are not used as a substrate for degradation. Using DpnI it is possible to remove the wild type DNA from the PCR sample. A small portion the PCR product

before and after DpnI digest is analyzed on an agarose gel (4.1.3.9). Bands on the gel with the DpnI digest signified that the PCR was successful. The mutated DNA was transformed (4.1.2.2) into either *E. coli* XL1-Blue or HB101.
This method requires the use of a high fidelity DNA polymerase like the *Pfu*$_{turbo}$ from Stratagene or the Phusion polymerase from Finnzymes, to ensure that no further mutations are introduced during amplification of the plasmid. We used the *Pfu*$_{turbo}$ polymerase for the *in vitro* mutagenesis. Note that by changing the polymerase changes to the PCR program may apply.
The tables below show the standard sample composition and PCR protocol.

component	amount
DNA template *	5 - 50 ng
dNTPs	0.2 mM (each)
Primer 1	125 ng
Primer 2	125 ng
Pfu$_{turbo}$ buffer	1x
Pfu$_{turbo}$ polymerase **	2,5 U
H_2O	@ 50 µl

* usually three samples were prepared for each mutation since the ratio of template to primes is a critical step in this method
** added later after first denaturation step

Table 4: sample composition for mutagenesis

1	99 °C	2 min	initial denaturing
2	90 °C	2 min (addition of *Pfu*$_{turbo}$)	pause to add polymerase
3	95 °C	30 s	denaturing
4	55 °C	1 min	annealing
5	68 °C	1 min / kb of plasmid length	elongation
6	68 °C	5 min	final elongation
7	8 °C	pause	storage

Table 5: standard *in vitro* mutagenesis PCR program

The steps 3 to 5 were repeated 18 times. For difficult mutations a slightly different PCR cycle protocol was employed. A cycle with a lower annealing temperature (44 °C) was introduced into the program and repeated for 10 times. Subsequently, a cycle with an annealing temperature of 55 °C was repeated for 20 times. The changes in the program are given in the table below.

1	99 °C	2 min	initial denaturing
2	90 °C	2 min (addition of *Pfu*$_{turbo}$)	pause to add polymerase
3 *	95 °C	0.5 min	denaturing
4 *	40°C	45 s	annealing
5 *	68 °C	2 min / kb of plasmid length	elongation
3 **	95 °C	0.5 min	denaturing
4 **	55 °C	45 s	annealing
5 **	72 °C	1 min / kb of plasmid length	elongation
6	72 °C	10 min	final elongation
7	8 °C	pause	storage

* repeated 10 times ** repeated 20 times

Table 6: Modified *in vitro* mutagenesis PCR program for difficult mutations

4.1.3.4 Two-step *in vitro* mutagenesis

The two-step *in vitro* mutagenesis is a method employed when introducing lager insertions or deletions into plasmid DNA.
For this protocol two pairs of primers are needed. Figure 38 schematically shows the procedure. One primer of each pair (primers 2 and 3) carries the desired mutation flanked at the 3'-end by approximately 10 to 20 nts of correct sequence. These primers have to be also partially complementary to each at the 5'-ends so that they can hybridize on a length of at least 10 nucleotides.

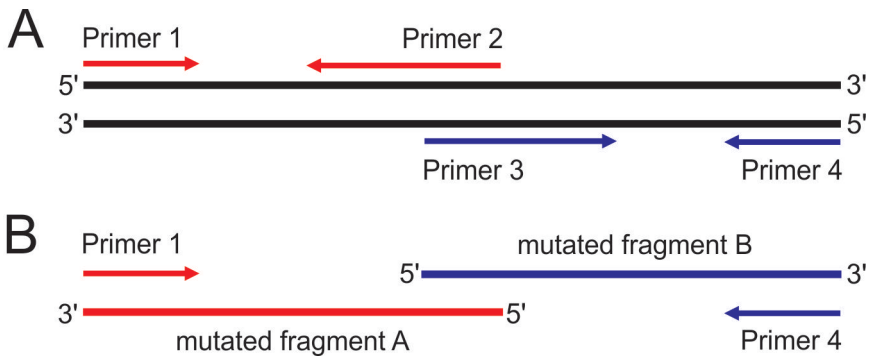

Figure 38: Model of the two-step mutagenesis PCR. In a first step the mutations were introduced by two separate PCRs using mutagenesis primers 1 and 2 for the first PCR and primers 3 and 4 for the second PCR reaction (A). The resulting DNA fragments of both PCRs partially overlap and can be used as a template for a third PCR (B) in which the primers 1 and 4 are used to fill in the gaps and amplify the mutated final fragment.

During the first step each primer pair is used to amplify two DNA fragments both carrying parts of the mutated region at their 5'-end. In the second step the two amplified fragments are combined and serve as a template for a PCR in which the two flanking primers (primers 1 and 4) not carrying the mutation are used to complete and amplify the mutated DNA fragment. The length of the final product was checked on an analytical agarose gel (4.1.3.9) and the fragment was cloned into a vector

backbone by restriction digest (4.1.3.5) using restriction sites near the end of the final PCR product and ligation (4.1.3.6).

4.1.3.5 Restriction digest of DNA

Restriction digests are usually used to provide DNA molecules with “sticky ends” for subsequent ligation or to check identity and integrity of DNA plasmids. Therefore, DNA molecules are incubated in certain buffers in the presence of restriction endonucleases. These nucleases can be obtained from several distributers like NEB or Fermentas.
The volume of the digest is highly variable depending on the amount of DNA that should be digested and the downstream application. Usually a sample has a final volume of 50 µl. The buffers needed are provided with the enzyme by the manufacturer and were used according to the manual’s specifications.
The amount of enzyme needed was calculated from the following formula:

amount of enzyme [µl] =

number of restriction sites in target molecule [pmol] / specific enzyme activity [pmol hits/µl]

Amounts calculated from this formula that were lower than 0.5 µl were rounded up to 0.5 µl since the used pipettes were not trustworthy with lower volumes.
Digests with multiple enzymes (double digests) were carried out following the suggestions provided by either thermoscientificbio.com/webtools/doubledigest/ or neb.com/tools-and-resources/interactive-tools/double-digest-finder.
The restriction was usually carried out in a water bath for 1 hour. The temperature of the incubation was dependent on the respective enzymes.
After digest the sample or a small portion of it was analyzed on an agarose gel (4.1.3.9) to check the sizes of DNA fragments after the digestion.

4.1.3.6 Ligation of DNA fragments

To fuse two different DNA molecules a ligation using the T4 DNA ligase was carried out. This enzyme catalyzes the formation of phosphordiester bonds between the 5’-phosphate of one and the 3’-OH of the other DNA molecule by hydrolyzing ATP. This reaction is more reliable when using DNAs with “sticky ends”, meaning DNAs carrying residues of the same restriction site at its respective ends.
A typical ligation reaction of 20 µl for cloning an insert into a vector backbone contained 25 ng of vector. The amount of insert depends on its length and the size of the vector. The necessary amount of insert was calculated by the following formula:

amount of insert [ng] = 5 x amount of vector [ng] x length of insert [bp] / length of vector [bp]

The concentration of the DNA fragments was assessed by photometric measurement in combination with gel analysis (4.1.3.9).
Besides the vector and the insert the ligation reaction also contained 400 U of the T4 DNA ligase and 1 x ligase reaction buffer. The ligation occurred at room temperature for 1 hour or overnight at 4 °C. After ligation the ligase was inactivated at 65 °C for 10 minutes when the resulting DNA was transformed into bacteria (4.1.2.2).

4.1.3.7 Phenol-chloroform extraction

This procedure is used to remove proteins from nucleic acids. During the protocol the watery sample containing nucleic acids and proteins is mixed with organic solvents, phenol and chloroform, and then centrifuged. After centrifugation two phases occur, a watery and an organic one. The nucleic acids remain in the watery phase; the proteins are denatured and partially solved in the organic phase.
The watery sample was mixed with one volume of Rotiphenol and vortexed for approximately 30 seconds. Subsequently, the watery phase of the sample (usually the upper phase depending on the salt concentration) was transferred into a new reaction tube. Next, one volume of a mixture (1:1) of phenol and chloroform / isoamyl alcohol (24:1) was added. After vortexing the sample was centrifuged again and the upper watery phase was transferred into a new reaction tube. The chloroform serves as a solvent for fatty acids. The isoamyl alcohol is added for a clearer phase separation.
In the last step of the extraction the sample was mixed with one volume of chloroform / isoamyl alcohol (24:1) for a final separation. In this step, the chloroform serves to remove traces of phenol from the watery sample. The watery phase was transferred into a new reaction tube. All centrifugation steps were carried out at 13000 rcf at room temperature for 5 minutes. Usually this procedure was followed by an ethanol precipitation (4.1.3.8) to concentrate the nuclei acids and to remove salt contaminations from the sample.

4.1.3.8 Precipitation of nucleic acids with ethanol

The ethanol precipitation was used to concentrate and clean nucleic acids of salt contaminations stemming from reaction buffers.
The sample is thoroughly mixed with three volumes of 99 % ethanol and 1/10 volume of 3 M sodium acetate. When low amounts of nucleic acids were expected 1 - 2 µl of Glycoblue (15 mg/ml) were added to increase the visibility of the expected RNA or

DNA pellet. For precipitation the mixture was incubated for one to several hours at -20 °C. After incubation the sample was centrifuged at 17000 rcf and 4 °C for 30 minutes. Following which the supernatant was carefully removed and discarded. Subsequently, the pellet was washed twice with 70 % ethanol and air-dried at 37 °C until the pellet changed color from milky white to transparent. At this step it was necessary to make sure that no ethanol remained with the pellet. The pellet was then dissolved in ddH_2O. The amount of ddH_2O depended on the expected RNA or DNA concentration and the intended downstream applications.

.

4.1.3.9 Separation of nucleic acids on an agarose gel

Non-radioactively labeled RNAs and DNAs were separated on a 1 -2 % TAE agarose gel depending on the expected size of the nucleic acid. Upon solidifying the agarose forms a sieve like structure. When an electric current is applied to the gel the negatively charged nucleic acids will move though the gel. Small fragments will pass thought the gel more quickly than larger ones, thus, the separation is based on the size of the nucleic acids. The resulting bands in the gel can be visualized by staining the gel with intercalating agents like ethidium bromide or cyber green and exposing it to UV light.

The samples were mixed with RNA or DNA sample buffer containing xylencyanole and bromphenol blue. These dyes served as a visual measure for fragment migration on the gel. Then the samples were loaded onto the gel and run at 100-150 V. 1 x TAE was used as a running buffer. When the bromophenol blue front reached the lower third of the gel, the run was stopped. Afterwards, the gel was incubated in a TAE - ethidium bromide bath for 10 - 30 minutes and subsequently exposed to UV light.

From preparative agarose gels the desired bands were cut out during UV-light exposure and the nucleic acids were purified using the Illustra GFX PCR DNA and Gel Band Purification Kit, following the manufacturer's protocol. Since UV light may lead to mutations in DNA it was necessary to reduce the time of exposure for cutting out the bands to a minimum.

4.1.3.10 Separation of radioactively labeled RNA on a polyacrylamide gel

To separate radioactively labeled RNAs the RNA was mixed with RNA sample buffer and loaded on a 6 -10 % polyacrylamide in TBE buffer gel with 7 M urea. An electric current of 100-150 V was then applied. Usually the gel was run until the xylencyanol band from the sample buffer reached the end of the gel. Gels that were used for estimating the RNA amount after *in vitro* transcription were run until the bromophenol

blue front reached approximately the middle of the gel, to ensure that the free nucleotides did not exit the gel. 1x TBE was used as a running buffer. After separation the RNA fragments were visualized by exposing them to X-ray film for several minutes up to several days. When low amounts of radioactivity were expected in the gel the exposure was amplified by putting the X-ray cassette in which the film was exposed at -80 °C.
For long time exposure (more than 1 hour) it was necessary to dry the gel before exposing it to the film. Therefore the gel was fixed with a 7.5 % acetic acid and 5 % ethanol fixer solution for 15 minutes, put on a piece of 3MM chromatography paper and dried for 2 hours at 80 °C on a gel dryer.

4.1.3.11 Preparation of duplex microRNAs

For transfection of eukaryotic cells double stranded microRNAs were required. To produce these miR duplexes the mature miR strand (miR mat, 100 µM) and the miR passenger strand (miR *, 100 µM) were mixed (1:1). Afterwards the sample was incubated in a PCR cycler starting at 90 °C and decreasing the temperature by 1 °C per minute to a final temperature of 4 °C. After cycling the sample was split into aliquots of 10 or 20 µl and stored at -20 °C.

4.1.4 Protein Biochemical Techniques

4.1.4.1 Argonaute protein specific RNA co-immunoprecipitation

The Argonaute (Ago) protein specific RNA co-immunoprecipitation (co-IP) was used to detect interaction of the Ago protein family members with parts of the HCV RNA in presence or absence of miR-122. The Ago proteins were pulled down from a crude cell extract containing radioactively labeled HCV RNA fragments. The pull down was accomplished by binding the proteins to specific antibodies coupled to magnetic beads. If HCV RNA and Ago proteins interact the HCV RNA is co-precipitated and could be detected by autoradiography.
First, 50 - 100 µl of magnetic protein A or G beads were washed with 500 µl PBS and resuspended in 1000 µl of PBS. The magnetic beads made it possible to use magnetic separation of the beads from a suspension without the need for centrifugation after washing steps. After washing the beads, antibodies were added and the suspension was rotated at 4 °C overnight (it was possible to shorten this step to 2 hours if necessary). The appropriate amount of antibody had to be determined for each antibody by testing during the run of the experiments; Table 7 shows the respective antibodies and the concentration at which they were used.

Second, a 9 cm dish of 80 - 90 % confluent HeLa cells was transfected (4.1.1.5) with 1 - 3 µg of radiolabeled RNA fragments comprising either the HCV 5'-UTR or 3'-UTR and the same amount of miR-122 or miR-124 as a control. 15 µl of the HCV RNA fragments stock (RNA transcript) were saved as a marker for RNA length. 6 hours post transfection the cells were washed twice with 1 ml of PBS and lysed on plate in 1 ml co-IP Lysis Buffer for 30 minutes at 4 °C. Meanwhile the antibody coupled beads were pelleted at 1000 rcf and 4 °C for 1 minute, washed once with co-IP wash buffer and resuspended in 500 ml PBS. After lysis the sample was centrifuged at 17000 rcf and 4 °C for 30 minutes to clear it from cell debris. 10 % of the lysate were saved as an input control to check the equal distribution of HCV RNA in the different samples and stored at 4 °C. The rest of the lysate was given to the antibody coupled magnetic beads. The samples were rotated at 4 °C for 3 hours. Next, the beads were pelleted at 1000 rcf and 4 °C for 1 minutes and the supernatant was discarded. Subsequently the beads were washed 4 times with 1 ml co-IP wash buffer, resuspended in 1 ml PBS and transferred to a new reaction tube. Before the PBS was discarded 10 % of the sample were saved as a control to check the efficiency of Ago binding in the samples by SDS-PAGE (4.1.4.3) and Western Blot (4.1.4.4).
Afterwards, 250 µl of proteinase K buffer and 10 µl of proteinase K [20 mg/ml] were added to the beads and the input sample. The samples were incubated at 65 °C for 15 minutes. To ensure that the beads did not sediment at the bottom of the reaction tube during the incubation, the tubes were flicked every 5 minutes. Meanwhile 235 µl proteinase K buffer were added to the saved 15 µl of the RNA transcript.
After incubation all samples, including input and RNA transcript, were centrifuged (1000 rcf, 4°C, 1 minute) and thoroughly mixed with 300 µl phenol. A centrifugation was carried out at 17000 rcf and 4 °C for 10 minutes, and the watery upper phase was transferred to a new reaction tube. Subsequently, the samples were mixed with 300 µl of chloroform and again centrifuged (17000, rcf 4°C, 10 minutes). The upper phase was then collected and an ethanol precipitation (4.1.3.8) was performed.
The resulting RNA pellets were thoroughly resuspended in 30 µl (co-IP samples) or 100 µl (input and transcript) of RNA sample buffer by pipetting and analyzed on a denaturing polyacrylamide gel (4.1.3.10).
For the RNA transcript and input controls it was necessary to heat the samples several times to 60 °C to accomplish satisfying resuspension. Before running the gels the input samples were diluted 1:100 in RNA sample buffer and 10 µl (0.1% of the total input sample) of this dilution were loaded on the gel. The RNA transcript was diluted 1:500 in RNA sample buffer and 10 µl of this dilution (~0.003 % of the original RNA transcript) were used for the co-IP sample gel, while 30 µl (~0,009 % of the original RNA transcript) were used for the input sample gel.

antibody	Amount per 100 µl magnetic beads	concentration	magnetic beads
rat-anti-Ago2 clone 11A9	5 µl	~1,5 mg/ml	protein G
rat-anti-Ago1 clone 4B8	5 µl	~1,5 mg/ml	protein G
rabit-anti-eIF3a *	5 µl	0.2 mg/ml	protein A
goat-anti-PTBP1	5 µl	0.5 mg/ml	protein G
mouse-anti-FLAG	5 µl	~3.8 mg/ml	protein G

* for eIF3a only 50 µl beads were used per sample

Table 7: Amount of antibodies used for anti-Ago – HCV RNA co-IPs

4.1.4.2 Immunoprecipitation

Immunoprecipitation (IP) was used to pull down proteins of interest using a specific antibody. The procedure can basically be divided into two parts, first the pre-clearing of the cell lysate and second the IP-step to pull out the desired protein. To prepare the lysate, a 9 cm dish of ~80 % confluent cells was washed twice with PBS and harvested in 800 µl IP-lysis buffer with a cell scraper. Following this the debris was pelleted by centrifugation (17000 rcf for 10 minutes at 4°C). Subsequently, the lysate was transferred into a new reaction tube. For the pre-clearing step, the cell lysate was rotated at 4 °C for 1 hour with native magnetic beads (25 µl beads per 200 µl lysate) to remove proteins biding unspecifically to the beads. After pre-clearing the beads were removed by centrifugation and the lysate was transferred into a new reaction tube containing new magnetic beads with the specific antibody. The IP occurred at 4 °C for 2 hours under constant rotation. Afterwards the beads were washed twice with IP/co-IP wash buffer and once with PBS. The proteins were released and denatured by adding 50 µl SDS sample buffer and heating the sample for 10 minutes at 95 °C. Finally, the proteins were analyzed by SDS-polyacrylamide gel (4.1.4.3) and Western Blot assay (4.1.4.4).
The amount of antibody and beads varied according to the amount of cells and the abundance of the protein of interest. For the anti-Ago2 IP 300 µl of the rat-anti Ago2 clone 11A9 hybridoma supernatant and 100 µl of magnetic protein G beads were used.

4.1.4.3 SDS-polyacrylamide gel electrophoresis (PAGE) of proteins

The SDS-polyacrylamide gel electrophoresis was based on the protocol described by Laemmli in 1970 (Laemmli, 1970). The bipartite SDS-PAGE is composed of the upper stacking gel and the lower resolving gel. The stacking gel has a pH of 6.8 and it also carries the wells for the samples. The resolving gel has a pH of 8.8 and usually takes up about 2/3 of the total gel. The proteins are denatured and linearized by SDS contained in the sample buffer and the running buffer. SDS leads to constant charge to mass ratios for different protein species in the sample. Thus the movement of the proteins towards the anode depends only on their size (ie, molecular weight). The running buffer contains glycine which at the pH of 6.8 in the stacking gel is mainly present in its zwitterion form and chloride ions (CL^-). Due to its zwitterionic form the glycine moves slowly though the stacking gel in comparison the negatively charged Cl^- ions which move much quicker. This leads to a zone of low ionic strength which is also a zone of high electric field strength in which the proteins move close to the glycine front. This leads the proteins to enter the resolving gel at virtually the same time. At pH 8.8 in the resolving gel the glycine deprotonates letting it run faster, thus, the field of low ionic strength dissipates and the proteins can separate depending on their size.
For the experiments the gels were poured following the instructions given in "Molecular cloning – a laboratory manual" by Sambrook, Fritsch and Maniatis (book 3, page 18.52, "Solution for Preparing Resolving Gels for Tris-Glycine SDS-PAGE"). The table below gives the recipe for the most commonly used acrylamide gel percentages.

	Stacking gel		Resolving gel	
	5 %	8 %	10 %	12 %
H_2O	1.4 ml	2.3 ml	1.9 ml	1.6 ml
30 % Bisacrylamide (19:1)	0.33 ml	1.3 ml	1.7 ml	2.0 ml
1.5 M Tris-HCl pH 6.8	0.25 ml			
1.5 M Tris-HCl pH 8.8		1.3 ml	1.3 ml	1.3 ml
SDS 10 %	0.02 ml	0.05 ml	0.05 ml	0.05 ml
APS 10 %	0.02 ml	0.05 ml	0.05 ml	0.05 ml
TEMED	0002 ml	0.005 ml	0.005 ml	0.005 ml
total	2 ml	5 ml	5 ml	5 ml

Table 8: Composition for SDS-PAGE stacking and resolving gels of different percentages

The samples for the SDS-PAGE were cooked at 95 °C for 10 minutes in the presence of SDS sample buffer, usually at a ratio of 1:1 (sample:sample buffer). Afterwards, the samples were shortly spun down to collect it at the bottom of the

reaction tube and pipetted into the wells of the gel. The gel was run at 100 - 180 V, until the bromphenol blue front from the sample buffer exited the gel. Usually a SDS-PAGE was followed by a Western Blot assay (4.1.4.4)

4.1.4.4 Western Blot

The Western Blot is used to detect proteins by a set of two antibodies. The primary antibody binds to the protein in question; the secondary antibody is covalently linked to a horseradish peroxidase and binds specifically to the Fc-part of the primary antibody. The peroxidase is in the run of the experiment used to oxidize a substrate that then emits light. This chemiluminiscence can then be detected by X-ray films.
In the first step of the procedure the proteins that were separated on a SDS-polyacrylamide gel (SDS-PAGE) (4.1.4.3) are transferred on a Polyvinylidenfluoride (PVDF) membrane by semi-dry electroblotting. Therefore, a 9 x 6 cm PVDF membrane is activated by immersing it in 100 % methanol for 1 minute and placed in the blotting chamber along with the gel. The blotting chamber was assembled in the following order: Three pieces (9 x 6 cm) of 3MM chromatography paper (Whatman paper) soaked in anode buffer, three pieces of Whatman paper soaked in anode buffer II, membrane, SDS-PAGE and three layers chromatography paper soaked in cathode buffer. It is necessary to make sure that no bubbles are between the different layers of paper, membrane and gel, otherwise some regions of the gel might not be blotted to the membrane.
After assembly an electric current of 43 mA per membrane is applied for 1.5 hours. After transfer the membrane is blocked in TBST with 10 % (w/v) dry milk (blocking buffer). The blocking is carried out under constant rocking either for 1 hour at room temperature or overnight at 4 °C.
Subsequently, the blocking buffer was discarded and the membrane was stained with an appropriate primary antibody in blocking buffer. Incubation with the primary antibody was performed at room temperature for 1 hour under constant agitation. Afterwards the antibody solution was discarded and membrane was washed thrice with TBST for 10 minutes. After washing the membrane was rocked for 1 hour in the secondary antibody solution, containing the peroxidase coupled antibody and blocking buffer. Finally the membrane was washed thrice with TBST and twice with TBS, each step taking 10 minutes. The SuperSignal West Femto Chemiluminescent substrate from Pierce was then added to the membrane, following the manufacturer's specifications. Therefore, the membrane was placed in a cut open, transparent plastic bag and 1 ml of the substrate was pipetted on top of it. Subsequently, the bag was closed and the membrane was incubated for 5 minutes at room temperature. After incubation the substrate was removed by wiping it out thoroughly and the bag

was sealed. Afterwards the membrane was exposed to x-ray film for several seconds to several hours.
The table below gives the antibodies and at what dilutions they were usually used.

Primary Antibody	Manufacturer	Dilution
rat-anti-Ago2 clone 11A9, hybridoma supernatant	G. Meister	1:50
rat-anti-ago2 clone 11A9, purified antibody	Sigma Aldrich	1:1000 – 1:3000
rat-anti-Ago1 clone 4B8	Sigma Aldrich	1:1000
Secondary Antibody	**Manufacturer**	**Dilution**
goat-anti-rat POD, light chain specific	Jackson ImmunoResearch	1:20000

Table 9: Antibodies and dilutions used for Western Blot analysis

4.1.4.5 Firefly Luciferase Assay

During the luciferase assay luciferin is converted into oxoluciferin by the luciferase of common eastern firefly *(Photinus pyralis)*. This oxidation is accompanied by emission of light which can be measured in a luminometer at a wavelength of 560 nm. Under substrate excess conditions, the emission of light is directly proportional to the amount of luciferase present and thus can be used to determine the translation efficiency of a RNA reporter construct coding for the firefly luciferase (Fluc).
For this assay 80 - 90 % confluent HuH-7 cells grown in a 6-well plate were transfected (4.1.1.5) with a RNA reporter construct under varying conditions. Three to nine hours post transfection the transfection medium was discarded and the cells were washed twice with approximately 1 ml of PBS. After washing the cells were lysed in the plate with 500 µl of Passive Lysis Buffer (PLB, Promega) at room temperature for 15 minutes under constant shaking. The lysates were transferred into a 2.0 ml reaction tube and centrifuged at 10000 rcf and 4 °C for 10 minutes to pellet the cell debris. At this point the samples may be stored for several days at -20 °C, or for prolonged storage periods -80 °C are advised. When thawing a sample it might be necessary to pellet the debris anew.
For the luciferase assay 30 µl of the lysate were used. During the procedure which 100 µl of the PJK Beetle Juice luciferase substrate were added. The measurement was carried out for 20 seconds in duplicates. To assess the unspecific background of the measurement either PLB alone or cell lysate of mock transfected cells was used as a blank.
The PJK Firefly Assay Beetle Juice substrate was prepared according to the manufacturer's specifications.

4.2 Materials

4.2.1 Bacteria

Strain	Company	Genotype
E. coli HB101	Promega	F⁻, thi-1, hsdS20 (rB⁻, mB⁻), supE44, recA13, ara-14, leuB6, proA2, lacY1, galK2, rpsL20 (strr), xyl-5, mtl-1
E. coli XL1-Blue	Stratagene	recA1, endA1, gyrA96, thi-1, hsdR17, supE44, relA1, lac [F´ proAB lacIqZ Δ M15 Tn10 (Tetr)]

4.2.2 Cell lines

Cell line	Source	Origin
HeLa	Bartenschlager laboratory, Heidelberg, Germany	Human cervix carcinoma
HuH-7	European collection of cell cultures (ECACC), Salisbury, UK	Human hepatocellular carcinoma

4.2.3 Kits

Kit	Company	Purpose
SuperSignal West Femto Chemiluminescent Substrate	Pierce	Western Blot substrate
Firefly Assay Beetle-Juice	PJK	luciferase substrate
Illustra GFX PCR DNA and Gel Band Purification Kit	GE healthcare	PCR clean up, band purification
NucleoBond PC100 Kit	Macherey-Nagel	Plasmid preparation, Maxi scale
RNeasy Mini Kit	Qiagen	RNA clean up
Wizard Plus SV Minipreps DNA purification System	Promega	Plasmid preparation, Mini scale

4.2.4 Chemicals and radiochemicals

Chemical	Company
10 x 0.5 % trypsin EDTA	Life Technologies GmbH, Darmstadt, Germany
Acetic Acid	Sigma-Aldrich Chemie GmbH, Taufkirchen, Germany
Agarose	Carl Roth GmbH & Co.KG, Karlsruhe, Germany
Ammonium Persulfate	Carl Roth GmbH & Co.KG, Karlsruhe, Germany
Bromophenol blue	Carl Roth GmbH & Co.KG, Karlsruhe, Germany
Chloroform	Sigma-Aldrich Chemie GmbH, Taufkirchen, Germany

Chemical	**Company**
Desoxyribonucleotidetriphosphates (dNTPs)	Carl Roth GmbH & Co.KG, Karlsruhe, Germany
Dimethyl Sulfoxide (DMSO)	Carl Roth GmbH & Co.KG, Karlsruhe, Germany
Di-sodium phosphate ($Na_2HPO_4 – 7H_2O$)	Carl Roth GmbH & Co.KG, Karlsruhe, Germany
Dulbacco's modified Eagle's medium (DMEM)	Life Technologies GmbH, Darmstadt, Germany
Easy tide α-^{32}P-UTP	PerkinElmer, Waltham, USA
Ethyendiamintetraacetic acid (EDTA)	Carl Roth GmbH & Co.KG, Karlsruhe, Germany
Ethanol (ACS reagent, > 99.5 %)	Sigma-Aldrich Chemie GmbH, Taufkirchen, Germany
Ethanol (denatured, 99%)	
Ethidiumbromide	Carl Roth GmbH & Co.KG, Karlsruhe, Germany
FBS gold	PAA Laboratories GmbH, Pasching, Austria
Filter Tips (10 µl, 200 µl, 1250 µl)	Sarstedt, Nümbrecht, Germany
Formamide	Carl Roth GmbH & Co.KG, Karlsruhe, Germany
Glycerol	Carl Roth GmbH & Co.KG, Karlsruhe, Germany
Glycine	Carl Roth GmbH & Co.KG, Karlsruhe, Germany
Glycoblue	Life Technologies GmbH, Darmstadt, Germany
Isoamylalcohol	Sigma-Aldrich Chemie GmbH, Taufkirchen, Germany
Lipofectamine 2000	Life Technologies GmbH, Darmstadt, Germany
Magnesium chloride ($MgCl_2$)	Carl Roth GmbH & Co.KG, Karlsruhe, Germany
Methanol	Carl Roth GmbH & Co.KG, Karlsruhe, Germany
Nonidet P-40, Biochemica [Ersatzprodukt] (NP-40)	AppliChem GmbH, Darmstadt, Germany
Pefablock	Roche GmbH, Mannheim, Germany
Penicillin/Streptomycin 100 x (Pen/Strep)	Life Technologies GmbH, Darmstadt, Germany
Potassium chloride (KCl)	Carl Roth GmbH & Co.KG, Karlsruhe, Germany
Potassium phosphate (KH_2PO_4)	Carl Roth GmbH & Co.KG, Karlsruhe, Germany
Proteinase K [20 mg/ml]	NEB, Ipswich, USA
Reaction Tubes (2 ml, Safe Lock)	Sarstedt, Nümbrecht, Germany
Ribonucleotidetriphosphates (rNTPs)	Carl Roth GmbH & Co.KG, Karlsruhe, Germany
Roti Phenol	Carl Roth GmbH & Co.KG, Karlsruhe, Germany
Rotiphorese Gel 40 (19:1)	Carl Roth GmbH & Co.KG, Karlsruhe, Germany
Skimmed milk powder	EDEKA Krenschker, Gießen, Germany
Sodium acetate	Carl Roth GmbH & Co.KG, Karlsruhe, Germany
Sodium chloride (NaCl)	Carl Roth GmbH & Co.KG, Karlsruhe, Germany
Sodium Dodecyl Dulfate (SDS)	Carl Roth GmbH & Co.KG, Karlsruhe, Germany
Sodium fluoride (NaF)	Sigma-Aldrich Chemie GmbH, Taufkirchen, Germany
TEMED (N,N,N',N'-Tetramethylethylendiamin)	Carl Roth GmbH & Co.KG, Karlsruhe, Germany
TriFast reagent	Peqlab Biotechnologie GmbH, Erlangen Germany
Tris base	Carl Roth GmbH & Co.KG, Karlsruhe, Germany
Tween20	Sigma-Aldrich Chemie GmbH, Taufkirchen, Germany
Urea	Carl Roth GmbH & Co.KG, Karlsruhe, Germany

Chemical	Company
Xylenecyanol blue	Carl Roth GmbH & Co.KG, Karlsruhe, Germany
β-Mercaptoethanol	Sigma-Aldrich Chemie GmbH, Taufkirchen, Germany
LB medium	Carl Roth GmbH & Co.KG, Karlsruhe, Germany

4.2.5 Enzymes

Enzyme	Company
DpnI	Fermentas
One Taq Polymerase	NEB
Pfu_{turbo} high fidelity DNA polymerase	Stratagene
Proteinase K	NEB
Sp6-RNA Polymerase	Fermentas
T7-RNA Polymerase	Fermentas
Various restriction enzymes	Fermentas or NEB

4.2.6 Consumables

Consumable	Company
9 cm tissue culture dish	Sarstedt, Nümbrecht, Germany
Autoclavable Waste Bags	Sarstedt, Nümbrecht, Germany
Chromatography Paper 3MM Chr (Whatman Paper)	VWR, Darmstadt, Germany
Filter Tips (10 µl, 20 µl, 200 µl, 1250 µl)	Sarstedt, Nümbrecht, Germany
Pipette Tips (10 µl, 200 µl, 1000 µl)	Sarstedt, Nümbrecht, Germany
PVDF Membrane Immobilon-P, 0.45 µm	Milipore, Billerica, USA
Reaction Tubes (15 ml, 50 ml)	Sarstedt, Nümbrecht, Germany
Reaction Tubes (2.0 ml safe lock)	Sarstedt, Nümbrecht, Germany
Sterile Serological Pipettes (5 ml, 10 ml, 25 ml)	Greiner, Frickenhausen, Germany
Tissue Culture Flasks (25 cm^2, 75 cm^2, 175 cm^2)	Sarstedt, Nümbrecht, Germany
Tissue culture plates (24-wells, 6-wells)	Sarstedt, Nümbrecht, Germany
Luminometer tubes 5ml, 75 x 12 mm, PS	Sarstedt, Nümbrecht, Germany
Gene Pulser / Micro Pulser electroporation cuvettes	Biorad, München, Germany

4.2.7 DNA Primer

Name	Sequence
3'-UTR-only for	5'-CGTCAGAAGCTAGCGATTTAGGTG-3'
HCMV-4986 for	5'-CCAATAGGCCGAAATCGGCAAAATCCC-3'
HCV 3X rev	5'-ACATGATCTGCAGAGAGGCCAG-3'

Name	Sequence
HCV-FL 334-363 rev	5’-GAGGTTTAGGATTCGTGCTCATGGTGCACG-3’
HCV-FL 380-406 rev	5’-GGCGTCTTCCATGGTTTTTCTTTGAGG-3’
HCV-FL m1m2 for	5’-CGACTCACTATAGGTGGCCCCGATTGGGGGCGAGCGCGGCTTCTAGATGTACAG -3’
HCV-FL m1m2 rev	5’-CTGTACATCTAGAAGCCGCGCTCGCCCCCAATCGGGGCCACCTATAGTGAGTCG -3’
miR122 site2-10nts-stem loop II fwd	5’-CATAGATCACTCCTCTCGAGGTGCCTGTGAGGAACTAC-3’
miR122 site2-10nts-stem loop II rev	5’-GTAGTTCCTCACAGGCACCTCGAGAGGAGTGATCTATG-3’
miR122 site2-20nts-stem loop II fwd	5’-CCATAGATCACTCCGACTGATCTCGAGGTGGACTCCTGTGAGGAAC-3’
miR122 site2-20nts-stem loop II rev	5’-GTTCCTCACAGGAGTCCACCTCGAGATCAGTCGGAGTGATCTATGG-3’
miR122 site2-5nts-stem loop II fwd	5’-CCACCATAGATCACTCCTCGAGCCTGTGAGGAACTACTGTC-3’
miR122 site2-5nts-stem loop II rev	5’-ACAGTAGTTCCTCACAGGCTCGAGGAGTGATCTATGGTGG-3’
NS5Bloop-3’UTRfwd	5’-GCAGGCTTAATACGACTCACTATAGCTCCTCCCCAACCGATGAAGGTTGGGGTAAACACTCCGGCC-3’
NS5Bloop-3’UTRrev	5’-ACATGATCTGCAGAGAGGCCAGTATCAGC-3’
RT-HCV pos. 233 – 253	5’-CTAGCAGTCTCGCGGGGGCAC-3’
RT-HCV pos. 9 – 29	5’-CGATTGGGGGCGACACTCCAC-3’

4.2.8 RNA Oligonucleotides

microRNA	Sequence
miR-122 mat	5’-℗UGGAGUGUGACAAUGGUGUUUG-3’
miR-122*	5’-℗AACGCCAUUAUCACACUAAAUA-3’
miR-124 mat	5’-℗UGGAGUGUGACAAUGGUGUUUGUC-3’
miR-124*	5’-℗GCAACGCCAUUAUCACACUAAAUA-3’

4.2.9 Plasmids

Plasmid *(also see appendix)*	**Producer**
3-UTRonly	Niepmann laboratory
pHCV - FL	Niepmann laboratory
pHCV - SIN	Niepmann laboratory
pHCV - FL miR-122 site2-5nts-stemloop II	Dominik Conrad, Niepmann laboratory
pHCV - FL miR-122 site2-10nts-stemloop II	Dominik Conrad, Niepmann laboratory
pHCV - FL miR-122 site2-20nts-stemloop II (later pHCV - FL stem)	Dominik Conrad, Niepmann laboratory

4.2.10 Antibodies and magnetic beads

Antibody / Magnetic Beads	**Company**
AffiniPure goat-anti-Rat, LightChain*Specific	Jackson ImmunoResearch, Newmarket, UK
goat-anti-PTBP1	Abcam, Cambridge, UK
Protein A magnetic beads	NEB, Ipswich, USA
Protein G magnetic beads	NEB, Ipswich, USA
rabit-anti-eIF3a	Abcam, Cambridge, UK
rat-anti-Ago1, clone 4B8	Sigma Aldrich, St. Louis, USA
rat-anti-Ago2, clone 11A9	Sigma Aldrich, St. Louis, USA

4.2.11 Laboratory Equipment

Device	**Company**
B15 petri dish incubator	Thermo Scientific GmbH, Dreieich, Germany
BioPhotometer	Eppendorf, Wesseling-Berzdorf, Germany
CB series CO_2 Incubator	Binder GmbH, Tuttlingen, Germany
Centrifuge 5417R	Eppendorf, Wesseling-Berzdorf, Germany
Cronex Lightning Plus X-ray cassette	DuPont, Wilmington, USA
Destamat, bi-destiller	Heraeus, Hanau, Germany
Digital-pH-Meter 644	Knick Elektronische Messgeräte GmbH & Co. KG, Berlin, Germany
Duomax 1030 shaker	Heidolph, Schwabach, Germany
Easyject Prima electroporator	EquiBio, Willstätt, Germany
ED240 hot-air cabinet	Binder GmbH, Tuttlingen, Germany
EPS 5007400 electrophoresis power supply	Pharmacia Fine Chemicals, Uppsala, Sweden
EPS 601 electrophoresis power supply	Amersham Bioscience, Glattbrugg, Switzerland
FastBlot B44 semidry blotting chamber	Biometra GmbH, Göttingen, Germany
GelDoc XR gel documentation system	BioRad, München, Germany
HA 2448 BS LaminAir lamina flow	Heraeus, Hanau, Germany
Heat-stir US152 magnetic stirrer	Stuart, Stone, UK
Isopropanol tank	Qualilab, Olivet, France
Julabo 7A water bath	Julabo, Seelbach, Germany

Device	Company
Julabo U3 water bath	Julabo, Seelbach, Germany
Labquake Rotator	Thermo Scientific GmbH, Dreieich, Germany
LB 124 Geiger counter	Berthold Technologies GmbH & Co.KG, Bad Wildbad, Germany
Leica DM IL invers microscope	Leica Microsystems, Wetzlar, Germany
Lumat LB 9501 luminometer	Berthold Technologies GmbH & Co.KG, Bad Wildbad, Germany
MagnaRack magnetic separation rack	Life Technologies GmbH, Darmstadt, Germany
MBT 250 heating block	Kleinfeld Labortechnik GmbH, Gehrden, Germany
Micropipettors (2 µl-1000 µl)	Gilson, Middleton, USA
Model 583 Gel Dryer	Biorad, München, Germany
Multifuge 3L-R	Heraeus, Hanau, Germany
Pipetboy comfort pipettor	Integra Biosciences GmbH, Fernwald, Germany
Polystar 100GE sealer	Rische + Herfurth GmbH, Hamburg, Germany
Severin 700 microwave	Severin, Sundern, Germany
Tecan infinite M200 multimode reader	Tecan Deutschland GmbH, Crailsheim, Germany
Thermicon T laboratory-type annealing furnace	Heraeus, Hanau, Germany
TProfessional PCR cycler	Biometra GmbH, Göttingen, Germany
V150 autoclave	Systec, Wettenberg, Germany
Vortex Genie 2	Scientific Industries, New York, USA

4.2.12 Buffers

4.2.12.1 Tissue Culture Buffers

10 x PBS	80 g NaCl 2 g KCl 26.8 g $Na_2HPO_4 – 7H_2O$ 2.4 g KH_2PO_4 @ 800 ml H_2O adjust pH 7.4 with HCl; adjust volume to 1 l with H_2O for 1 x PBS dilute 1:10 with de-ionized H_2O; sterilize by autoclaving
0.5 % Trypsin EDTA	dilute 10 x 0.5 % Trypsin EDTA 1:10 in 1 x PBS
DMEM + 10 % FBS + 1% Pen/Strep (DMEM 10 %)	add 50 ml FBS gold and 5 ml Pen/Strep to 500 ml DMEM
DMEM + 20 % FBS + 10 % DMSO (cryomedium)	add 10 ml FBS gold and 5ml DMSO @ 50ml DMEM

4.2.12.2 Gel Buffers

10 x TBE (Tris-borate)	108 g	Tris
	55 g	Boric Acid
	40 ml	0.5 M EDTA (pH. 8.0)
	@ 1 l	ddH_2O
50 x TAE (Tris-acetate)	242 g	Tris
	100 ml	0.5 M EDTA (pH 8.0)
	57.1 ml	Acetic Acid
	@ 1 l	ddH_2O

4.2.12.3 Co-IP Buffers

RNA Sample Buffer	80 %	Formamide
	10 %	Gycerol
	50 mM	EDTA pH 7.5
	few grains bromphenolblue and xylenecyanole	
	@ 20 ml	ddH_2O
Proteinase K Buffer	200 mM	Tris-HCl pH 7.5
	300 mM	NaCl
	25 mM	EDTA pH 7.5
	2 %	SDS
	@ 50 ml	ddH_2O
Co-IP Lysis Buffer	25 mM	Tris-HCl pH 7.5
	150 mM	KCl
	2 mM	EDTA pH 7.5
	0.5 mM	DTT
	0.5 %	NP-40
	@ 250 ml	ddH_2O
Co-IP-Wash Buffer	50 mM	Tris-HCl pH 7.5
	0.3 M	NaCl
	5 mM	$MgCl_2$
	0.05 %	NP-40
	@ 500 ml	ddH_2O
Fixer solution	7.5 %	Acetic Acid
	5 %	Ethanol
	@ 1 l	de-ionized H_2O
Chloroform/Isoamylalcohol	24 ml	Chloroform
	1 ml	Isoamylalcohol

4.2.12.4 IP Buffers

IP-Lysis buffer	20 mM	Tris-HCl, pH 7.5
	150 mM	NaCl
	0.5 %	Nonidet P-40
	2 mM	EDTA
	0.5 mM	DTT
	1 mM	NaF
	1 mM	Pefablock
	@ 250 ml	ddH_2O
IP-Wash Buffer	50 mM	Tris-HCl pH 7.5
	0.3 M	NaCl
	5 mM	$MgCl_2$
	0.05 %	NP-40
	@ 500 ml	ddH_2O

4.2.12.5 SDS-PAGE Buffers

Acrylamide 30 %	Dilute 150 ml Rotiphorese Gel 40 (19:1) with H_2O to a final volume of 200 ml	
1.5 M Tris pH 8.8 (resolving gel buffer)	90.75 g	Tris
	@400 ml	H_2O
	adjust pH to 8,8 with HCl; adjust volume to 500 ml	
1.5 M Tris pH 6.8 (stacking gel buffer)	90.75 g	Tris
	@400 ml	H_2O
	adjust pH to 6,8 with HCl; adjust volume to 500 ml	
10 % SDS (w/v)	5 g	Sodium Dodecyl Sulfate
	@ 50 ml	H_2O
10 % APS	0.1 g	Ammonium Persulfate
	@ 10 ml	H_2O
10 x SDS Running Buffer	10 g	SDS
	30 g	Tris
	144 g	Glycine
	@ 1 l	de-inonized H_2O,
	for 1 x SDS Running Buffer dilute 1:10	

SDS Sample Buffer	20 %	Glycerol
	20 %	β-Mercaptoethanol
	60 %	10 % SDS
	125 mM	Tris
	few grains of Bromephenole blue	
	@ 25 ml	ddH_2O

4.2.12.6 Western Blot Buffer

Cathode Buffer	3 g	Tris
	@ 800 ml	H_2O
	adjust pH to 9.4 with HCl,	
	add 100 ml Methanol, adjust volume to 1 l	
Anode Buffer I	36.3 g	Tris
	@ 800 ml	H_2O
	adjust pH to 10.4 with HCl,	
	add 100 ml Methanol, adjust volume to 1 l	
Anode Buffer II	3 g	Tris
	@ 800 ml	H_2O
	adjust pH to 10.4 with HCl,	
	add 100 ml Methanol, adjust volume to 1 l	
10 x TBS	60.5 g	Tris
	87.6 g	NaCl
	@ 800 ml	H_2O
	adjust pH to 7.5 with HCl,	
	adjust volume to 1 l; for 1 x TBS dilute 1:10 de-ionized H_2O	
TBS + 0.25 % Tween20 (TBST)	add 2.5 ml Tween20 to 1 l of 1 x TBS	
TBST + 10 % milk powder (blocking buffer)	add 10 g of skimmed milk powder to 100 ml TBST	

5 Glossary

5.1 Abbreviations

µ	micro (10^{-6})
Ago	Protein of the argonaute family
AmpR	Ampicilline resistance
ApoE	Apolipoprotein E
Arg	Arginine
ATP	Adenosine triphosphate
ATX2	Ataxin 2
bp	Base pairs
BSC	Bio safety cabinet
CD81	Cluster of Differenciation 81
CLDN1	Claudin-1
CSFV	Classical swine fever virus
ddH2O	Double distilled water
DDX	DEAD-box helicase
DMEM	Dulbecco's modified Eagle's medium
DNA	Desoxyribonucleic acid
DNase	Desoxyribonuleic acid endonuclease
dNTP	Desoxy ribonucleic acid tri phosphate
E. coli	Escherischia coli
ECACC	European collection of cell cultures
eIF	Eukaryotic (translation)Initiation Factor
ER	Endoplasmic reticulum
et al.	et alii (and others)
EtBr	ethidium bromide
FBS	Fetal bovine serum
FLuc	Firefly luciferase
FMDV	Foot and mouth disease
GAG	glycosaminoglycan
GBV-B	GB-virus B
h	hour
HCC	hepatocellular carcinoma
HCl	Hydrochloric acid
HCV	Hepatitis C virus
His	Histidine
hnRNP	heterogenous ribonucleoproteins
HSC	Heat shock cognate protein
IFITM1	Interferone induced transmembrane protein 1
IFN	Interferone
Ig	immune globulin
IMP-1	insulin-like growth factor-II mRNA-binding protein

IP	immunoprezipitation
IRES	internal Ribosome entry site
ITAF	IRES trans-acting factor
kb	kilo bases
kDa	kilo Dalton
KO	Knock out
l	liter
LB	Lysogeny Broth
LD	lipid droplet
LSm	like SM protein
M	Molar mol/l
m	milli (10^{-3})
mat	mature
min	minute
miR	microRNA
miR*	Passanger strand of miR duplexes
miRNP complex	microRNA-protein complex
mRNA	messanger RNA
NEB	New England Biolabs
NP-40	Nonidet P-40
NS	Nonstructural protein
NSAP1	NS1-associated protein 1
Nt(s)	Nucleotide(s)
OCLN	Occludin
OD	optical density
ORF	open reading frame
P	phosphate
PABP	poly(A) binding protein
PACT	Protein kinase R-associated activator
PAGE	Polyacrylamide gel electrophoresis
P-body	processing body
PBS	phosphate buffered saline
PCBP1	Poly(rC)-binding protein 1
PCR	polymerase chain reaction
PEG	polyethylene glycol
Pen/Strep	Penicillin/Streptomycin solution
pH	Decimal cologarithm of hydrogen concentration
PLB	Passive lysis buffer
pre	precursor
pri	primary
PTB	Polypyrimidine tract-binding protein
PVDF	Polyvinylidene fluoride
Py	poly-pyrimidine tract
rcf	relative centrifugal force
RISC	RNA induces silencing complex
RLuc	Renilla luciferase
RNA	ribonucleic acid

RNase	RNA endonuclease
rNTP	ribonucleic acid tri-phosphate
rpm	rounds per minute
RRM	RNA recognition motif
RT-PCR	reverse transcriptase-PCR
rUTP	Uridine triphosphate
s	second
SIN	short and in frame
SL	Stem loop
SR-BI	Scavenger receptor BI
$t_{1/2}$	half-life
TAE	Tris-acetate-EDTA buffer
Taq	*thermo aquaticus*
TBE	Tris-borate-EDTA buffer
TBS	Tris buffered saline
TBST	Tris buffered saline with Tween20
TGF-β	Transforming growth factor-β
TRBP	HIV-1 TAR RNA-binding protein
tRNA	transfer RNA
$tRNA_i^{Met}$	Initiator tRNA
U	Unit
UTR	untranslated region
UV	Ultra violet
V	Volt
v/v	Volume/Volume
VR	Variable region
w/v	Weight/volume
WHO	World health organization
wt	Wild type

5.2 Figures

5.3 Tables

5.4 Citations

Andre P, Komurian-Pradel F, Deforges S, Perret M, Berland JL, Sodoyer M, Pol S, Brechot C, Paranhos-Baccala G, Lotteau V (2002) Characterization of low- and very-low-density hepatitis C virus RNA-containing particles. *J Virol* **76:** 6919-6928

Ariumi Y, Kuroki M, Kushima Y, Osugi K, Hijikata M, Maki M, Ikeda M, Kato N (2011a) Hepatitis C virus hijacks P-body and stress granule components around lipid droplets. *J Virol* **85:** 6882-6892

Ariumi Y, Kuroki M, Maki M, Ikeda M, Dansako H, Wakita T, Kato N (2011b) The ESCRT system is required for hepatitis C virus production. *PLoS One* **6:** e14517

Bai S, Nasser MW, Wang B, Hsu SH, Datta J, Kutay H, Yadav A, Nuovo G, Kumar P, Ghoshal K (2009) MicroRNA-122 inhibits tumorigenic properties of hepatocellular carcinoma cells and sensitizes these cells to sorafenib. *J Biol Chem* **284:** 32015-32027

Baltimore D (1971) Expression of animal virus genomes. *Bacteriol Rev* **35:** 235-241

Bankwitz D, Steinmann E, Bitzegeio J, Ciesek S, Friesland M, Herrmann E, Zeisel MB, Baumert TF, Keck ZY, Foung SK, Pecheur EI, Pietschmann T (2010) Hepatitis C virus hypervariable region 1 modulates receptor interactions, conceals the CD81 binding site, and protects conserved neutralizing epitopes. *J Virol* **84:** 5751-5763

Barba G, Harper F, Harada T, Kohara M, Goulinet S, Matsuura Y, Eder G, Schaff Z, Chapman MJ, Miyamura T, Brechot C (1997) Hepatitis C virus core protein shows a cytoplasmic localization and associates to cellular lipid storage droplets. *Proc Natl Acad Sci U S A* **94:** 1200-1205

Barreau C, Dutertre S, Paillard L, Osborne HB (2006) Liposome-mediated RNA transfection should be used with caution. *Rna* **12:** 1790-1793

Bartenschlager R, Frese M, Pietschmann T (2004) Novel insights into hepatitis C virus replication and persistence. *Adv Virus Res* **63:** 71-180

Behrens SE, Tomei L, De Francesco R (1996) Identification and properties of the RNA-dependent RNA polymerase of hepatitis C virus. *Embo J* **15:** 12-22

Beitzinger M, Meister G (2011) Experimental identification of microRNA targets by immunoprecipitation of Argonaute protein complexes. *Methods Mol Biol* **732:** 153-167

Berezhna SY, Supekova L, Sever MJ, Schultz PG, Deniz AA (2011) Dual regulation of hepatitis C viral RNA by cellular RNAi requires partitioning of Ago2 to lipid droplets and P-bodies. *Rna* **17:** 1831-1845

Berry KE, Waghray S, Mortimer SA, Bai Y, Doudna JA (2011) Crystal structure of the HCV IRES central domain reveals strategy for start-codon positioning. *Structure* **19:** 1456-1466

Bhanja Chowdhury J, Shrivastava S, Steele R, Di Bisceglie AM, Ray R, Ray RB (2012) Hepatitis C virus infection modulates expression of interferon stimulatory gene IFITM1 by upregulating miR-130A. *J Virol* **86:** 10221-10225

Boulant S, Montserret R, Hope RG, Ratinier M, Targett-Adams P, Lavergne JP, Penin F, McLauchlan J (2006) Structural determinants that target the hepatitis C virus core protein to lipid droplets. *J Biol Chem* **281:** 22236-22247

Bradley DW, McCaustland KA, Cook EH, Schable CA, Ebert JW, Maynard JE (1985) Posttransfusion non-A, non-B hepatitis in chimpanzees. Physicochemical evidence that the tubule-forming agent is a small, enveloped virus. *Gastroenterology* **88:** 773-779

Bressanelli S, Stiasny K, Allison SL, Stura EA, Duquerroy S, Lescar J, Heinz FX, Rey FA (2004) Structure of a flavivirus envelope glycoprotein in its low-pH-induced membrane fusion conformation. *Embo J* **23:** 728-738

Brown EA, Zhang H, Ping LH, Lemon SM (1992) Secondary structure of the 5' nontranslated regions of hepatitis C virus and pestivirus genomic RNAs. *Nucleic Acids Res* **20:** 5041-5045

Bruni R, Marcantonio C, Tritarelli E, Tataseo P, Stellacci E, Costantino A, Villano U, Battistini A, Ciccaglione AR (2011) An integrated approach identifies IFN-regulated microRNAs and targeted mRNAs modulated by different HCV replicon clones. *BMC Genomics* **12:** 485

Bung C, Bochkaeva Z, Terenin I, Zinovkin R, Shatsky IN, Niepmann M (2010) Influence of the hepatitis C virus 3'-untranslated region on IRES-dependent and cap-dependent translation initiation. *FEBS Lett* **584:** 837-842

Castanotto D, Sakurai K, Lingeman R, Li H, Shively L, Aagaard L, Soifer H, Gatignol A, Riggs A, Rossi JJ (2007) Combinatorial delivery of small interfering RNAs reduces RNAi efficacy by selective incorporation into RISC. *Nucleic Acids Res* **35:** 5154-5164

Castoldi M, Vujic Spasic M, Altamura S, Elmen J, Lindow M, Kiss J, Stolte J, Sparla R, D'Alessandro LA, Klingmuller U, Fleming RE, Longerich T, Grone HJ, Benes V, Kauppinen S, Hentze MW, Muckenthaler MU (2011) The liver-specific microRNA miR-122 controls systemic iron homeostasis in mice. *J Clin Invest* **121:** 1386-1396

Chang J, Nicolas E, Marks D, Sander C, Lerro A, Buendia MA, Xu C, Mason WS, Moloshok T, Bort R, Zaret KS, Taylor JM (2004) miR-122, a mammalian liver-specific microRNA, is processed from hcr mRNA and may downregulate the high affinity cationic amino acid transporter CAT-1. *RNA Biol* **1:** 106-113

Chendrimada TP, Gregory RI, Kumaraswamy E, Norman J, Cooch N, Nishikura K, Shiekhattar R (2005) TRBP recruits the Dicer complex to Ago2 for microRNA processing and gene silencing. *Nature* **436:** 740-744

Choo QL, Kuo G, Weiner AJ, Overby LR, Bradley DW, Houghton M (1989) Isolation of a cDNA clone derived from a blood-borne non-A, non-B viral hepatitis genome. *Science* **244:** 359-362

Chu CY, Rana TM (2006) Translation repression in human cells by microRNA-induced gene silencing requires RCK/p54. *PLoS Biol* **4:** e210

Coller KE, Heaton NS, Berger KL, Cooper JD, Saunders JL, Randall G (2012) Molecular determinants and dynamics of hepatitis C virus secretion. *PLoS Pathog* **8:** e1002466

Conrad KD, Giering F, Erfurth C, Neumann A, Fehr C, Meister G, Niepmann M (2013) MicroRNA-122 dependent binding of Ago2 protein to hepatitis C virus RNA is associated with enhanced RNA stability and translation stimulation. *PLoS One* **8:** e56272

Corless L, Crump CM, Griffin SD, Harris M (2010) Vps4 and the ESCRT-III complex are required for the release of infectious hepatitis C virus particles. *J Gen Virol* **91:** 362-372

Coulouarn C, Factor VM, Andersen JB, Durkin ME, Thorgeirsson SS (2009) Loss of miR-122 expression in liver cancer correlates with suppression of the hepatic phenotype and gain of metastatic properties. *Oncogene* **28:** 3526-3536

Czech B, Hannon GJ (2011) Small RNA sorting: matchmaking for Argonautes. *Nat Rev Genet* **12:** 19-31

Dmitriev SE, Terenin IM, Andreev DE, Ivanov PA, Dunaevsky JE, Merrick WC, Shatsky IN (2010) GTP-independent tRNA delivery to the ribosomal P-site by a novel eukaryotic translation factor. *J Biol Chem* **285:** 26779-26787

Dreux M, Pietschmann T, Granier C, Voisset C, Ricard-Blum S, Mangeot PE, Keck Z, Foung S, Vu-Dac N, Dubuisson J, Bartenschlager R, Lavillette D, Cosset FL (2006) High density lipoprotein inhibits hepatitis C virus-neutralizing antibodies by stimulating cell entry via activation of the scavenger receptor BI. *J Biol Chem* **281:** 18285-18295

Egger D, Wolk B, Gosert R, Bianchi L, Blum HE, Moradpour D, Bienz K (2002) Expression of hepatitis C virus proteins induces distinct membrane alterations including a candidate viral replication complex. *J Virol* **76:** 5974-5984

Esau C, Davis S, Murray SF, Yu XX, Pandey SK, Pear M, Watts L, Booten SL, Graham M, McKay R, Subramaniam A, Propp S, Lollo BA, Freier S, Bennett CF, Bhanot S, Monia BP (2006) miR-122 regulation of lipid metabolism revealed by in vivo antisense targeting. *Cell Metab* **3:** 87-98

Filbin ME, Kieft JS (2011) HCV IRES domain IIb affects the configuration of coding RNA in the 40S subunit's decoding groove. *Rna* **17:** 1258-1273

Filipowicz W, Bhattacharyya SN, Sonenberg N (2008) Mechanisms of post-transcriptional regulation by microRNAs: are the answers in sight? *Nat Rev Genet* **9:** 102-114

Fraser CS, Doudna JA (2007) Structural and mechanistic insights into hepatitis C viral translation initiation. *Nat Rev Microbiol* **5:** 29-38

Friebe P, Lohmann V, Krieger N, Bartenschlager R (2001) Sequences in the 5' nontranslated region of hepatitis C virus required for RNA replication. *J Virol* **75:** 12047-12057

Gastaminza P, Cheng G, Wieland S, Zhong J, Liao W, Chisari FV (2008) Cellular determinants of hepatitis C virus assembly, maturation, degradation, and secretion. *J Virol* **82:** 2120-2129

Giering F (in preparation) Translationseffizienz des HCV-RNA-Genoms unter verschiedenen Bedingungen und Analyse von Translations-Initiationskomplexen. MD Ph.D Thesis, Bioschemisches Institut, Justus Liebig-University, Giessen

Gingras AC, Raught B, Sonenberg N (1999) eIF4 initiation factors: effectors of mRNA recruitment to ribosomes and regulators of translation. *Annu Rev Biochem* **68:** 913-963

Goergen D, Niepmann M (2012) Stimulation of Hepatitis C Virus RNA translation by microRNA-122 occurs under different conditions in vivo and in vitro. *Virus Res* **167:** 343-352

Gosert R, Egger D, Lohmann V, Bartenschlager R, Blum HE, Bienz K, Moradpour D (2003) Identification of the hepatitis C virus RNA replication complex in HuH-7 cells harboring subgenomic replicons. *J Virol* **77:** 5487-5492

Gregory RI, Yan KP, Amuthan G, Chendrimada T, Doratotaj B, Cooch N, Shiekhattar R (2004) The Microprocessor complex mediates the genesis of microRNAs. *Nature* **432:** 235-240

Gwack Y, Kim DW, Han JH, Choe J (1996) Characterization of RNA binding activity and RNA helicase activity of the hepatitis C virus NS3 protein. *Biochem Biophys Res Commun* **225:** 654-659

Haase AD, Jaskiewicz L, Zhang H, Laine S, Sack R, Gatignol A, Filipowicz W (2005) TRBP, a regulator of cellular PKR and HIV-1 virus expression, interacts with Dicer and functions in RNA silencing. *EMBO Rep* **6:** 961-967

He LF, Alling D, Popkin T, Shapiro M, Alter HJ, Purcell RH (1987) Determining the size of non-A, non-B hepatitis virus by filtration. *J Infect Dis* **156:** 636-640

Henke J (2010) Einfluss der leberspezifischen microRNA-122 auf die Regulation der Translation der Hepatitis C Virus-RNA. Ph.D Thesis, Biochemisches Institut, Justus Liebig-University, Giessen

Henke JI, Goergen D, Zheng J, Song Y, Schüttler CG, Fehr C, Jünemann C, Niepmann M (2008) microRNA-122 stimulates translation of hepatitis C virus RNA. *Embo J* **27:** 3300-3310

Hoofnagle JH (2002) Course and outcome of hepatitis C. *Hepatology* **36:** S21-29

Huang L, Hwang J, Sharma SD, Hargittai MR, Chen Y, Arnold JJ, Raney KD, Cameron CE (2005) Hepatitis C virus nonstructural protein 5A (NS5A) is an RNA-binding protein. *J Biol Chem* **280:** 36417-36428

Huys A, Thibault PA, Wilson JA (2013) Modulation of Hepatitis C Virus RNA accumulation and translation by DDX6 and miR-122 are mediated by separate mechanisms. *PLoS One epub ahead of print*

Ishida H, Tatsumi T, Hosui A, Nawa T, Kodama T, Shimizu S, Hikita H, Hiramatsu N, Kanto T, Hayashi N, Takehara T (2011) Alterations in microRNA expression profile in HCV-infected hepatoma cells: involvement of miR-491 in regulation of HCV replication via the PI3 kinase/Akt pathway. *Biochem Biophys Res Commun* **412:** 92-97

Jackson RJ, Hellen CU, Pestova TV (2010) The mechanism of eukaryotic translation initiation and principles of its regulation. *Nat Rev Mol Cell Biol* **11:** 113-127

Jangra RK, Yi M, Lemon SM (2010) Regulation of hepatitis C virus translation and infectious virus production by the microRNA miR-122. *J Virol* **84:** 6615-6625

Janssen HL, Reesink HW, Lawitz EJ, Zeuzem S, Rodriguez-Torres M, Patel K, van der Meer AJ, Patick AK, Chen A, Zhou Y, Persson R, King BD, Kauppinen S, Levin AA, Hodges MR (2013) Treatment of HCV infection by targeting microRNA. *N Engl J Med* **368:** 1685-1694

Jeong SW, Jang JY, Chung RT (2012) Hepatitis C virus and hepatocarcinogenesis. *Clin Mol Hepatol* **18:** 347-356

Jopling CL, Yi M, Lancaster AM, Lemon SM, Sarnow P (2005) Modulation of hepatitis C virus RNA abundance by a liver-specific MicroRNA. *Science* **309:** 1577-1581

Khvorova A, Reynolds A, Jayasena SD (2003) Functional siRNAs and miRNAs exhibit strand bias. *Cell* **115:** 209-216

Kim DW, Gwack Y, Han JH, Choe J (1995) C-terminal domain of the hepatitis C virus NS3 protein contains an RNA helicase activity. *Biochem Biophys Res Commun* **215:** 160-166

Kim JH, Park SM, Park JH, Keum SJ, Jang SK (2011) eIF2A mediates translation of hepatitis C viral mRNA under stress conditions. *Embo J* **30:** 2454-2464

Kim VN, Han J, Siomi MC (2009) Biogenesis of small RNAs in animals. *Nat Rev Mol Cell Biol* **10:** 126-139

Krützfeldt J, Rajewsky N, Braich R, Rajeev KG, Tuschl T, Manoharan M, Stoffel M (2005) Silencing of microRNAs in vivo with 'antagomirs'. *Nature* **438:** 685-689

Kutay H, Bai S, Datta J, Motiwala T, Pogribny I, Frankel W, Jacob ST, Ghoshal K (2006) Downregulation of miR-122 in the rodent and human hepatocellular carcinomas. *J Cell Biochem* **99:** 671-678

Laemmli UK (1970) Cleavage of structural proteins during the assembly of the head of bacteriophage T4. *Nature* **227:** 680-685

Lagos-Quintana M, Rauhut R, Lendeckel W, Tuschl T (2001) Identification of novel genes coding for small expressed RNAs. *Science* **294:** 853-858

Lanford RE, Hildebrandt-Eriksen ES, Petri A, Persson R, Lindow M, Munk ME, Kauppinen S, Orum H (2010) Therapeutic silencing of microRNA-122 in primates with chronic hepatitis C virus infection. *Science* **327:** 198-201

Lee Y, Hur I, Park SY, Kim YK, Suh MR, Kim VN (2006) The role of PACT in the RNA silencing pathway. *Embo J* **25:** 522-532

LeFebvre AK, Korneeva NL, Trutschl M, Cvek U, Duzan RD, Bradley CA, Hershey JW, Rhoads RE (2006) Translation initiation factor eIF4G-1 binds to eIF3 through the eIF3e subunit. *J Biol Chem* **281:** 22917-22932

Lindenbach BD (2013) Viron Assembly and Release. *Current Topics in Microbiology and Immunology* **369**:199-218

Liu J, Valencia-Sanchez MA, Hannon GJ, Parker R (2005) MicroRNA-dependent localization of targeted mRNAs to mammalian P-bodies. *Nat Cell Biol* **7:** 719-723

Liu X, Wang T, Wakita T, Yang W (2010) Systematic identification of microRNA and messenger RNA profiles in hepatitis C virus-infected human hepatoma cells. *Virology* **398:** 57-67

Lohmann V (2013) Hepatitis C Virus RNA Replication. *Current Topics in Microbiology and Immunology* **369:** 167-98

Lohmann V, Korner F, Herian U, Bartenschlager R (1997) Biochemical properties of hepatitis C virus NS5B RNA-dependent RNA polymerase and identification of amino acid sequence motifs essential for enzymatic activity. *J Virol* **71:** 8416-8428

Lund E, Guttinger S, Calado A, Dahlberg JE, Kutay U (2004) Nuclear export of microRNA precursors. *Science* **303:** 95-98

Machlin ES, Sarnow P, Sagan SM (2011) Masking the 5' terminal nucleotides of the hepatitis C virus genome by an unconventional microRNA-target RNA complex. *Proc Natl Acad Sci U S A* **108:** 3193-3198

Makeyev AV, Liebhaber SA (2002) The poly(C)-binding proteins: a multiplicity of functions and a search for mechanisms. *Rna* **8:** 265-278

Maraia RJ, Lamichhane TN (2011) 3' processing of eukaryotic precursor tRNAs. *Wiley Interdiscip Rev RNA* **2:** 362-375

Marintchev A, Edmonds KA, Marintcheva B, Hendrickson E, Oberer M, Suzuki C, Herdy B, Sonenberg N, Wagner G (2009) Topology and regulation of the human eIF4A/4G/4H helicase complex in translation initiation. *Cell* **136:** 447-460

Martino L, Pennell S, Kelly G, Bui TT, Kotik-Kogan O, Smerdon SJ, Drake AF, Curry S, Conte MR (2012) Analysis of the interaction with the hepatitis C virus mRNA reveals an alternative mode of RNA recognition by the human La protein. *Nucleic Acids Res* **40:** 1381-1394

McLauchlan J, Lemberg MK, Hope G, Martoglio B (2002) Intramembrane proteolysis promotes trafficking of hepatitis C virus core protein to lipid droplets. *Embo J* **21:** 3980-3988

Miyamoto H, Okamoto H, Sato K, Tanaka T, Mishiro S (1992) Extraordinarily low density of hepatitis C virus estimated by sucrose density gradient centrifugation and the polymerase chain reaction. *J Gen Virol* **73 (Pt 3):** 715-718

Modis Y, Ogata S, Clements D, Harrison SC (2004) Structure of the dengue virus envelope protein after membrane fusion. *Nature* **427:** 313-319

Moradpour D, Englert C, Wakita T, Wands JR (1996) Characterization of cell lines allowing tightly regulated expression of hepatitis C virus core protein. *Virology* **222:** 51-63

Moradpour D, Penin F (2013) Hepatitis C virus proteins: from structure to function. *Curr Top Microbiol Immunol* **369:** 113-142

Moradpour D, Penin F, Rice CM (2007) Replication of hepatitis C virus. *Nat Rev Microbiol* **5:** 453-463

Mortimer SA, Doudna JA (2013) Unconventional miR-122 binding stabilizes the HCV genome by forming a trimolecular RNA structure. *Nucleic Acids Res* **41:** 4230-4240

Muerhoff AS, Leary TP, Simons JN, Pilot-Matias TJ, Dawson GJ, Erker JC, Chalmers ML, Schlauder GG, Desai SM, Mushahwar IK (1995) Genomic organization of GB viruses A and B: two new members of the Flaviviridae associated with GB agent hepatitis. *J Virol* **69:** 5621-5630

Murakami Y, Aly HH, Tajima A, Inoue I, Shimotohno K (2009) Regulation of the hepatitis C virus genome replication by miR-199a. *J Hepatol* **50:** 453-460

Nasheri N, Singaravelu R, Goodmurphy M, Lyn RK, Pezacki JP (2011) Competing roles of microRNA-122 recognition elements in hepatitis C virus RNA. *Virology* **410:** 336-344

Nielsen SU, Bassendine MF, Burt AD, Martin C, Pumeechockchai W, Toms GL (2006) Association between hepatitis C virus and very-low-density lipoprotein (VLDL)/LDL analyzed in iodixanol density gradients. *J Virol* **80:** 2418-2428

Niepmann M (2009) Internal translation initiation of picornaviruses and hepatitis C virus. *Biochim Biophys Acta* **1789:** 529-541

Niepmann M (2013) Hepatitis C virus RNA translation. *Curr Top Microbiol Immunol* **369:** 143-166

Orom UA, Lund AH (2010) Experimental identification of microRNA targets. *Gene* **451:** 1-5

Orom UA, Nielsen FC, Lund AH (2008) MicroRNA-10a binds the 5'UTR of ribosomal protein mRNAs and enhances their translation. *Mol Cell* **30:** 460-471

Pang PS, Pham EA, Elazar M, Patel SG, Eckart MR, Glenn JS (2011) Structural map of a microRNA-122: hepatitis C virus complex. *J Virol* **86:** 1250-1254

Parent R, Qu X, Petit MA, Beretta L (2009) The heat shock cognate protein 70 is associated with hepatitis C virus particles and modulates virus infectivity. *Hepatology* **49:** 1798-1809

Paulin FE, Campbell LE, O'Brien K, Loughlin J, Proud CG (2001) Eukaryotic translation initiation factor 5 (eIF5) acts as a classical GTPase-activator protein. *Curr Biol* **11:** 55-59

Pawlotsky JM (2013) Treatment of chronic hepatitis C: current and future. *Curr Top Microbiol Immunol* **369:** 321-342

Pedersen IM, Cheng G, Wieland S, Volinia S, Croce CM, Chisari FV, David M (2007) Interferon modulation of cellular microRNAs as an antiviral mechanism. *Nature* **449:** 919-922

Pestova TV, Kolupaeva VG (2002) The roles of individual eukaryotic translation initiation factors in ribosomal scanning and initiation codon selection. *Genes Dev* **16:** 2906-2922

Pestova TV, Shatsky IN, Fletcher SP, Jackson RJ, Hellen CU (1998) A prokaryotic-like mode of cytoplasmic eukaryotic ribosome binding to the initiation codon during internal translation initiation of hepatitis C and classical swine fever virus RNAs. *Genes Dev* **12:** 67-83

Petri S, Dueck A, Lehmann G, Putz N, Rüdel S, Kremmer E, Meister G (2011) Increased siRNA duplex stability correlates with reduced off-target and elevated on-target effects. *Rna* **17:** 737-749

Pietschmann T, Zayas M, Meuleman P, Long G, Appel N, Koutsoudakis G, Kallis S, Leroux-Roels G, Lohmann V, Bartenschlager R (2009) Production of infectious genotype 1b virus particles in cell culture and impairment by replication enhancing mutations. *PLoS Pathog* **5:** e1000475

Ploss A, Evans MJ, Gaysinskaya VA, Panis M, You H, de Jong YP, Rice CM (2009) Human occludin is a hepatitis C virus entry factor required for infection of mouse cells. *Nature* **457:** 882-886

Ploss A, Rice CM (2009) Towards a small animal model for hepatitis C. *EMBO Rep* **10:** 1220-1227

Prentoe J, Jensen TB, Meuleman P, Serre SB, Scheel TK, Leroux-Roels G, Gottwein JM, Bukh J (2011) Hypervariable region 1 differentially impacts viability of hepatitis C virus strains of genotypes 1 to 6 and impairs virus neutralization. *J Virol* **85:** 2224-2234

Rand TA, Petersen S, Du F, Wang X (2005) Argonaute2 cleaves the anti-guide strand of siRNA during RISC activation. *Cell* **123:** 621-629

Randall G, Panis M, Cooper JD, Tellinghuisen TL, Sukhodolets KE, Pfeffer S, Landthaler M, Landgraf P, Kan S, Lindenbach BD, Chien M, Weir DB, Russo JJ, Ju J, Brownstein MJ, Sheridan R, Sander C, Zavolan M, Tuschl T, Rice CM (2007) Cellular cofactors affecting hepatitis C virus infection and replication. *Proc Natl Acad Sci U S A* **104:** 12884-12889

Roberts AP, Lewis AP, Jopling CL (2011) miR-122 activates hepatitis C virus translation by a specialized mechanism requiring particular RNA components. *Nucleic Acids Res* **39:** 7716-7729

Rodriguez A, Griffiths-Jones S, Ashurst JL, Bradley A (2004) Identification of mammalian microRNA host genes and transcription units. *Genome Res* **14:** 1902-1910

Rogers GW, Jr., Richter NJ, Merrick WC (1999) Biochemical and kinetic characterization of the RNA helicase activity of eukaryotic initiation factor 4A. *J Biol Chem* **274:** 12236-12244

Rüdel S, Flatley A, Weinmann L, Kremmer E, Meister G (2008) A multifunctional human Argonaute2-specific monoclonal antibody. *Rna* **14:** 1244-1253

Saini HK, Griffiths-Jones S, Enright AJ (2007) Genomic analysis of human microRNA transcripts. *Proc Natl Acad Sci U S A* **104:** 17719-17724

Sambrook, Fritsch, Maniatis (1989) *Molecular Cloning - A Laboratory Manual* 2nd Edition edn.: Cold Spring Harbor Press.

Scheller N, Mina LB, Galao RP, Chari A, Gimenez-Barcons M, Noueiry A, Fischer U, Meyerhans A, Diez J (2009) Translation and replication of hepatitis C virus genomic RNA depends on ancient cellular proteins that control mRNA fates. *Proc Natl Acad Sci U S A* **106:** 13517-13522

Schwarz DS, Hutvagner G, Du T, Xu Z, Aronin N, Zamore PD (2003) Asymmetry in the assembly of the RNAi enzyme complex. *Cell* **115:** 199-208

Seeff LB (2002) Natural history of chronic hepatitis C. *Hepatology* **36:** S35-46

Shimakami T, Yamane D, Jangra RK, Kempf BJ, Spaniel C, Barton DJ, Lemon SM (2012a) Stabilization of hepatitis C virus RNA by an Ago2-miR-122 complex. *Proc Natl Acad Sci U S A* **109:** 941-946

Shimakami T, Yamane D, Welsch C, Hensley L, Jangra RK, Lemon SM (2012b) Base pairing between hepatitis C virus RNA and microRNA 122 3' of its seed

sequence is essential for genome stabilization and production of infectious virus. *J Virol* **86:** 7372-7383

Shwetha S, Gouthamchandra K, Chandra M, Ravishankar B, Khaja MN, Das S (2013) Circulating miRNA profile in HCV infected serum: novel insight into pathogenesis. *Sci Rep* **3:** 1555

Simmonds P, Holmes EC, Cha TA, Chan SW, McOmish F, Irvine B, Beall E, Yap PL, Kolberg J, Urdea MS (1993) Classification of hepatitis C virus into six major genotypes and a series of subtypes by phylogenetic analysis of the NS-5 region. *J Gen Virol* **74 (Pt 11):** 2391-2399

Simons JP-M, TJ; Leary, TP; Dawson, GJ; Desai, SM; Schlauder, GG; Muerhoff, AS; Erker, JC; Buijk, SL; Chalmers, ML; Van Sant, CL; Mushahwar, IK (1995) Identification of two flavivirus-like genomes in GB hepatitis agent. *Proc Natl Acad Sci* **92:** 3401-3405

Song Y, Friebe P, Tzima E, Jünemann C, Bartenschlager R, Niepmann M (2006) The hepatitis C virus RNA 3'-untranslated region strongly enhances translation directed by the internal ribosome entry site. *J Virol* **80:** 11579-11588

Spencer PBJ (2012) Genetic Code Redundancy and its Influence on the encoded Polypeptides. *Comput Struct Biotechnol J* **1**

Stapleton JT, Foung S, Muerhoff AS, Bukh J, Simmonds P (2011) The GB viruses: a review and proposed classification of GBV-A, GBV-C (HGV), and GBV-D in genus Pegivirus within the family Flaviviridae. *J Gen Virol* **92:** 233-246

Suzich JA, Tamura JK, Palmer-Hill F, Warrener P, Grakoui A, Rice CM, Feinstone SM, Collett MS (1993) Hepatitis C virus NS3 protein polynucleotide-stimulated nucleoside triphosphatase and comparison with the related pestivirus and flavivirus enzymes. *J Virol* **67:** 6152-6158

Tamai K, Shiina M, Tanaka N, Nakano T, Yamamoto A, Kondo Y, Kakazu E, Inoue J, Fukushima K, Sano K, Ueno Y, Shimosegawa T, Sugamura K (2012) Regulation of hepatitis C virus secretion by the Hrs-dependent exosomal pathway. *Virology* **422:** 377-385

Terenin IM, Dmitriev SE, Andreev DE, Shatsky IN (2008) Eukaryotic translation initiation machinery can operate in a bacterial-like mode without eIF2. *Nat Struct Mol Biol* **15:** 836-841

Thomssen R, Bonk S, Propfe C, Heermann KH, Kochel HG, Uy A (1992) Association of hepatitis C virus in human sera with beta-lipoprotein. *Med Microbiol Immunol* **181:** 293-300

Tscherne DM, Jones CT, Evans MJ, Lindenbach BD, McKeating JA, Rice CM (2006) Time- and temperature-dependent activation of hepatitis C virus for low-pH-triggered entry. *J Virol* **80:** 1734-1741

Tsukiyama-Kohara K, Iizuka N, Kohara M, Nomoto A (1992) Internal ribosome entry site within hepatitis C virus RNA. *J Virol* **66:** 1476-1483

Unbehaun A, Borukhov SI, Hellen CU, Pestova TV (2004) Release of initiation factors from 48S complexes during ribosomal subunit joining and the link between establishment of codon-anticodon base-pairing and hydrolysis of eIF2-bound GTP. *Genes Dev* **18:** 3078-3093

Vasudevan S, Tong Y, Steitz JA (2007) Switching from repression to activation: microRNAs can up-regulate translation. *Science* **318:** 1931-1934

Vieyres G, Thomas X, Descamps V, Duverlie G, Patel AH, Dubuisson J (2010) Characterization of the envelope glycoproteins associated with infectious hepatitis C virus. *J Virol* **84:** 10159-10168

Wang C, Sarnow P, Siddiqui A (1993) Translation of human hepatitis C virus RNA in cultured cells is mediated by an internal ribosome-binding mechanism. *J Virol* **67:** 3338-3344

Weinlich S, Hüttelmaier S, Schierhorn A, Behrens SE, Ostareck-Lederer A, Ostareck DH (2009) IGF2BP1 enhances HCV IRES-mediated translation initiation via the 3'UTR. *Rna* **15:** 1528-1542

Welsch S, Miller S, Romero-Brey I, Merz A, Bleck CK, Walther P, Fuller SD, Antony C, Krijnse-Locker J, Bartenschlager R (2009) Composition and three-dimensional architecture of the dengue virus replication and assembly sites. *Cell Host Microbe* **5:** 365-375

WHO. (2012) Hepatitis C Facts Sheet World Health Organization.

Wilson JA, Zhang C, Huys A, Richardson CD (2011) Human Ago2 is required for efficient microRNA 122 regulation of hepatitis C virus RNA accumulation and translation. *J Virol* **85:** 2342-2350

Yuasa T, Ishikawa G, Manabe S, Sekiguchi S, Takeuchi K, Miyamura T (1991) The particle size of hepatitis C virus estimated by filtration through microporous regenerated cellulose fibre. *J Gen Virol* **72 (Pt 8):** 2021-2024

Zein NN (2000) Clinical significance of hepatitis C virus genotypes. *Clin Microbiol Rev* **13:** 223-235

Zeisel MB, Felmlee DJ, Baumert TF (2013) Hepatitis C virus entry. *Curr Top Microbiol Immunol* **369:** 87-112

Zhang X, Daucher M, Armistead D, Russell R, Kottilil S (2013) MicroRNA expression profiling in HCV-infected human hepatoma cells identifies potential anti-viral targets induced by interferon-alpha. *PLoS One* **8:** e55733

6 Appendix

6.1 Plasmid maps

6.1.1 pHCV-FL

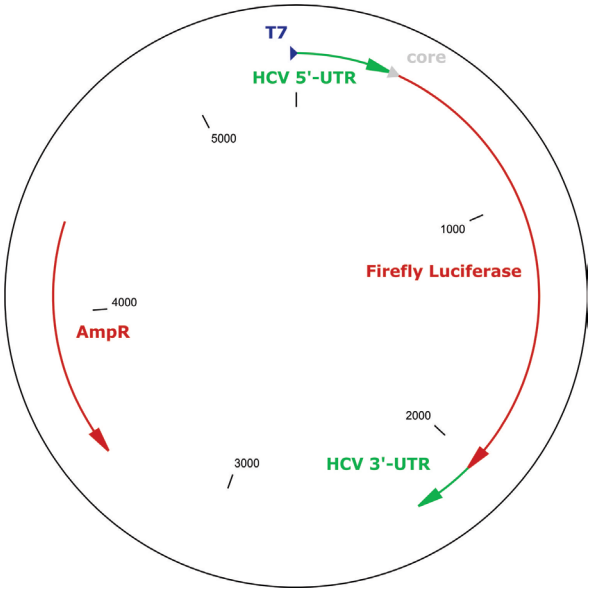

feature	description	start - stop [nt]
T7	Promoter for T7 RNA polymerase	5393 - 5410
HCV 5'-UTR	Sequence of the HCV 5'-untranslated region	1 - 341
Core I	Fragment of the HCV Core coding sequence	342 – 374
Firefly luciferase	ORF for the firefly luciferase	375 - 2027
HCV 3'-UTR	Sequence of the HCV 3'-untranslated region	2028 – 2248
AmpR	Ampicillin resistance gene	4327 – 3467

Description: Given are the relative positions of structural features present on the pHCV-FL expression plasmid. The T7 RNA polymerase promoter can be used to *in vitro* transcribe a HCV RNA reporter construct comprising the firefly luciferase ORF, flanked by the HCV 5'- and 3'-UTR. The Core linker is necessary for the proper folding of the HCV 5'-UTR after *in vitro* transcription. In opposite direction the location of the Ampicillin resistance gene is given, which is necessary for selection and amplification of the plasmid. The plasmid a ha total size of 5410 nts.

6.1.2 pHCV-FL miR-122 site 2-5nts-stem loop II

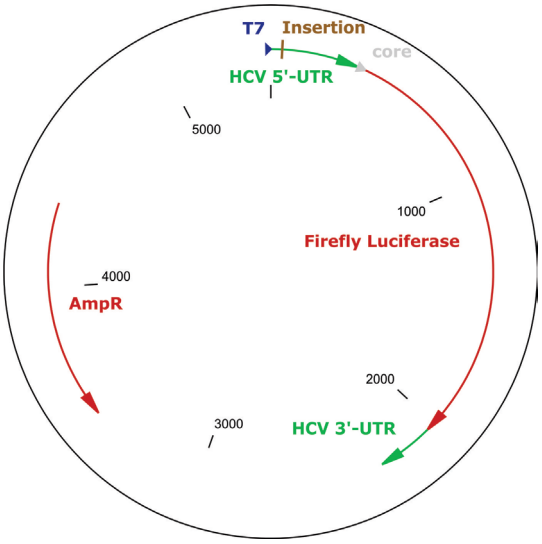

feature	description	start - stop [nt]
T7	Promoter for T7 RNA polymerase	5393 - 5410
HCV 5'-UTR	Sequence of the HCV 5'-untranslated region	1 - 351
Insetion	5 nts insertion including a *Xba*I restriction site	43 - 47
Core l	Fragment of the HCV Core coding sequence	347 – 379
Firefly luciferase	ORF for the firefly luciferase	380 - 2032
HCV 3'-UTR	Sequence of the HCV 3'-untranslated region	2033 – 2253
AmpR	Ampicillin resistance gene	4332 – 3473

Description: Given are the relative positions of structural features present on the pHCV-FL miR-122 site 2-5nts-stem loop II expression plasmid. The T7 RNA polymerase promoter can be used to *in vitro* transcribe a HCV RNA reporter construct comprising the firefly luciferase ORF, flanked by the HCV 5'- and 3'-UTR. The 5'-UTR carries an insertion of 5 nts between miR-122 site 2 and stem loop II of the HCV IRES. The insertion was generated by Quick Change *in vitro* mutagenesis, using a *Xba*I restriction site to identify positive mutations. The Core linker is necessary for the proper folding of the HCV 5'-UTR after *in vitro* transcription. In opposite direction the location of the Ampicillin resistance gene is given, which is necessary for selection and amplification of the plasmid. The plasmid has a total size of 5415 nts.

6.1.3 pHCV-FL miR-122 site 2-10nts-stem loop II

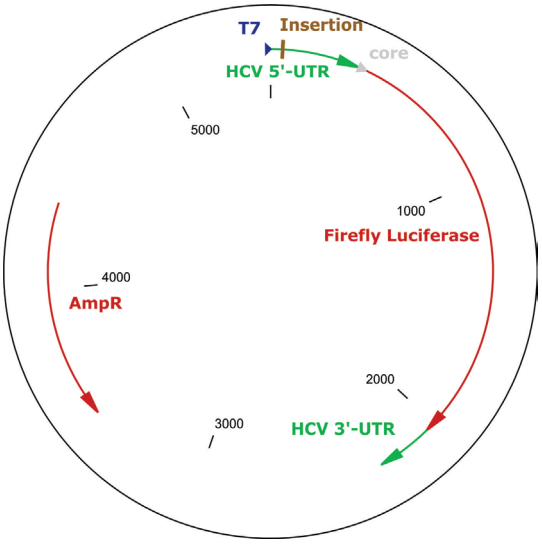

feature	description	start - stop [nt]
T7	Promoter for T7 RNA polymerase	5393 - 5410
HCV 5'-UTR	Sequence of the HCV 5'-untranslated region	1 - 351
Insetion	10 nts insertion including a *Xba*I restriction site	43 - 52
Core I	Fragment of the HCV Core coding sequence	342 – 374
Firefly luciferase	ORF for the firefly luciferase	385 - 2037
HCV 3'-UTR	Sequence of the HCV 3'-untranslated region	2038 – 2258
AmpR	Ampicillin resistance gene	4337 – 3477

Description: Given are the relative positions of structural features present on the pHCV-FL miR-122 site 2-10nts-stem loop II expression plasmid. The T7 RNA polymerase promoter can be used to *in vitro* transcribe a HCV RNA reporter construct comprising the firefly luciferase ORF, flanked by the HCV 5'- and 3'-UTR. The 5'-UTR carries an insertion of 10 nts between miR-122 site 2 and stem loop II of the HCV IRES. The insertion was generated by Quick Change *in vitro* mutagenesis, using a *Xba*I restriction site to identify positive mutations. The Core linker is necessary for the proper folding of the HCV 5'-UTR after *in vitro* transcription. In opposite direction the location of the Ampicillin resistance gene is given, which is necessary for selection and amplification of the plasmid. The plasmid has a total size of 5420 nts.

6.1.4 pHCV-FL stem

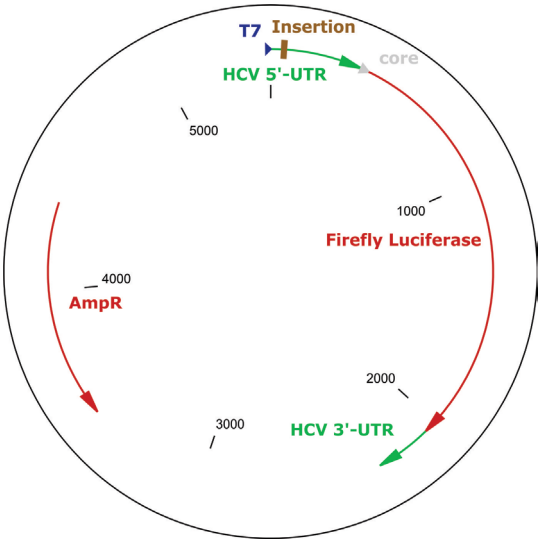

feature	description	start - stop [nt]
T7	Promoter for T7 RNA polymerase	5393 - 5410
HCV 5'-UTR	Sequence of the HCV 5'-untranslated region	1 - 361
Insetion	20nts insertion including a *Xba*I restriction site	43 - 62
Core I	Fragment of the HCV Core coding sequence	362 – 394
Firefly luciferase	ORF for the firefly luciferase	395 - 2047
HCV 3'-UTR	Sequence of the HCV 3'-untranslated region	2048 – 2268
AmpR	Ampicillin resistance gene	4347 – 3487

Description: Given are the relative positions of structural features present on the pHCV-FL stem expression plasmid. The T7 RNA polymerase promoter can be used to in vitro transcribe a HCV RNA reporter construct comprising the firefly luciferase ORF, flanked by the HCV 5'- and 3'-UTR. The 5'-UTR carries an insertion of 20 nts between miR-122 site 2 and stem loop II of the HCV IRES. The insertion was generated by Quick Change in vitro mutagenesis, using a *Xba*I restriction site to identify positive mutations. When transcribed the insertion forms an artificial stem loop in the HCV 5'-UTR masking the two miR-122 sites, redering them unable to hybridize to miR-122. The Core linker is necessary for the proper folding of the HCV 5'-UTR after *in vitro* transcription. In opposite direction the location of the Ampicillin resistance gene is given, which is necessary for selection and amplification of the plasmid. The plasmid has a total size of 5430 nts.

6.1.5 pHCV-SIN

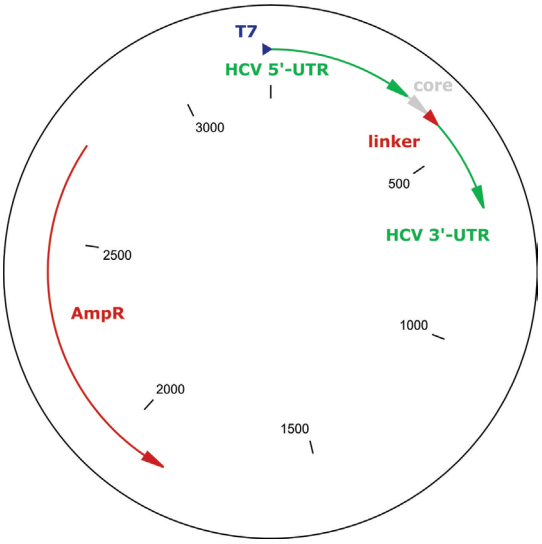

feature	description	start - stop [nt]
T7	Promoter for T7 RNA polymerase	3219 - 3235
HCV 5'-UTR	Sequence of the HCV 5'-untranslated region	1 - 341
Core	Fragment of the HCV Core coding sequence	342 -+ 402
Linker	Part of the firefly luciferase ORF	403 - 437
HCV 3'-UTR	Sequence of the HCV 3'-untranslated region	438 - 658
AmpR	Ampicillin resistance gene	2737 – 1877

Description: Given are the relative positions of structural features present on the pHCV-SIN expression plasmid. The T7 RNA polymerase promoter can be used to *in vitro* transcribe a HCV RNA reporter construct comprising a small linker comprised of parts of the core protein and firefly luciferase coding sequence, flanked by the HCV 5'- and 3'-UTR. In opposite direction the location of the Ampicillin resistance gene is marked, which is necessary for selection and amplification of the plasmid. The plasmid has a total size of 3235 nts.

6.1.6 3’-UTR only

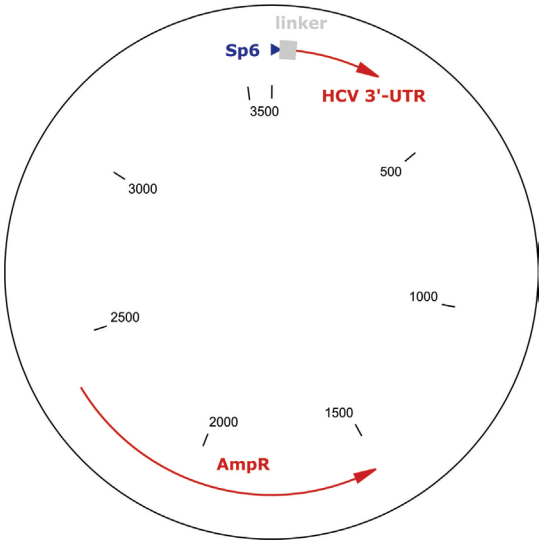

feature	description	start - stop [nt]
Sp6	Promoter for Sp6 RNA polymerase	1 - 21
Linker	Small linker sequence derived from the firefly luciferase ORF	22 - 62
HCV 3’-UTR	Sequence of the HCV 3’-untranslated region	63 - 283
AmpR	Ampicillin resistance gene	2370 - 1510

Description: Given are the relative positions of structural features present on the 3’-UTR only expression plasmid. The Sp6 RNA polymerase promoter can be used to *in vitro* transcribe a HCV RNA reporter construct comprising a small liker sequence derived from the firefly luciferase ORF, flanked downstream by the HCV 3’-UTR. The linker is necessary for the proper folding of the HCV 3’-UTR after *in vitro* transcription. In opposite direction the location of the Ampicillin resistance gene is given, which is necessary for selection and amplification of the plasmid. The plasmid has a total size of 3571 nts.

6.2 Publications

6.2.1 Peer-reviewed Journals

K.D. Conrad, F. Giering, C. Erfurth, A. Neumann, C. Fehr, G. Meister and M. Niepmann. 2013. microRNA-122 dependent binding of Ago2 protein to Hepatitis C virus RNA is associated with enhanced RNA stability and translation stimulation. PLoS One 8(2):e56272.

C. Fehr, **K.D. Conrad** and M. Niepmann. 2012. Differential stimulation of hepatitis C virus RNA translation by microRNA-122 in different cell cycle phases. Cell Cycle 11(2):277-285

6.2.2 Contributions to congresses

K. Dominik Conrad, Florian Giering, Corinna Erfurth, Angelina Neumann, Carmen Fehr, Gunter Meister and Michael Niepmann. Ago2 protein mediates miR-122-dependent stimulation of Hepatitis C virus IRES RNA translation in a distance-dependent manner.
Poster; 19th International Symposium on Hepatitis C Virus and Related Viruses; Venice (Italy); October 2012.

K.Dominik Conrad, Florian Giering, Corinna Erfurth, Agelina Neumann, Carmen Fehr, Gunter Meister and Michael Niepmann. Ago2 protein loads microRNA-122 to the Hepatitis C Virus 5'-untranslated region to stimulate translation.
Poster; Meeting on Transaltional Control of Cold Spring Harbor; New York (USA); September 2012.

Dagmar Goergen, **K. Dominik Conrad**, Carmen Fehr, Florian Giering and Michael Niepmann. Mechanisms of stimulation of Hepatitis C Virus RNA translation by microRNA-122.
Poster; 22nd Annual Meeting of the Society for Virology; Essen (Germany); March 2012.

Dagmar Goergen, **K. Dominik Conrad** and Michael Niepmann. Mechanisms of stimulation of Hepatitis C Virus RNA translation by microRNA-122.
Poster; 18th International Symposium on Hepatitis C Virus and Related Viruses; Seattle (USA); September 2011.

Carmen Fehr, **K. Dominik Conrad** and Michael Niepmann. Differential stimulation of Hepatitis C Virus RNA translation by miR-122 in different cell cycle phases.
Poster; 18th International Symposium on Hepatitis C Virus and Related Viruses; Seattle (USA); September 2011.

Eidesstattliche Erklärung

Ich erkläre:

Ich habe die vorgelegte Dissertation selbstständig und ohne unerlaubte fremde Hilfe und nur mit den Hilfen angefertigt, die ich in der Dissertation angegeben habe.
Alle Textstellen, die wörtlich oder sinngemäß aus veröffentlichten Schriften entnommen sind, und alle Angaben, die auf mündlichen Auskünften beruhen, sind als solche kenntlich gemacht.
Bei den von mir durchgeführten und in der Dissertation erwähnten Untersuchungen habe ich die Grundsätze guter wissenschaftlicher Praxis, wie sie in der „Satzung der Justus-Liebig-Universität Gießen zur Sicherung guter wissenschaftlicher Praxis“ niedergelegt sind, eingehalten.

Gießen im Juli 2013

K. Dominik Conrad

Acknowledgements

First of all, I would like to thank Prof. Michael Niepmann for providing the research topic, funding and laboratory space for conducting this work. Furthermore, I would like to thank him for the scientific support during the whole process.

Special thanks go to Prof. Albrecht Bindereif for taking over the part of a first supervisor in the faculty of biology at Justus Liebig University Giessen.

In addition I want to thank the IRTG “Enzymes and Multienzyme complexes acting on Nucleic Acids” for providing the funding for travels and soft skill workshops.

Finally I would like to thank Dr. Michaela Beitzinger and Prof. Gunter Meister for the various discussions as well as providing a lot of anti-Ago protein specific antibodies and for technical support during the anti-Ago co-IP development.